PERFORMANCE EVALUATION AND OPTIMISATION OF SURFACE GRINDING PROCESS FOR GRINDING OF ALUMINIUM BASED METAL MATRIX COMPOSITES USING RESPONSE SURFACE METHODOLOGY AND A NOVEL GENETIC ALGORITHM APPROACH

Thesis
Submitted in partial fulfilment of the requirements for the degree of

DOCTOR OF PHILOSOPHY

by

MR. DAYANANDA PAI K

DEPARTMENT OF MECHANICAL ENGINEERING
NATIONAL INSTITUTE OF TECHNOLOGY KARNATAKA,
SURATHKAL, MANGALORE – 575025

February, 2013

"Let each man take the path according to his capacity, understanding and temperament. His true guru will meet him along that path"

-Swami Sivananda

D E C L A R A T I O N

by the Ph.D. Research Scholar

I hereby *declare* that the Research Thesis/Synopsis entitled "*Performance evaluation and Optimisation of Surface Grinding Process for grinding of Aluminium based Metal Matrix Composites using Response Surface Methodology and a Novel Genetic Algorithm Approach"*, which is being submitted to the **National Institute of Technology Karnataka, Surathkal** in partial fulfillment of the requirements for the award of the Degree of **Doctor of Philosophy** in Mechanical Engineering is *a bonafide report of the research work carried out by me. The material contained in this Research Thesis/Synopsis has not been submitted to any University or Institution for the award of any degree.*

Dayananda Pai K.
(ME05P02)

Department of Mechanical Engineering

Place: NITK-Surathkal
Date: 22-02-2013

C E R T I F I C A T E

This is to *certify* that the Research Thesis entitled "Performance Evaluation and Optimisation of Surface Grinding Process for Grinding of Aluminium based Metal Matrix composites using Response Surface Methodology and a Novel Genetic Algorithm Approach" submitted by Dayananda Pai K. (Register Number: ME05P02) as the record of the research work carried out by him, is *accepted as the Research Thesis submission* in partial fulfillment of the requirements for the award of degree of **Doctor of Philosophy**.

(Dr. Shrikantha S.Rao)
Research Guide

(Dr. G.C. Mohan Kumar)
Chairman - DRPC

ACKNOWLEDGEMENT

This dissertation was only possible with the guidance and the help of several individuals who have contributed and extended their valuable assistance in the preparation and completion of this study.

First and foremost, my utmost gratitude to my research guide Dr. Shrikantha S. Rao, Associate Professor, Department of Mechanical Engineering, National Institute of Technology Karnataka for guiding me at each and every stage, right from identifying the research problem till the completion of this research work. Dr. Shrikantha S. Rao has been my inspiration for the successful completion of this research work.

I take this opportunity to thank Prof. G.C.Mohan Kumar, H.O.D., Department of Mechanical Engineering, National Institute of Technology, Karnataka-Surathkal, for the moral support extended to me during my research work in the campus and for his kind concern and consideration regarding my academic requirements.

I thank Dr. Sandeep Sancheti, former Director, National Institute of Technology Karnataka-Surathkal for giving me an opportunity to carry out my research work at the Institute.

I am highly indebted to the RPAC members, Dr. K.V. Gangadharan, Professor, Department of Mechanical Engineering, and Dr. Sripathi U., Professor, Department of Electronics and Communication Engineering, National Institute of Technology, Karnataka for their critical review of my research work, suggestions and support during the progress and pre synopsis assessment meetings.

I am extremely thankful to Dr. Suresh Hebbar and Dr. S.M. Kulkarni of Mechanical Engineering Department, National Institute of Technology, Karnataka for guiding me to successfully complete the course work.

My sincere thanks are due, to Dr. Rio G.L. D'Souza, Dean(Academics) and Professor, Computer Science Engineering, St. Joseph Engineering College, Mangalore, and Mr. Vipin, Project Manager, Infosys Technologies, Mangalore, for their valuable suggestions during genetic algorithm code development.

I am grateful to Dr. Raviraj Shetty, Associate Professor, Mechanical and Manufacturing engineering Department, Manipal Institute of Technology, Manipal, for helping and continuously motivating me throughout my research work.

I would like to thank the Head of the Composite Structure Division, VSSC Trivendrum, for providing the specimen required for conducting experiments.

I am very grateful to Dr. Ramamohan Pai, Head of Aeronautical and Automobile Engineering, Manipal Institute of Technology, Manipal University, Manipal, for supporting my work at all the stages.

The supporting work and other help rendered by Mr. Murali, Lab Technician, Mechanical Engineering Department, M.I.T. Manipal, in conducting the experiments is solicited.

I am highly indebted to my mother Smt. Sharada L.Pai for her encouraging words and instilling fresh dose of confidence in me whenever I faced problems. Successful outcome of this project would definitely cherish one of her dreams.

Role of my children Aniketh and Abhijith and my wife Supritha, cannot go unmentioned here. I am thankful to them for their kind patience and best wishes.

Finally, I wish to thank all the people who helped me directly or indirectly for the successful completion of my research work and the one above all of us, the omnipresent God, for answering my prayers for giving me the strength to plod on, despite hurdles. Thank you so much Dear Lord.

ABSTRACT

Aluminium-based metal matrix composites (MMCs) reinforced with ceramic particles are the advanced materials known for their good damping properties, high specific strength and high wear resistance. MMCs are increasingly used in aeronautical and automobile industries and in military applications. In addition, the sporting goods industry has also been in the forefront of MMCs development to capitalise on the materials high specific properties.

Despite many advantages, full implementation of MMCs is cost-prohibitive. This is partially due to the poor machinability of the materials. Although near-net-shape MMC components can be produced, finishing is still required for obtaining the desired dimensional accuracy and surface finish. Significant cost and fabrication problems, including machining, must be overcome for the successful application of these composites. Surface finish and surface integrity are important for surface sensitive parts subjected to fatigue. Unconventional processes produce better surface finish but they results in subsurface damage during the machining of MMCs. Hence, finishing processes such as grinding and allied abrasive machining are used to improve the surface integrity of machined MMCs.

The grindability of aluminium-based MMCs reinforced with ceramic particles is investigated in this dissertation. By the analysis of variance, a complete realization of the grinding process and their effects was achieved. Mathematical model is established for specific energy, metal removal rate and surface roughness from Response surface methodology (RSM). The main objective of this research is to determine the favourable grinding conditions for aluminium-based MMCs reinforced with ceramic particles. Not many researchers have attempted the optimisation of the surface grinding process by considering the specific energy as a performance parameter during grinding of MMCs. A novel approach of multi-objective optimization based on Genetic Algorithm and Desirability function approach was conducted to achieve the desired objective. Very few research works have been attempted towards multi objective optimisation involving surface roughness, metal removal rate and specific energy as the performance parameters in total.

The first part of the presented research concentrates on influence of process variables on specific energy, metal removal rate and surface roughness obtained in

grinding of Al6061-SiC_{35P} composites using Taguchi's design of experiments. From the above investigation, it is observed that feed is the dominant factor affecting the specific energy. Depth of cut is the dominant factor affecting the Metal removal rate and volume percentage of SiC is the dominant factor affecting the surface roughness.

The second part of presented research concentrates on mathematical modelling RSM. From the study, it is revealed that the second order RSM model developed for the performance parameters indicates good fit with the experimental results. Desirability function approach for multi-objective optimisation is adopted to choose the process variables that are favourable to achieve the optimal values of specific energy, metal removal rate and surface roughness.

The third part of the research involves the application of novel genetic algorithm on multi objective optimisation of specific energy (u), metal removal rate (Q_w) and surface roughness (R_a). The results obtained from this novel genetic algorithm were compared with RSM and the results obtained were in fairly close agreement.

Finally, the confirmatory experiments were carried out to validate the results obtained from RSM and novel genetic algorithm. From the experiments, it was observed that, deviation between the experimental and predicted responses were within 14%. However novel genetic algorithm compilation consumes less amount time in comparison to conventional non-dominated genetic algorithm (NSGA-II). Hence from the study, it can be concluded that the developed novel genetic algorithm model can be effectively used for the prediction of specific energy, metal removal rate and surface roughness.

The understanding gained from Taguchi's design of experiments, RSM, Desirability function approach and novel genetic algorithm in this research can be used to develop future guidelines for grinding of aluminium-based MMCs reinforced with ceramic particles.

Key words: discontinuously reinforced aluminium composites (DRACs), Specific energy, Metal removal, rate, surface roughness, Taguchi design of experiments, Response surface methodology, Novel genetic algorithm.

CONTENTS

Nomenclature

Symbol	*Abbreviation*	*Units*
a	Depth of cut	mm
ANOVA	Analysis of variance	---
D	Global Desirability Function	---
e	Residuals from the residual analysis	---
E_c	Elastic modulus of composite	N/m^2
E_m	Elastic modulus of matrix	N/m^2
E_p	Elastic modulus of particle	N/m^2
f	Feed	m/s
F'_t	Specific Tangential grinding force	N/mm
H_0	Null hypothesis	---
H_1	Alternate hypothesis	---
m	Mass of the material removed	grams
MS	Mean square	---
N	Population size	---
p	Levels of indipendent variables	---
P_t	Population Generated	---
Q_t	Offspring population	---
Q'_w	Specific Material Removal Rate	$mm^3/mm \cdot s$
R_t	Intermediate population	---

S	Particle aspect ratio	---
SS_E	Sum of the square of the error	---
SS_R	Sum of the square of residuals	---
SS_T	Sum of the square of the total	---
u	Specific energy	J/mm^3
V_f	Volume fraction of the fibre	mm^3
V_m	Volume fraction of the matrix	mm^3
V_p	Volume fraction of the particle	mm^3
v_s	Grinding wheel speed	m/s
v_w	Work speed	mm/s
w	Width of grinding wheel	mm
β	Coefficients of Regression equation	---
$d(\hat{y})$	Local Desirability Function	---
σ_c	Yield sterngth of the composite	N/m^2
σ_m	Yield strength of the matrix	N/m^2
ρ_c	Density of Composite	kg/mm^3
ρ_m	Density of matrix material	kg/mm^3
ρ_f	Density of fibre material	kg/mm^3
$\in$	Random error in regression	---

Chapter 1

INTRODUCTION

The term “composite” widely refers to a combination of two or more distinct materials having interface between them. It is a system composed of a discrete constituent (the reinforcement) distributed in a continuous phase (the matrix), and which derives its distinguishing characteristics from the properties of its constituents, from the shape, size and orientation of the constituents, and from the properties of the boundaries (interfaces) between different constituents. Metal matrix composites (MMCs) are composed of an element or an alloy matrix in which a second phase is embedded and distributed to achieve some property improvement. MMCs are a class of materials with a wide variety of structural, wear, and thermal management applications. Metal-matrix composites are capable of providing higher-temperature operating limits than their base metal counterparts, and they can be tailored to give improved strength, stiffness, thermal conductivity, abrasion resistance, creep resistance, or dimensional stability [ASM Hand book, Vol 21, 2001]. Unlike polymer-matrix composites, they are nonflammable, do not outgas in a vacuum, and suffer minimal attack by organic fluids such as fuels and solvents. MMCs tend to have higher strength to weight and stiffness to density ratios, as compared to monolithic metals [ASM Hand book, Vol 21, 2001].

In Aluminium Matrix Composites (AMCs) one of the constituents is aluminium/aluminium alloy, which forms percolating network and is termed as matrix phase. The other constituent is embedded in this aluminium/aluminium alloy matrix and serves as reinforcement, which is usually non-metallic such as SiC, TiC, TiB_2, fly ash Al_2O_3 etc. AMCs are intended to substitute monolithic materials including aluminium alloys, ferrous alloys, titanium alloys steel and polymer based composites in several applications. It is now recognised that in order to substitute monolithic materials for AMCs in engineering system, there is a compelling need to redesign the whole system to gain additional weight and volume savings. In fact according to the UK Advisory Council

on Science and Technology, AMCs can be viewed either as a replacement for existing materials, but with superior properties, or as a means of enabling radical changes in system or product design [Surappa 2003].

First section of this chapter explains the properties, characteristics, and production of MMCs. Second section describes the basic grinding variables and grinding of MMCs. A brief introduction about multi objective optimisation is cited in third section.

1.1 PROPERTIES OF MMCs

Properties of MMCs can be varied by altering the nature of constituents and their volume fraction. Particle-reinforced Aluminium Matrix Composites (PMACs), often called as discontinuously reinforced Aluminium metal matrix composites (DRACs), constitute 5 – 20 % of the new advanced materials [El-Gallab and Sklad 1998]. These composites generally contain equiaxed ceramic reinforcements with an aspect ratio less than 5. Ceramic reinforcements are generally oxides or carbides or borides (Al_2O_3 or SiC or TiB_2) and present in volume fraction less than 30% when used for structural and wear resistance applications. However, in electronic packaging applications reinforcement volume fraction could be as high as 70% [Surappa 2003]. In general, DRACs are manufactured either by solid state (Powder Metallurgy processing) or liquid state (stir casting, infiltration and in-situ) processes. The microstructure of the processed composites influences and has a great effect on the mechanical properties. Based on the size, shape and amount of the second phase, the property of the composite varies. Generally, increasing the weight fraction of the reinforcement phase in the matrix leads to an increased stiffness, yield strength and ultimate tensile strength. However, the low ductility of particulate reinforced MMCs is the major drawback that prevents their usage as structural components in some applications.

1.1.1 Basic properties of composite materials

In the field of metal matrix composite (MMC), particle reinforced matrix materials are considered to be a replacement for steel in the automobile and machine industry. Useful

performance characteristics of these composites have been gradually recognised and many MMC components are produced in these industries. The inclusion of hard particles in the ductile matrix material strengthens the composite with excellent mechanical properties such as increased yield and tensile strength. The mechanical properties of the metal matrix composite can be engineered by varying the shape, the size, the volume fraction, and the orientation of the reinforced particles [Huda et al. 1996].

The reinforcement of metals can have many different objectives. The reinforcement of light metals opens up the possibility of application of these materials in areas where weight reduction has first priority. There are several other property improvements due to reinforcement. They are;

- Greater strength
- Improved stiffness
- Improved high temperature properties
- Controlled thermal expansion coefficient
- Thermal/heat management
- Enhanced and tailored electrical performance
- Improved abrasion and wear resistance
- Control of mass (especially in reciprocating applications)
- Improved damping capabilities
- Improved corrosion resistance.

Determination of the basic properties of composite materials was conducted by many of the researchers in science and engineering. J.C. Maxwell in 1873 and Lord Rayleigh in 1892 computed the effective conductivity of composites consisting of a matrix and certain distribution of spherical particles **[**Broutman et al. 1967]. A fiber composite is highly anisotropic and has many stiffness and strength parameters. The strength and stiffness in the fiber direction are higher than those in the transverse direction. Furthermore, the matrix properties may be strongly influenced by

environmental changes such as heating, cooling and moisture absorption. It results in enormous varieties of property changes making the analytical modeling more complex.

One of the most important factors determining the properties of composite is the relative proportion of the matrix and the reinforcing phases. The relative proportions can be given as the weight fractions or the volume fractions. Among these, the volume fractions are extensively used in the theoretical analysis of composite materials

Volume fraction of the fiber, $V_f = \frac{v_f}{v_c}$ (1.1)

Volume fractions of the matrix, $V_m = v_m / v_c = 1 - V_f$ (1.2)

where, v_f, v_m and v_c are the volumes of the fiber, matrix and the composite respectively [Jones1992, Kaw 1997].

1.1.2 Characteristics of the composite materials

Composites consist of one or more discontinuous phases embedded in a continuous phase. The discontinuous phase is usually harder and stronger than the continuous phase and is called the 'reinforcement' or 'reinforcing' material, where as the continuous phase is termed as the 'matrix'.

Properties of composites are strongly dependent on the properties of their constituents, their distribution and the interactions among them. Apart from the above said properties, the size, density, type of reinforcing particles, and its distribution have a pronounced effect on the performance of particulate composites. The variables affecting the distribution of particles are solidification rate, fluidity, type of reinforcement, and the method of incorporation. The concentration and orientation of the reinforcement will also affect the properties of composites [Das et al., 1989].

The shape of the discontinuous phase (which may by spherical, cylindrical, or rectangular cross-sanctioned prisms or platelets), the size and size distribution (which influence the texture of the material) and volume fraction determine the interfacial area, which plays an important role in determining the extent of the interaction between the

reinforcement and the matrix. Concentration, usually measured as volume or weight fraction, determines the contribution of a single constituent to the overall properties of the composite. It is not only the single most important parameter influencing the properties of the composite, but also an easily controllable manufacturing variable used to alter its property. The orientation of the reinforcement affects the isotropy of the system.

1.2 CLASSIFICATION OF COMPOSITE MATERIALS

Composite materials can be classified in different ways [Agarwal and Broutman 1980]. Classification based on the geometry of a representative unit of reinforcement is convenient since it is the geometry of the reinforcement which is responsible for the mechanical properties and high performance of the composites. The two broad classes of composites are (1) Particulate composites and (2) Fibrous composites.

1.2.1 Particulate composites

Among all the AMCs, particle reinforced AMCs constitute largest quantity of composites produced and utilised on volume and weight basis[Surappa 2003].These composites are often called as discontinuously reinforced composites. As the name indicates, the reinforcement is of particle nature (platelets are also included in this class). It may be spherical, cubic, tetragonal, a platelet, or other regular or irregular shapes, but it is approximately equiaxed. In general, particles are not very effective in improving the fracture resistance but they enhance the stiffness of the composite to a limited extent. Particle fillers are widely used to improve the properties of matrix materials such as to modify the thermal and electrical conductivities, improve performance at elevated temperatures, reduce friction, increase wear and abrasion resistance, improve machinability, increase surface hardness and reduce shrinkage. These composites are isotropic in nature and can be subjected to a variety of secondary forming operations such as extrusion, rolling and forging.

1.2.2 Fibrous composites

A fiber is characterised by its length being much greater compared to its cross-sectional dimensions. Fibrous composites contain reinforcements with an aspect ratio of greater than 5, but are not continuous. These composites are either short-fibre composites or whisker-reinforced composites. The dimensions of the reinforcement determine its capability of contributing its properties to the composite. Fibers are very effective in improving the fracture resistance of the matrix since a reinforcement having a long dimension discourages the growth of incipient cracks normal to the reinforcement that might otherwise lead to failure, particularly when reinforced with brittle matrices.

Fibers, known for their small cross sectional dimensions, are not used directly in engineering applications. Hence they are embedded in matrix materials to form fibrous composites. The matrix will bind the fibers together, transfer loads to the fibers, and protect them against environmental degradation and damage due to handling.

Mechanical properties of whisker reinforced composites are superior compared to particle or short fibre reinforced composites. However, in the recent years usage of whiskers as reinforcements in AMCs is fading due to perceived health hazards and, hence of late commercial exploitation of whisker reinforced composites has been very limited. Short fibre reinforced AMCs display characteristics in between that of continuous fibre and particle reinforced AMCs.

Man-made filaments or fibers of non polymeric materials exhibit much higher strength along their length since large flaws, which may be present in the bulk material, are minimised because of the small cross-sectional dimensions of the fiber. In the case of polymeric materials, orientation of the molecular structure is responsible for high strength and stiffness.

1.3 PRODUCTION OF METAL MATRIX COMPOSITES

Metal matrix composite materials are produced by casting, powder metallurgy, atomisation and reactive processing methods. By means of casting methods, composite

materials reinforced by dispersion particles, platelets, non-continuous (short) fibres and continuous (long) fibres [Kainer 1997] as well as composite materials with hybrid reinforcement composed of particles and fibres are produced. By powder metallurgy methods, composite materials reinforced by dispersion particles, platelets, non-continuous fibres and continuous fibres are manufactured. Atomisation is a spray forming method and reactive processing involves exothermic dispersion.

1.3.1. Production of composite materials by casting methods

Composites are produced through casting method by blending of reinforcing elements in molten alloy matrix reinforced with dispersion particles and short fibres [Corbin and Wilkinson1994]. Normally mixing process is performed under atmospheric pressure and reinforcing elements should be characterised by good wettability by the molten metal alloy. Reinforcing particles showing poor wettability with the molten alloy can be covered with layers improving the mutual wettability; for instance in the case of graphite strengthening particles in A356 aluminium alloy, they were covered with nickel to improve the mutual wettability [Ames and Alpas 1995].

1.3.1.1 Stir casting process (Al6061Composites):

In this method Al6061 alloy in the form of ingots were used for the preparation of MMC's. The cleaned metal ingots were melted to the desired super heating temperature of 750^0C- 800°C in graphite crucibles under a cover of flux in order to minimise the oxidation of molten metal. 3-phase electrical resistance furnace shown in Figure 1.1 is used for melting. The super heated molten metal was degassed at a temperature of 780°C. SiC particulates, preheated to around 600°C were then added to the molten metal and stirred continuously by using mechanical stirrer shown in Figure 1.1. The stirring time varies between 5 – 8 minutes at an impeller speed of 250-300 rpm. During stirring, Magnesium is added in small quantities to increase the wettability of SiC particles. The dispersion of the preheated SiC particulates was achieved in accordance with the vortex method. The melt with the reinforced particulates were poured into the dried, coated, cylindrical permanent metallic moulds to produce the desired castings.

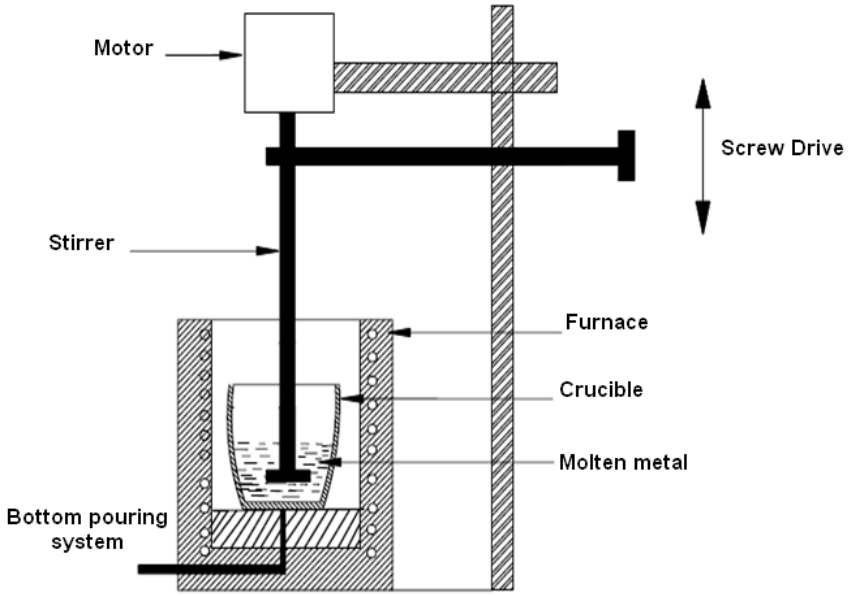

Figure 1.1 Schematic of Stir casting process

1.3.1.2 Squeeze casting process:

Currently, the most common production method of composite materials is infiltration of porous preforms made of ceramic fibres under pressure with molten light alloys. There are direct squeeze casting and indirect squeeze casting of preliminary heated preforms, and these processes are shown schematically in Figure 1.2.

Direct squeeze casting is applied for the production of composite elements characterised by relatively simple shapes, and casting dies for direct squeeze casting are relatively simple and of reasonable price. The application of indirect squeeze casting makes possible the production of more complex composite parts, but it results in more expensive casting dies.

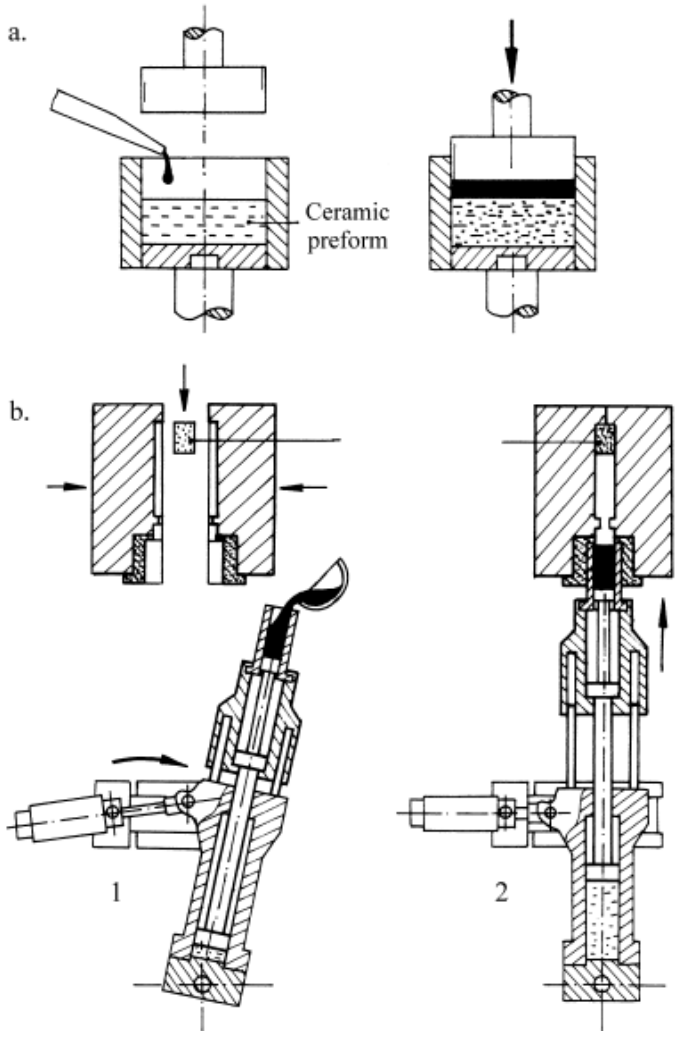

[1]**Figure 1.2**. Production of cast composite materials by (a) direct squeeze casting method and (b) indirect squeeze casting method.

1.3.2 Production of composite materials by powder metallurgy methods

Powder metallurgy methods are based on the classical blending of matrix powders and reinforcing elements (dispersion powders, platelets and ceramic fibres) and further cold pressing and sintering followed by plastic working (forging, extrusion). Cold plastic

[1] *Courtesy: Kaczmar J.W. "The production and application of metal matrix composite materials", Journal of Materials Processing Technology 106 (2000) 58-67*

working is normally applied when a green part is preliminary sintered and hot plastic working occurs when only cold pressing is applied.

The method described above, on account of its simplicity, is applied widely for the production of composite materials with magnesium alloys matrix, aluminium alloys matrix, and copper matrices [Kaczmar J.W. 1989].

Mechanical alloying is nowadays one of the most widely applied methods for the production of composite materials reinforced by dispersion particles. The process is performed in a high-energy ball mill (attritor), making possible the introduction of hard dispersion particles into a relatively soft metal matrix. The composite powders, so produced are then pressed and consolidated by hot plastic working (extrusion, forging or hot isostatic pressing) or cold pressed, sintered and cold plastic worked. The mechanical alloying technique is applied for the production of composite materials, materials characterised by very fine grains, amorphous materials and magnetic materials [Bowman et al. 1995].

1.3.3 Spray forming

The idea of the spray forming process is based on the atomisation of metal matrix powders with simultaneous injection of dispersion powders on the substrate and is nowadays increasingly more widely applied for the production of large size elements from composite materials and is shown schematically in Figure 1.3.

By means of the spray forming process, composite powders reinforced with dispersion particles can also be manufactured. Further, by powder metallurgy methods (pressing, sintering, hot plastic working) composite materials can be manufactured. This process has such advantages as the possibility of introduction of different reinforcing particles, and makes it possible to have an effect on the chemical reactions between matrix and reinforcement. This leads to production of in situ composite materials.

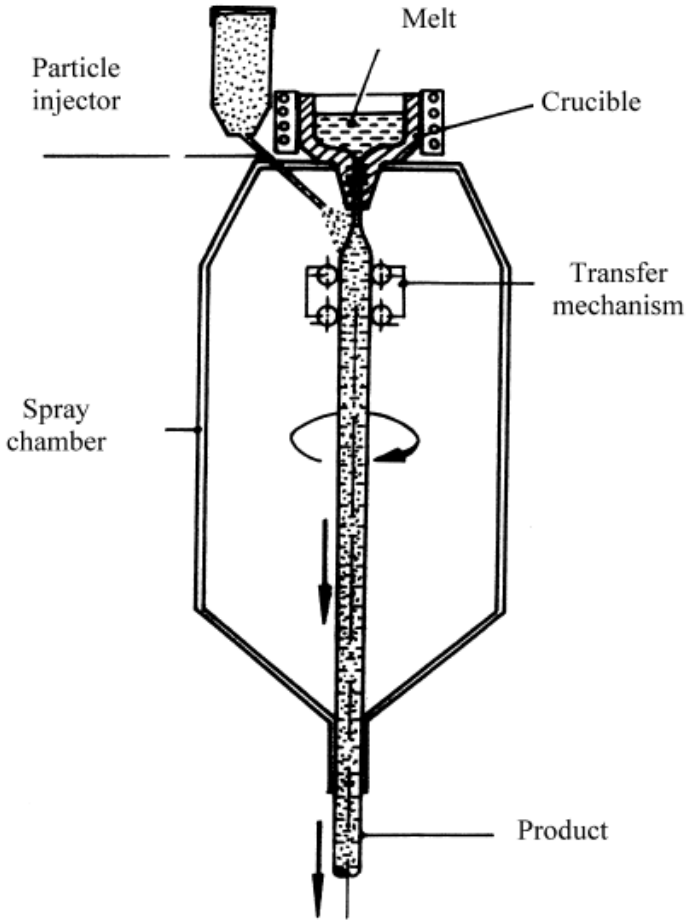

[2]**Figure 1.3** Spray forming process

Due to the relatively low heat convection during the atomisation process, it can be realised at relatively low temperatures, which is due to the limited chemical reactions at the interphases. This makes possible the production of such combinations of metal matrix and ceramic particles that would react intensively at elevated temperatures (for instance during the squeeze casting process) when harmful chemical compounds would be formed at the interphases.

[2] *Courtesy: Kaczmar J.W. "The production and application of metal matrix composite materials", Journal of Materials Processing Technology 106 (2000) 58-67*

On account of the high cooling rate, the materials produced are characterised by relatively small grains, increased solid state solubility, and the possibility of forming non-equilibrium phases and the lack of macro segregation.

1.3.4. XD^{TM} process (Reactive Processing)

The XD^{TM} (Exothermic Dispersion) process was developed by Martin Marietta Corporation (1987) for fabricating in-situ composites. It is a rather different approach to MMC manufacture than the methods mentioned in the previous sections. In this process, the matrix metal is mixed with compounds with which it reacts exothermally. When this mixture is heated to a high temperature (usually above the melting point of the matrix or to a point where a self-propagating reaction takes place), the constituent components react exothermally to form a dispersion of submicroscopic reinforcing particles in the matrix. Hence the name "XD", since the particles of the reinforcing phase are formed exothermally at high temperatures, they tend to be very stable during subsequent processing and use at elevated temperatures. A wide range of ceramic compounds can be formed by the XD^{TM} process [Martin Marietta Corporation 1987]. However, the two that have received wide attention are TiB_2 and TiC. These can be formed by the following reactions.

$$2B + Ti + Al \xrightarrow{yields} TiB_2 + Al$$

and

$$C + Ti + Al \xrightarrow{yields} TiC + Al$$

There is little information in the open literature regarding (i) the cost of materials produced by the XD^{TM} process, (ii) the porosity levels in the as-reacted materials, and (iii) the control of the size and spacing of the reinforcing particles. The production of a variety of MMCs by this process has been reported. These include matrices of Ai, Ti, Fe, Cu, Pb, and Ni as well as inter-metallics such as TiAl, Ti_3AI, and NiAl [Lewandowski et al. 1988, Christodoulou et al. 1988].

1.4. ENGINEERING PROPERTIES AND APPLICATIONS OF MMCs

A brief discussion of some engineering properties of particle-reinforced MMCs is presented here to show how these properties are influenced by the addition of ceramic particles to aluminum alloys. The enhancement of specific stiffness, specific strength, wear and creep resistance, and the reduction of density and coefficient of thermal expansion are some of the most attractive features of MMCs. Table 1.1 lists the engineering property of the prominent alloys and the Al-SiC composites. The correct selection of reinforcement is very important in yielding desired resultant material properties. An improper reinforcement selection may lead to less-than-desirable composite materials properties, difficulty in fabrication of end product, and high cost.Stiffness is a critical design parameter for many engineering components because the avoidance of excessive elastic deflection in service is the principal overriding consideration. A typical potential application of improved creep resistance is in the development of high-temperature components, such as turbine engine parts where the aim is to replace some heavy components with components made of much lighter substitute materials.

Table 1.1 Mechanical Properties of SiC particle-Reinforced Aluminium [Kutz 2008]

Property	**Aluminium (6061-T6)**	**Titanium (6Al-4V)**	**Steel (4340)**	**Composie particle volume fraction**		
				25	**55**	**70**
Modulus (GPa)	69	113	200	114	186	265
Tensile yield strength (MPa)	275	1000	1480	400	495	225
Tensile ultimate strength (MPa)	310	1100	1790	485	530	225
Elongation (%)	15	5	10	3.8	0.6	0.1
Density g/cm^3	2.77	4.43	7.76	2.88	2.96	3.00
Specific modulus GPa	5	26	26	40	63	88

1.4.1 Stiffness

Elastic modulus is one mechanical property that is always significantly increased by the addition of ceramic particles into a metallic alloy. The enhancement of stiffness achieved by the addition of the reinforcement is retained at high temperatures and this is of great benefit in the design of rotating parts, support members, and structural bodywork. Examples of applications that depend primarily on stiffness include drive shafts, electronic instrument racks, bicycle frames, and inertial guidance spheres for missiles.

The elastic modulus of composite increases with the volume fraction of the reinforcing phase and can be calculated from the rule of mixtures (ROM) expression. It should be noted that the ROM is appropriate for estimating the Young's modulus of continuous reinforcement, but it overestimates that of discontinuous reinforcement. Hence this has been modified in the Halpin-Tsai equation, [Halpin et al. 1967]

$$E_c = \frac{E_m(1+2sqV_p)}{1-qV_p} \tag{1.3}$$

where

$$q = \frac{\left(\frac{E_p}{E_m}-1\right)}{\left(\frac{E_p}{E_m}+2s\right)}$$

and E_c, E_m, E_p are the elastic moduli of the composite, matrix, and particle, respectively, s is the particle aspect ratio, and V_p, the volume fraction of the particle. The elastic modulus can also be calculated using the Eshelby equivalent inclusion method, and this approach is also known to be in good agreement with experimental data.

1.4.2 Elongation

It can be seen from Table 1-1 that a major limitation in the engineering properties of aluminium alloys is the rather high ductility (as quantified by percent elongation). The tensile elongation decreases with increasing particle content. Similarly, tensile elongation decreases with increased aging time in heat treatable alloys [ASM Hand Book Vol. 2,

2000]. The increase in stiffness and decrease in ductility with increasing particle content reflect the interactions between particles and the intervening matrix within MMCs.

Previous work has demonstrated that composite failure is associated with particle cracking and voids formation in the matrix within clusters of particles. Lloyd, 1994 Manoharan et al. 1990 and Whitehouse and Clyne 1993 have suggested that, particle fracture is more prevalent in coarser particles than in the finer ones due to the higher probability of finding crack-initiating defects in the former than in the latter particles. The failure associated with particle clusters is attributed to the higher stress generated in such regions. It has been reported that matrix deformation between closely spaced elastic particles would be highly constrained resulting in local stress levels which are many times the matrix flow stress [Miracle and Donaldson 2001]. This behavior has been confirmed by continuum modeling [Whitehouse et al. 1992; Christman et al. 1989]. Further, larger the particle size, more the load due to conventional fiber loading and end loading mechanisms. For Al-SiCp composites, it has been observed that particle cracking is an important failure mechanism for composites containing particles of size greater than 20 microns [Lloyd, 1989].The geometry of the reinforcement in MMCs has been shown to markedly affect matrix deformation behavior [Lloyd, 1989, Whitehouse and Clyne 1993, Brockenbrough et al. 1991, Padkin *et al.* 1987]. This is largely due to the fact that, the matrix stress and strain fields developed in response to external loads vary appreciably with the geometry of the reinforcing phase [Christman et al.1989, Brockenbrough et al. 1991, Tvergaard 1990]. This has, in turn, been shown to alter fracture behavior particularly near the matrix/reinforcement interface. Song et al. (1996) studied the effects of particle shape on the fracture and ductility of a spherical and an angular particle-reinforced 6061Al composite using scanning electron microscope (SEM) and transmission electron microscope (TEM). It was found that although the spherical particulate composite showed a slightly lower yield strength and work hardening rate, the ductility was significantly higher than the angular counterpart. The SEM fractography examination showed that during tensile loading, the spherical composite failed via void nucleation and

linking in the matrix near the reinforcement matrix interface whereas the angular composite failed through particle fracture and matrix ligament rupture.

Experimental evidence in the literature shows that voids nucleate preferentially at the sharp corners of the reinforcements [Manoharan et al. 1990, Christman et al.1989, Nutt et al. 1987, Dragone and Nix 1990]. Fisher and Gurland (1981) have discussed the factors that tend to favor the formation of voids, which results in premature failure of the composite. FEM modeling has predicted that composites with spherical reinforcements have a higher ductility due to the lower matrix triaxiality [Song et al. 1996, Llorca et al. 1991]. Therefore, a feasible way to improve composite ductility is to use spherical reinforcements to reduce stress concentrations and thereby bring about changes in the stress distribution throughout the composite.

The stress distributions created around and within hard particles in a deforming matrix have been studied [Watt et al. 1996]. The way a particle gathers stress to itself depends on the elastic misfit between the two phases. The stress concentrations at sharp corners of the reinforcements give rise to intense localised plastic flow [Manoharan et al. 1990, Dragone and Nix 1990, Christman et al. 1989]. The onset of local plastic deformation leads at first to plastic relaxation, but with further deformation, localised strain hardening once again leads to high stresses next to the particles [Watt et al. 1996].

Due to the complexity of the stress fields, dislocation glide, void nucleation, and growth in the matrix during plastic deformation proceed differently from those commonly found in unreinforced alloys [Shi et al. 1994]. The particles are known to carry much higher stresses than the matrix. This transfer of stress to the particles and the associated near-particle perturbations affect the failure modes, stiffening, and strength observed in MMCs.

1.4.3 Strength

Mc Danels, (1985) carried out the first extensive study of the strength of several discontinuous MMCs reinforced with SiC whisker, particle and reported up to 60% increase in yield and ultimate tensile strengths. The exact value depended on the volume fraction of reinforcement, the type of alloy and its temper, and processing of the composite. Although subsequent work by different authors essentially confirmed these findings, the reported experimental data show a large degree of scatter due to differences in the material quality, processing routes, and testing parameters.

Numerous strengthening mechanisms that may operate in particle-reinforced MMCs have been discussed in the literature and the behavior has been extensively modeled mathematically [Christman et al. 1989, Arsenault et al. 1991, Levy and Papazian1991, Humphreys 1998]. The strengthening process in the composite has been modeled based on two different approaches, namely, the continuum approach and the micromechanics approach. The continuum shear lag model, originally developed by Cox in 1952 and later modified by many researchers [Piggot, 1980, Nardone and Prewo1986], gives the composite strength (σ_c) for a particulate composite as:

$$\sigma_c = \sigma_m \left[V_p \left(\frac{S+4}{4} \right) + V_m \right] \tag{1.4}$$

where (σ_m) is the matrix yield stress, V_m, and V_p, are the volume fractions of the matrix and particle respectively, and S is the particle aspect ratio. The aspect ratios typically used for particulate MMCs vary from 1.0-1.5. The major difficulty with the continuum approach lies with its inability to account for the influence of the particles on the micromechanics of deformation. These include the very high work hardening at low strains as well as modification in microstructure such as grain size and dislocation density.

In the micromechanics approach the micro structural effects arising from the presence of the particles are considered. The possible strengthening mechanisms reported

by Clyne and Withers1993, Arsenault et al. 1991, Levy and Papazian 1991 and Humphreys 1998 are: (i) dislocation strengthening due to difference in coefficient of thermal expansion between the matrix and the reinforcing particles (ii) dispersion strengthening caused by the resistance of closely spaced hard particles to the passing of dislocations (iii) strengthening from grain size refinement (iv) work-hardening due to the strain misfit between the elastic reinforcing particles and the plastic matrix. The extent to which the different mechanisms operate will depend on the microstructure and processing of the particular composite.

In general, there are relatively few applications where the main attraction of using the MMCs stems from the greater strength offered, especially at room temperature. While the presence of ceramic particles improves the modulus at higher temperatures, they do not add significantly to the high temperature strength. Only a small improvement in strength over the monolithic alloy is retained at higher temperatures. The reason for this behavior is that the strengthening mechanisms operating in MMCs at low temperatures are relaxed at high temperatures. Thus the composite strength is primarily controlled by the high temperature strength of the matrix.

1.4.4 Wear resistance

Although different wear applications require different reinforcement types to achieve optimal wear rate reduction, there are many situations where wear rates are reduced by factors of up to ten by the introduction of the reinforcement. This property makes MMCs very attractive for bearings, bushings, cylinder liners, and brake rotors. In some cases, it is advantageous to control the distribution of reinforcement so as to provide material of high wear resistance in selected surface areas while other regions are suitably tough, strong, or thermally conducting. This can be done by selective reinforcement of critical areas through spray deposition or some other route. In general, it is important for wear resistance to be combined with other properties such as high thermal conductivity (to dissipate frictional heat) and high stiffness (to avoid wear from excessive deflections).

1.4.5 Applications of MMCs

Aluminum alloys are preferred engineering material for automobile, aerospace and mineral processing industries for various high performing components that are being used for variety of applications owing to their lower weight, higher strength and excellent thermal conductivity. Among several series of aluminum alloys, heat treatable Al6061 and Al7075 are much explored. Among them Al6061 alloy are highly corrosion resistant and are easily available in nature [Rohatgi 1993].

Mechanical properties of DRACs are inferior compared to whisker/short fibre/continuous fibre reinforced AMCs but far superior compared to unreinforced aluminium alloys. These composites are isotropic in nature and can be subjected to a variety of secondary forming operations including extrusion, rolling and forging. Discontinuously reinforced metal-matrix composite (DRMMC) materials systems are commonly used in applications that require high specific materials properties, enhanced fatigue resistance, improved wear resistance, controlled expansion, or the ability to absorb neutron radiation (boron carbide). Additionally, DRMMC may be designed to yield a materials system that offers multiple roles. Some examples of multiple roles are DRMMC material systems that offer high strength and fatigue resistance for aerospace and mechanical applications, thermal management coupled with expansion control for space-borne applications, moderate strength and neutron absorption capabilities for nuclear applications, high strength and wear resistance for heavy equipment applications, and impact/energy dissipation for armor applications.

1.5. BASIC GRINDING PROCESS VARIABLES

In the current century grinding is still often involved in the manufacturing of many products and components not only because the shaping technology such as sintering is not as accurate as required by the size specifications but also the economics involved [Marinescu et al. 2007]. The grinding process is almost chosen exclusively for finishing purposes since grinding has a high material removal rate combined with a moderate precision in comparison with other abrasive machining processes. However, it is well

known that the process may induce damage at the machined surface and specific energy involved is much higher compared to other machining processes. The surface damage may affect the functional properties of the material being ground. The integrity of the material at the machined surface may not always be obvious but is vitally important in many situations. The cracks may reduce the mechanical strength of a component. It may also be important to avoid tensile residual stresses that reduce strength and shorten service life. All these aspects of quality require careful design and control of the grinding process variables.

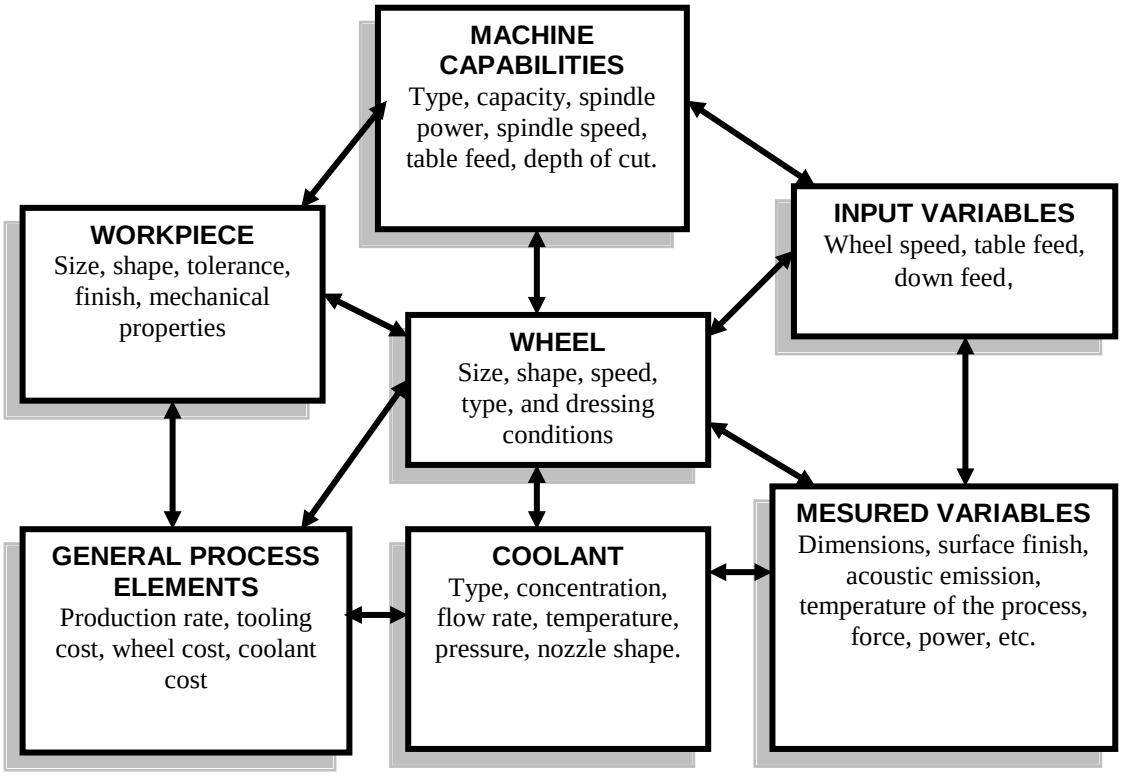

Figure 1.4 Major process elements of surface grinding

Figure 1.4 shows the major elements for a surface grinding process. Prior to selecting a fabrication process, the engineer usually knows the workpiece requirements – the desired size, shape, dimensions, tolerances, surface finish, and other elements related to the form and function of the workpiece. The required production rate is also usually

known. These elements, combined with the budget, strongly influence the engineer's selection of an appropriate grinding machine, tooling, etc. These process elements are fixed based on design criteria and production requirements.

There are many parameters in grinding that influence each other. A problem that continues to confront the manufacturing industry is establishment of efficient grinding conditions. This includes choosing a suitable grinding conditions and establishing the values of grinding parameters such as grinding ratio, material removal rate, specific energy, surface roughness and establishing dressing parameters.

The basic grinding variables may be divided into four categories [Rowe 2009]

(i) The output variables of the system comprise the work piece quality, productivity and cost, which should meet the design and manufacturing requirements. The output variables are therefore the main variables to be controlled.

(ii) The process variables include power, force, temperature and vibration. The process variables are affected by the grinding conditions and affect the output variables. For example, higher the forces applied during the grinding process, the faster is the material removal rate. But the force also affects the other output variables such as surface roughness, the dynamic structure of the system and the onset of thermal damage etc.

(iii) The input conditions may be divided in to the grinding conditions which are selectable and other conditions which are uncontrolled. Uncontrolled variables, e.g. material properties, cannot be changed by the operator but have a significant effect on the grinding process and output variables. The grinding conditions consist of the grinding wheel, the coolant, the dressing conditions and the grinding kinematics conditions. The kinematic variables affecting the process and output variables are:

a. wheel speed v_s m/s
b. work speed v_w, m/s
c. feed rate f, mm/s
d. depth of grind a, mm

(iv) Grinding conditions: The criterion for the selection of the grinding conditions is that the output variables must meet the requirements of design and manufacturing. The grinding conditions selected by the selection system may be considered as the solution to the grinding problem, where the operator presents the description of the grinding problem to the system.

(v) Grinding wheel: The grinding wheel characteristics have a direct effect on process efficiency, accuracy, surface roughness and surface integrity. It is therefore essential to select an appropriate grinding wheel. The best wheel for an application is a compromise between the ability to cut rapidly and the ability to hold form, maintain the surface roughness requirements and last a long time before dressing is required [ASM Handbook Vol. 21, 2000]. The specification of the grinding wheel consists of five parts:

(a) abrasive type
(b) abrasive grit size
(c) grade
(d) structure
(e) bond

The engineer has more latitude when it comes to the selection of an appropriate grinding wheel, truing and dressing method, and coolant. These choices are based largely on prior experience, machinability data handbook and recommendations from the manufacturers of grinding wheels and coolants. Once these process elements are chosen, they are usually held constant for convenience.

Perhaps the most difficult part of planning the process is making intelligent decisions regarding appropriate values for material removal rate, wheel speed, table speed, down feed and cross feed. It requires the understanding of factors affecting grinding conditions.

Grinding involves a large number of interacting variables. Before designing the selection system, it is necessary to decide which variables should feature in the selection

process. Consideration is therefore given to the relationships and interactions between these variables.

1.6. GRINDING OF DISCONTINUOUSLY REINFORCED ALUMINIUM COMPOSITES (DRACs)

Grinding is a complex process as there are several parameters in grinding that influence each other [malkin and Guo 2008]. These include the type of the grinding wheel, type of workpiece, wheel speed, cross feed, in-feed, depth of cut, dressing parameters, etc. Many of these parameters in grinding will influence each other [Li 1999]. A problem that continues to confront the manufacturing industry is establishment of efficient grinding conditions. This includes choosing a suitable grinding wheel, establishing the values of grinding process variables that are suitable for given conditions. The search for higher productivity, cost reduction, production systems flexibility, better surface and /or dimensional quality, besides development of new materials, is becoming more and more important in machined products industries, aiming to keep, or even increase their market share, in the global world.

The aluminium alloy reinforced with discontinuous ceramic reinforcements is rapidly replacing conventional materials in various automotive, aerospace and automobile industries. But Al/SiC-MMCs machining is one of the major problems, which resist its wide spread engineering application [Allison and Cole 1993]. Though DRAC's are produced to near net shaped products, final finishing is still required for obtaining the desired finish and dimensional accuracy. Therefore finishing processes such as grinding are used to improve the performance parameters of machined discontinuously reinforced aluminium composites. Grinding of DRACs is still a challenge for an industry. It is mainly because of the reason that when Al/SiC-MMC specimen slides over a hard grinding wheel during grinding, it always presents a newly formed surface to the same portion of the cutting edge and consequently due to friction, high temperature and pressure the particles of the Al/SiC-MMC adhere to the grinding wheel. In this way more

particles will join up with those already adhering and results in poor surface finish, lower material rate and higher specific energy [Manna and Bhattacharya 2003].

1.7. PERFORMANCE PARAMETERS IN GRINDING PROCESS

Performance of any machining process is depending on the output that is obtained from the process. The performance parameters in grinding process are specific energy, surface roughness, material removal rate, grinding ratio, surface integrity, residual stresses etc. All these parameters depends on the type of material to be ground, type of grinding wheel, type of lubricants used, machine dynamics and grinding conditions[Rowe 2009]. Dominant Performance parameters in grinding are grinding ratio, surface finish, specific energy, and material removal rate.

Specific energy is an important performance parameter in grinding, because it defines the temperature at the wheel-work interface [Ren et al. 2009]. It is defined as energy consumed per unit volume of metal removed. Typically, the specific energies involved in grinding are much larger than in other metal-cutting operation. In other metal-cutting operations the shearing accounts for about 75% of the total chip formation energy and for chip-tool friction the remaining 25% [Allison and Cole 1993]. But in grinding, virtually, all the energy expended is converted into heat. Since the chip-formation process in grinding is extremely rapid, owing to the high grinding speed and large strains, the process should be nearly adiabatic. This means that there is no sufficient time for any significant amount of the heat generated by plastic flow to be conducted away during deformation. Any change in grinding parameters such as depth of cut, feed rate, or grinding speed, or the characteristics of the grinding wheel such as grit size, bonding, and porosity, can have a great influence on heat generation and hence the specific energy[Tawakoli et al. 2007].

Choudhury and El-Baradie (1999) noted that the grinding force is highly affected by feed rate and slightly by grinding speed. This shows that the feed rate is a dominant parameter and it plays a very important role on the grinding force and hence the specific

energy. Any plausible physical model of the grinding process should be able to quantitatively account for the magnitude of the specific grinding energy and its dependence on the operating parameters. A combination of low grinding speed with low depth of grind leads to high specific energy [Brinksmeier et. al. 2006]. This effect can be used for a controlled subsurface work-hardening. Chen et al (1996) concluded that a fine dressing condition produces a high density of cutting edges which results in a reduced chip size and hence a higher grinding power. Likewise, a coarse dressing condition will often result in a lower grinding power. Blunt grains on the wheel surface result in higher sliding friction and ploughing forces and accentuate the increase of specific energy at small depths of cut. [Malkin and Guo 2008]

In a more practical sense, the specific energy is also related to the grinding power and the force components. The grinding power, which is equal to the product of the force component tangential to the wheel surface and the wheel velocity, is especially important for calculating specific energy in grinding [Shaw 1996].

Specific energy (u) also called as specific grinding energy is defined as the amount of spindle power required to remove a unit volume of work piece material. The operating conditions that give the lowest value of specific grinding energy are desirable. Specific grinding energy *'u'* is given by;

$$u = \frac{F_t * v_s}{Q_w} \quad \text{J/mm}^3 \tag{1.5}$$

where, F_t is grinding force in N, v_s is the wheel speed in m/s, and Q_w is the material removal rate in mm^3/s.

Specific energy is an important performance parameter in grinding, because it is directly related to the temperature at the wheel-work interface. Typically, the specific energies involved in grinding are much larger than in other metal-cutting operation. Hence

in order to achieve the improved productivity specific energy should be kept as low as possible.

Surface roughness and material removal rate are the other two performance parameters in grinding. Surface roughness of a component will define the corrosion resistance, surface texture and integrity of a finished product. Machined surface roughness is an important research topic relating to the quality of manufacturing process. In recent past, tremendous advancement in precision of products is envisaged [Allison and Cole 1993]. Hence more attention was attracted towards surface roughness in every stage of design and manufacturing of a product.

Material removal rate on the other hand defines the productivity of a process. Higher the material removal rate, better the productivity. Any machining process demands better surface roughness (R_a), higher material removal rate (MRR) lower cutting forces while keeping the energy consumption to the minimum. Excessive forces acting on grinding surfaces cause defects on specimen during grinding [Inasaki 1980]. Removal depth and table feeding rate are the only controlling factors for a conventional grinding system. It is a well-known fact that high MRR and very good surface finish while keeping the energy consumption at minimum can never be achieved simultaneously in a grinding process. This is an age-long problem and continuous efforts are being made by different researchers all over the world to fulfill such an objective. A compromise is always sought between the performance parameters so that an optimal solution is obtained during the process.

Hence in this present work an attempt is made for multi objective optimisation of the performance parameters such as specific energy, material removal rate and surface roughness based on the grinding process variables during surface grinding of Al6061-SiC_{35p} composites.

1.8 MULTI OBJECTIVE OPTIMISATION

Performance characteristics of a process are often characterised by a group of responses which are measurements of one or several characteristics of quality. These responses are generally correlated and can be expressed in different measuring units. In embodiment design stage, the problem is to find the optimal levels of the parameters by combining the different responses. Several criteria were developed by different authors in order to define a global optimisation function of the responses (for example: loss function, desirability function, performance index of production).

In a general way, the optimisation criteria are based on:

- the distance to the target value (to minimise the deviations compared to the target values)
- the variance of the responses (to minimise variability or to maximise the robustness with the noise).
- sensitivity of the response to the weak variations (to maximise the robustness with the fluctuations of the parameters of control).

Development of logical methodologies to optimise the grinding parameters requires a fundamental knowledge of the prevailing grinding mechanisms and their influence on the resulting surface damage and mechanical properties. Process modeling and optimisation are two important issues in grinding [Brinskmeier et al 1998]. The grinding processes are characterised by a multiplicity of dynamically interacting process variables. Surface finish, material removal rate and specific energy are considered to be the important factors in predicting performance of grinding operation. Hence in the present work, multi objective optimisation by desirability function approach and a novel genetic algorithm approach are applied.

1.8.1 Desirability function

Desirability function is a mathematical method to find the optimum values of input parameters and performance parameters (response) concurrently by using the optimum

input parameters levels. It is an effective tool for multi objective optimisation. The desirability function approach to simultaneously optimise the multiple equations was originally proposed by Harrington (1965) and later improved by Derringer and Suich (1980). Essentially, the approach is to translate the functions to a common scale [0, 1], combine them using the geometric mean and optimise the overall metric. The method involves transformation of each predicted response, $\hat{y}_i$ to a dimensionless partial desirability function d_i, which includes the researcher's priorities and desires when building the optimisation procedure. One or two-sided functions are used, depending on whether each of the n responses has to be maximised or minimised, or has an allotted target value.

1.8.2 Genetic Algorithm

Genetic algorithms (GAs) have been extensively used to optimise complicated production systems. GAs are known for their robustness and effective overall search capabilities It is a global optimisation algorithm, and the objective function does not need to be differentiable. This allows the algorithm to be used in solving difficult problems, such as multimodal, discontinuous or noisy systems. As no single solution can be considered as the best in a multi objective optimisation problem, the single solution reported has limited use.

The GA generally preferred for large and complex cutting process parameter optimisation problems, is based on three basic operators, viz., reproduction, crossover, and mutation, in order to offer a population of solutions [Holland 1975**]**. The mechanics of GA is simple, involving copying of binary strings and the swapping of the binary strings. The simplicity of operation and computational efficiency are the two main attractions of the GA approach.

GA is very appealing for single and multi objective optimisation problems and some of its advantages are as follows [Deb 2008]:

(i) As it is not based on gradient-based information, it does not require the continuity or convexity of the design space.

(ii) It can explore large search space and its search direction or transition rule is probabilistic, not deterministic, in nature, and hence, the chance of avoiding local optimality is more.

(iii) It works with a population of solution points rather than a single solution point as in conventional techniques, and provides multiple near-optimal solutions.

(iv) It has the ability to solve convex multiple objectives and non-linear response function problems, and it may be applied to both discrete and continuous objective functions.

The algorithm creates new population from an initial random population (obtained from different feasible combination of process decision variables) by reproduction, crossover, and mutation in an iterative process. The selection, crossover and mutation on initial population create a new generation, which is evaluated with pre-defined termination criteria. The procedure continues by considering current population as initial population till the termination criteria are reached.

1.9 OBJECTIVES

The primary aim of the present work is to study the performance parameters such as material removal rate, specific energy and surface roughness during surface grinding of DRACs. The emphasis of the study is on the influence of various grinding variables on machining of DRACs using Design of experiments, since the performance parameters are greatly affected by type of workpiece and grinding variables. Besides this, the other objectives of this dissertation are

- Application of Analysis of Variance (ANOVA) for overall understanding of variables affecting the grinding process.
- Application of response surface methodology for developing a multi objective second order regression equation for performance parameters such as surface

roughness, material removal rate and specific energy during grinding of Al6061-SiC_{35p} composites by varying the volume percentage of SiC, feed and depth of cut.

- Checking the adequacy of the model by Analysis of variance.
- Optimisation of process parameters using desirability function principles.
- Application of novel genetic algorithm, a multi objective genetic algorithm approach for optimisation of the process parameters.

Therefore the scope of the dissertation encompasses study on the influence of various grinding process variables and optimisation of performance parameters during grinding of DRACs. The research work involves four phases

- Studying the influence of various grinding process variables on grinding of DRACs.
- Developing the mathematical model for the performance parameters.
- Multi objective optimisation of grinding process parameters using desirability function approach.
- Application of novel genetic algorithm for optimisation of grinding process parameters.

1.10 ORGANISATION OF THE THESIS

The report begins with introduction to the topic in Chapter 1. It is followed by Chapter 2, discussing the state-of-art of work pertaining to grinding of the DRACs. A number of 'technology voids' or 'areas for further work' were identified based on the literature review, from which subsequently, the statement of objectives and detailed action plan of this work was evolved. The details of experimental procedures conducted are discussed in Chapter 3. These include description of workpiece material, grinding tests, grinding force measurement, volume of metal removed, ground work-piece surface, Design of experiments and Response surface methodology. The effect of grinding process variables on specific energy, material removal rate and surface roughness using Taguchi's design of experiments are discussed in chapter 4. A complete realisation of the process is discussed in this chapter.

Application of response surface methodology for specific energy, MRR and surface roughness is discussed in chapter 5. In this chapter the regression models were developed for each of the performance parameters and they were further analysed and optimised by employing desirability function approach. Chapter 6 is devoted for the optimisation of the performance parameters based on novel genetic algorithm. This novel method requires less number of computations compared to the conventional non-dominated genetic algorithm (NSGA-II). In Chapter 7 the report concludes with the overall conclusions and future scope of work.

Chapter 2

LITERATURE REVIEW

The literature review on the grinding of discontinuously reinforced aluminium composites (DRACs) is categorised into two parts:

- Experimental Studies
- Analytical and Numerical Investigation

A summary of the literature review is given at the end of the chapter.

2.1 EXPERIMENTAL STUDIES

Many engineering applications involve the usage of advanced aerospace composites such as Al-SiC composites. These materials feature a high strength to weight ratio, resistance to chemical degradation, wear resistance and low density. The effective use of composites in aerospace and other applications demands the grinding of ceramic components with good surface finish and low surface damage. Although near-net-shape Al-SiC components can be produced, final finishing is still required for obtaining the desired final dimensions and surface finish. Relatively soft aluminium matrix reinforced with hard ceramic fibres poses a challenge to the researchers in obtaining the satisfactory performance characterises.

The main problem concerning the use of composites in industries is the complexity involved in machining because of the high hardness and low fracture toughness of the reinforcing materials. Machining of these composites is characterised by high specific energy, poor surface roughness, high grinding zone temperature, higher surface degradation and lower productivity.

Di Ilio et al. (1996) investigated the machining characteristics of Al2009-SiC_{15P}, Al2009-SiC_{20P} and Al2009-SiC_{25P}. The results show that the presence of the reinforcement enhances the machinability in terms of both surface roughness and particle size. Reinforced Al alloys exhibit lower tendency to clog the grinding wheel, when compared to a non-reinforced Al alloy. They observed that, surface roughness is

lower with composite having a lower particle size and surface roughness and tangential force shows decreasing trend with increasing hardness.

Ronald et al. (2009) conducted experiments with powder compacted 2124 aluminium alloy reinforced with SiC particles (5μm 30% by vol.). They considered wheel speed and depth of cut as variables. Two types of wheels viz, electroplated and Resonoid bonded were used. They observed that, the electroplated wheel experiences higher temperature with low depth of grinding, while a visible reduction in temperature can be seen with higher depth of grinding. Resin bonded wheel gave a better surface finish compared to the electroplated wheel. As a whole, resin bonded wheel performed better than electroplated wheel.

In another investigation on grinding of Al2009-SiC and Al6062-SiC with 32A46 IV grinding wheel, Di Ilio et al. (2009) developed a modelling of the grinding process based on empirical relations and observed that sliding component of the specific grinding energy is almost negligible with respect to the cutting component, which shows a decreasing exponential trend as the removal rate increases and the workpiece surface roughness can be related with the equivalent chip thickness through a power relationship; it shows a decreasing linear trend as the hardness of workpiece material increases.

Di Ilio and Paoletti (2000) conducted an experimental study on the grindability of metal matrix composites. Machining by abrasive tools different types of grinding wheels, made with both conventional abrasives and superabrasives are used. It has been found that the decrease in cutting ability of the grinding wheels is mainly caused by clogging of the active surface due to chip adhesion rather than by flattening of the grits caused by the abrasion of the hard reinforcement. Among the types of grinding wheels employed in experimental tests, the ones manufactured with conventional abrasives and open structure have given better performances than those with superabrasives in terms of low clogging, low grinding forces and better surface finish.

Zhong (2003) presented results obtained from the grinding of aluminium-based metal matrix composites reinforced with either aluminium oxide (Al_2O_3) or silicon carbide (SiC) particles using grinding wheels made of SiC in a vitrified matrix or

diamond in a resin-bonded matrix. Grinding using a 3000-grit diamond wheel at depths of cut of 1 μm and 0.5 μm produced ductile streaks on the Al_2O_3 particles and the SiC particles, respectively. There was almost no subsurface damage except for rare cracked particles when fine grinding with the diamond wheel.

Zhong and Hung (2002) in another investigation concluded that rough grinding with SiC wheel followed by fine grinding with a fine grit diamond wheel will produce no ductile streak on the alumina/aluminium composites.

Agarwal and Rao (2005) investigated the grinding characteristics, surface integrity and material removal mechanisms of SiC ground with diamond wheel on surface grinding machine. The surface and subsurface characteristics of the ground silicon carbide showed that the material removal associated with this material was primarily due to the dislodgement of individual grains, resulting from microcracks along the grain boundaries. They concluded that the grinding force and specific grinding energy could be, therefore, considerably reduced.

Agarwal and Rao **(**2008) in another work developed a new analytical surface roughness model on the basis of the stochastic nature of the grinding process, governed mainly by the random geometry and the random distribution of cutting edges. This model has been validated by the experimental results of silicon carbide grinding.

Abdullah et al. (2007) studied wheel wear and workpiece surface roughness in creep-feed grinding of tungsten carbide with 20% cobalt binder using a resin-bonded nickel-coated diamond wheel. Experiments have shown that the wheel wear increased and surface roughness decreased with increased feed rate, on the other hand, wheel wear and surface roughness decreased with increased wheel speed.

Veeresh Kumar et al. (2010) aimed to present the experimental results of the studies conducted regarding hardness, tensile strength and wear resistance properties of Al6061-SiC and Al7075-Al_2O_3 composites. The composites are prepared using the liquid metallurgy technique, in which 2-6 wt. % of particulates were dispersed in the base matrix. The increased percentage of these reinforcements contributed to increased

hardness and density of the composites. The dispersed SiC in Al6061 alloy and Al_2O_3 in Al7075 alloy contributed to enhancing the tensile strength of the composites.

Monici et al. (2006) have investigated the effect of type and amount of cutting fluid on tangential cutting force, specific grinding energy, acoustic emission, diametrical wear, roughness, and residual stress. To analyse the influence of these variables, an optimised fluid application methodology was developed to reduce the amount of fluid used in the grinding process and improve its performance in comparison with the conventional fluid application. The results revealed that, in every situation, the optimised application of cutting fluid significantly improved the efficiency of the process, particularly the combined use of neat oil and CBN grinding wheel.

Ling Yin et al. (2005) conducted experiments with high removal rate (up to 16.6 mm^3/s per mm) grinding of alumina and alumina–titania with respect to material removal and basic grinding parameters using a resin-bonded 160 mm grit diamond wheel at the speeds of 40 and 160 m/s, respectively. There were no distinct differences in surface roughness and morphology for both materials ground at either conventional or high speed. An increase in specific removal rate caused more rapid increases in normal and tangential forces obtained at the conventional grinding speed than those at higher speed.

The research from Brinksmeier and Giwerzew (2003) deals with the quantification of the size effect in grinding. Main physical quantity characterising the size effect is specific grinding energy. Since higher specific grinding energy values were found to increase the absolute values of compressive residual stresses and their penetration depth, low cutting speeds and low depth of cut are considered to be promising for advanced investigations aimed at further development of this new technology.

Reddy and Rao (2006) investigated the role of solid lubricant assisted machining with graphite and molybdenum disulphide lubricants on surface quality, cutting forces and specific energy while machining AISI 1045 steel using cutting tools of different tool geometry. The performance of solid lubricant assisted machining has

been studied in comparison with that of wet machining. The results indicate that there is a considerable improvement in the process performance with solid lubricant assisted machining as compared to that of machining with cutting fluids. The use of solid lubricants has been successful in reducing cutting forces, specific energy, surface finish, and chip size. Experimental findings reveal that the friction generated between tool and workpiece has been significantly reduced in molybdenum disulphide assisted machining as compared with graphite and wet assisted machining.

Ramesh et al. (2001), conducted high speed grinding experiments on Al_2O_3, SiC and ZrO_2 materials using diamond grinding wheel. Authors conclude that grinding force decreased and surface finish is improved with increase in wheel speed. They also found that specific energy decreased with increase in specific material removal rate.

Wilk and Barbara (2008) carried out cut-off tests of aluminium composites reinforced with Al_2O_3 and Si_3N_4 particulates. The result indicates that, wear of resin bonded diamond wheels was large, with a good finish on the cut-off surfaces. In contrast, in the case of metal bonds, the wheel wear was insignificant, but there was a tendency to gumming up of the grinding wheel active surface.

Malkin and Ritter (1989) in their research presented grinding mechanisms for ceramic materials and their influence on the finished surface and mechanical properties. The machining approach has typically involved measurement of the grinding forces and specific energy coupled with microscopic observations of the surface morphology and grinding detritus. This study gives an insight in to grinding behaviour and strength degradation while grinding ceramics.

Bifano and Fawcett (1991) considered specific grinding energy as an in-process measurement to monitor the ductile grinding of ceramics. The specific energy was shown to remain relatively constant for ductile regime grinding but decreased according to a power law relationship with increasing material removal rate for brittle regime grinding.

Chiu and Malkin (1993) simulated cylindrical plunge grinding operations. The simulation does not predict the exact performance of the grinding process but instead captures the main effects during the grinding cycle. The grinding model consists of analytical and empirical mathematical models and predicts the grinding forces and power, actual material removal, thermal damage, thermal expansion, wheel wear, workpiece roughness and roundness.

Comley et al. (2006) demonstrated the application of high efficiency deep grinding to cylindrical plunge grinding cycle for an automotive steel and cast iron. Author used thermal modelling to optimise the grinding process. Both thermal modelling and experimental measurements have established that low workpiece temperatures are possible even when specific material removal rates of 2000 mm^3/mm-s are achieved. Surface integrity studies based on microstructural analysis and Barkhausen noise have also demonstrated the effectiveness of the process

Shih et al. (2003) presented the results of grinding zirconia using wheels with fine grain size SiC and dense vitreous bond. Wheel wear results demonstrated that this type of SiC wheel could grind fully and partially stabilised zirconia (PSZ) very effectively. X-ray diffraction showed no monoclinic phase in the PSZ debris. This suggests that, during grinding, the low thermal conductivity of zirconia and SiC, compared to that of diamond, facilitates heat retention in the chip and softens the work-material. This makes the efficient grinding of PSZ possible.

El-Gallab and Sklad (1998) explain the surface integrity of machined Al-20%SiC particulate metal-matrix composites (PMMC). Dry high speed turning tests, at different cutting speeds, feed rates and depths of cut were conducted. The cutting tests were carried out using PCD. Surface roughness measurements show that the surface roughness improves with an increase in the feed rate and the cutting speed, but slightly deteriorates with an increase in the depth of cut. It is also found that machining this type of composites is most economical and safe at a speed of 894 m/min, a depth of cut of 1.5 mm and feed rates as high as 0.45 mm/rev, when the surface roughness, did not exceed 2.5 μm.

Kannan Kishawy (2006) investigated the effect of cutting parameters and particulate properties on the microhardness variations. It is found that lower the reinforcement volume fraction and the coarser the particulates, the higher are the variations in matrix microhardness. The microhardness measurements on the aluminium matrix beneath the machined layer showed higher values when machining under wet conditions with reduced depth of plastically deformed zone.

2.2 ANALYTICAL AND NUMERICAL INVESTIGATION

Analysis of an experimental work is an important aspect of study among the researchers. The experimental work supported by modelling and analysis can help an experimenter to visualise the process more closely and to conclude the outcome of his experimental work. There are several stochastic and deterministic techniques for analysing a machining process.

The experimenter is always interested in finding the solution for optimisation of the process which gives the maximum yield at minimum cost. In grinding process the experimenter will try to develop a model of the grinding process and to optimise the performance parameters such as surface roughness, material removal rate, specific energy, temperature, grit ratio etc. Manufacturing industries are interested in simultaneous optimisation of several parameters and to establish the control on the process.

The research work from Krajnik (2006) describes a systematic methodology for empirical modelling and optimisation of the plunge centreless grinding process. The central composite response surface design has been employed to develop a second-order surface roughness model. The final goal of experimental study focuses on determination of optimum centreless grinding system set-up and operating conditions for minimisation of surface roughness. The analysis of variance proved that the grinding wheel dressing condition most significantly affects the ground surface roughness. It is also observed that surface roughness is affected by the geometrical grinding gap set-up factor and the control wheel speed. The computer-aided single-objective optimisation, solved by non-linear programming and genetic algorithm, is

applied. The results of two different optimisation approaches for determination of optimal operating conditions are compared.

Kwak and Kim (2008) developed a second order response surface model for surface roughness and grinding force. The author used AC8A Aluminium alloy with SiC and Mg powder as reinforcing material. The grain size of the grinding wheel, specimen table speed and depth of cut were taken as parameter to study the surface roughness on the specimen. The second-order response surface models were developed and the usefulness of the developed models was verified. It is observed that the decreased value of table feed and depth of cut will result in better surface roughness. They also concluded that the optimum content of SiC and Mg in AC8A aluminium alloy is30wt % and 9wt% respectively.

Kwak J.S. (2005) made an attempt to apply Taguchi and response surface methodologies for the geometric error. The effect of grinding parameters on the geometric error was evaluated and optimum grinding conditions for minimising the geometric error were determined. A second-order response model for the geometric error was developed and the utilisation of the response surface model was evaluated with the constraints of the surface roughness and the material removal rate. It is observed that the depth of cut was a dominant parameter for geometric error followed by the grain size.

Hung et al. (1997) studied the grindability of metal matrix composites reinforced with SiC particles. A two-level factorial experiment was set up to investigate the effects of reinforcement volume, grinding parameters, and grinding wheel materials. While increasing the force and specific energy in grinding, the SiC particles are fractured along cleavage planes rather than being machined by grinding grains. Smearing of aluminum matrix masks the effect of grinding parameters on surface finish measurement. Increasing material removal rate causes an increase in grinding forces but a decrease in of specific energy. Diamond wheels are recommended for both rough- and fine-grinding of the tested composites.

Shetty R. et al. (2009) presented the study on Taguchi’s optimisation methodology, which is applied to optimise cutting parameters in turning of age

hardened Al6061-15% vol. SiC 25 μm particle size metal matrix composites with Cubic boron nitride inserts (CBN) KB-90 grade using steam as cutting fluid. The turning parameters evaluated are speed, feed, depth of cut, nozzle diameter and steam pressure. A series of experiments are conducted to relate the cutting parameters on surface roughness, tool wear, cutting force, feed force, and thrust force. From the analysis using Taguchi's method, results indicate that among the all-significant parameters, steam pressure is the most significant parameter.

Shetty R. et al. (2008) in another work discussed the use of Taguchi's design of experiments and response surface methodology (RSM) for minimising the surface roughness in turning of discontinuously reinforced aluminium composites (DRACs) having aluminum alloy 6061 as the matrix and containing 15 vol. % of silicon carbide particles with a mean diameter of 25μm under dry cutting condition. The effect of cutting parameters on surface roughness is evaluated and the optimum cutting condition for minimising the surface roughness is determined. A second-order model is established between the cutting parameters and the surface roughness using RSM. The experimental results reveal that the most significant machining parameter for surface roughness is feed, followed by cutting speed.

Wattanutchariya and Pintasee (2006) applied RSM for optimisation of milling parameters for surface finishing. The two controlled parameters were spindle speed and feed rate. Three materials: aluminum, brass and cast iron were tested. It was found that at the significant level of 95% the suitable production factors (spindle speed and feed rate) for CNC milling of Aluminum with optimal 0.25 μm surface roughness were 1,400 rpm and 50 mm/min, whereas the 1.31 μm of brass were 1,000 rpm and 100 mm/min; and the conditions for cast iron with 2.57 μm were 800 rpm and 20 mm/min, respectively.

Ginta et al. (2009) developed an approach to establish models for tool life in end milling of titanium alloy Ti–6Al– 4V using uncoated carbide inserts under dry conditions. Central composite design (CCD) was employed in developing the tool life model in relation to primary cutting parameters such as cutting speed, axial depth of cut and feed. Flank wear has been considered as the criteria for tool failure and the

wear was measured. The first-order and the second-order model were established and contour plots were developed. The adequacy of the predictive model was verified using analysis of variance (ANOVA) at 95% confidence level.

Brinksmeier (2006) in his study explains about model developed by Lippock wherein the author compared his regression analysis based model, for grinding forces and surface roughness in cylindrical precision grinding, with vitrified bonded CBN grinding wheels with his model based on neural networks. Author detected only little differences concerning the simulation quality regarding surface roughness. In contrast the regression analysis based model performed significantly better regarding the simulation of grinding forces

Choudhury and Baradieb (1999) describe machinability assessment of nickel base super alloy (inconel 718) in turning operations using coated and uncoated carbide inserts under dry conditions. Response models (tool life, surface roughness, and cutting force) were developed utilising the factorial design of experiment and RSM. The adequacy of the different response models has been judged by analysing the variance. From the plot of dual response (surface roughness and material removal rate) contours, one can choose cutting parameters for higher material removal rates without sacrificing surface finish. Dual response contours of tool life and surface roughness have also been presented. For a given surface finish, these contours help to predict the cutting conditions for maximum tool life.

In another finding Brinksmeir et al. (1998) built up two different regression models for the computation of the specific normal and tangential force in external and internal plunge grinding of 100Cr6 with vitrified bonded CBN wheels. Both contain cutting speed as the input variable. One is additionally calculated by transversal feed rate and radial feed, the other by speed ratio and material removal rate. The correlation coefficient is best for a full factorial design of experiment and decreases if it is partially factorial. Afterwards he compares his regression models for specific normal and tangential forces to other methods finding that they can compete with results from artificial neural networks and are superior to models based on fuzzy logic. Modeling

of roughness and residual stresses resulted in insufficient correlation coefficients for all model types, whereby regression models show the least.

Sivasakthivel et al. (2010) developed a mathematical model for machining Al6063 alloy to predict the tool wear in terms of machining parameters such as helix angle of cutting tool, spindle speed, feed rate, axial and radial depth of cut. Central composite rotatable second order RSM was employed to create a mathematical model and the adequacy of the model was verified using analysis of variance.

Slowik and Slowik (2008) used an evolutionary algorithm for multi-objective optimisation of a surface grinding process in order to minimise production cost and surface roughness or to minimise production cost and maximise production rate. Factors such as wheel speed, workpiece speed, depth of dressing and lead of dressing were the variables considered.

Venu Gopal et al. (2003) carried out experiments to study the effect of wheel parameters; grain size, grain density and grinding parameters; depth of cut and feed on the surface roughness and surface damage. The significance of the grinding parameters on the selected responses was evaluated using analysis of variance. Mathematical models were developed using the experimental data considering only the significant parameters. A genetic algorithm (GA) code has been developed to optimise the grinding conditions for maximum material removal, using a multi-objective function model, by imposing surface roughness and surface damage constraints. The choice of including manufacturer's constraints on the basis of functional requirements of the component for maximising the production rate was also embedded in the GA code.

Saravanan and Sachidanandam (2001) developed a GA based optimisation procedure to optimise grinding conditions, viz. wheel speed, workpiece speed, depth of dressing and lead of dressing, using multi-objective function model with a weighted approach for surface grinding process. The procedure evaluates the production cost and production rate for the optimum grinding condition, subjected to constraints such as thermal damage, wheel wear parameters, machine tool stiffness and surface finish.

Saravanan et al. (2002) in another investigation developed a GA based optimisation procedure to optimise the surface grinding process using a multi-objective function model. Ten process variables are considered in this work. The procedure evaluates the production cost and production rate for the optimum grinding conditions, subject to constraints such as thermal damage, wheel-wear parameters, machine-tool stiffness and surface finish. A worked example is used to illustrate how this procedure can be used to produce an optimum production rate, low production cost, and fine surface quality of the surface grinding process.

Suresh et al. (2002) presented their work which deals with the study and development of a surface roughness prediction model for machining mild steel, using RSM. The experiment was carried out with TiN-coated tungsten carbide (CNMG) cutting tools, for machining mild steel work-pieces covering a wide range of machining conditions. A second order mathematical model, in terms of machining parameters, was developed for surface roughness prediction using RSM. This model gives the factor effects of the individual process parameters. The two-stage effort of obtaining a surface roughness model by surface response methodology, and optimisation of this model by GAs, has resulted in a fairly useful method of obtaining process parameters in order to attain the required surface quality.

Palanikumar (2008) discussed the use of Taguchi and response surface methodologies for minimising the surface roughness in machining glass fiber reinforced (GFRP) plastics with a polycrystalline diamond (PCD) tool. The experiments have been conducted using Taguchi's experimental design technique. The cutting parameters used are cutting speed, feed and depth of cut. A second-order model has been established between the cutting parameters and surface roughness using RSM. The experimental results reveal that the most significant machining parameter for surface roughness is feed followed by cutting speed.

Sidda Reddy et al. (2009) performed studies to deal with the development of surface roughness prediction model for machining of aluminum alloys, using adaptive neuro-fuzzy inference system (ANFIS). The ANFIS model has been developed in terms of machining parameters for the prediction of surface roughness using trained

data. The Experimental validation runs were conducted for validating the model. The RSM is also applied to model the same data. The ANFIS results are compared with the RSM results. Comparison results showed that the ANFIS results are superior to the RSM results

Jeyapaul et al. (2006) in their approach take advantage of both the Taguchi method and GA, which forms a robust and practical methodology in tackling multiple response optimisation problems. The work also presents a case study to illustrate the potential of this powerful integrated approach for tackling multiple response optimisation problems. The variance analysis is also an integral part of the study, which identifies the most critical and statistically significant parameters. The model is validated with gear hobbing process with multiple response characteristics. It has been demonstrated that a multiple response optimisation problem can be effectively tackled by using GA to generate a single weighed S/N ratio as a performance indicator.

The aim of the study by Kwak et al. (2006) was to analyse effectively the grinding power spent during the process and the surface roughness of the ground workpiece in the external cylindrical grinding of hardened SCM440 steel using the response surface method. The surface roughness was also measured and evaluated according to the change of the grinding conditions. Response surface models were developed to predict the grinding power and the surface roughness using the experimental results. Based on experimental results, increasing the depth of cut affected the grinding power more than increasing the traverse speed. In addition, increasing the depth of cut changed the maximum height of the surface roughness more than the centerline average height.

Johnson et al. (2008) in their work developed a grinding force model to predict the forces during the face grinding of cast iron and aluminum alloy 319. Design of experiments method is used to create a response surface of four process parameters: feed rate, inclination angle of the grinding wheel profile, offset angle between the grinding wheel and the workpiece, and the peripheral speed of the wheel. For each material, three polynomial equations are determined by regression analysis to represent the forces in three directions. The model shows better accuracy for cast iron

than aluminium alloy. The feed rate and inclination angle have the most significant effect on the grinding forces.

Tawakoli et al. (2007) presents some of the very good results of the systematic research works that were done to reduce heat generation by special conditioning using a single-point diamond dressing tool. A new idea is based on the T-Tool and T-Tool profile concept is introduced. Based on this concept, the reduction of cutting edges by definite conditioning of the grinding wheel produces a specific structure on the wheel surface, giving more chance to each cutting edge to do real cutting action. This paper focused on the heat generation and chip formation and showed that with special conditioning, it is possible to reduce the static cutting edges as a source of rubbing and to optimise chip formation, which both have a significant influence on heat generation and on workpiece surface integrity. A reduced contact layer can lower cutting forces, heat generation, and temperature in the contact zone.

Lee et al. (2007) in their work, carried out optimisation based on the available model to obtain optimum parameters for silicon carbide grinding via particle swarm optimisation (PSO) based on the objective of maximising MRR with reference to surface finish and damage. The effect of parameters such as feed rate, depth of cut and grit size has been studied in silicon carbide grinding. In this work, optimal machining conditions were obtained for the maximisation of the MRR subject to some constraints. Based on statistical analysis of various constraint values of surface roughness and number of flaws, simulation results obtained in this machining process for PSO are comparatively better to GA approach.

Hooda et al. (2007) in their work utilised 2 separate L9 Taguchi fractional factorial arrays to study the creep-feed grinding process of gamma titanium alloy (γ-TiAl) and burn resistant titanium alloy (BuRTi). It is concluded that γ -TiAl alloy was easier to grind than the BuRTi alloy with an average, a 10 times higher G-ratio, 10% lower maximum power, 25% lower maximum specific energy, 28% lower tangential force and 15% lower average workpiece surface roughness for the same operating parameter levels. The results point to the use of diamond superabrasive wheels with

improved grit thermal conductivity in order to minimise workpiece surface burn and cracking while possibly reducing wheel wear.

Hwang and Malkin (1999) in their work made an attempt to account for the specific grinding energy and its dependence on the grit depth of cut by modifying a previous upper-bound plowing model to include the effect of rounding at the tip of the triangle-shaped cutting tool. Using this approach, the shape of the cross-sectional cutting profile is calculated which matches the upper bound solution to experimental measurements of the specific grinding energy.

In another investigation Hwang et al. (1999) reported about the ‘size effect’ for specific energy in grinding of silicon nitride. Experimental measurements over a wide range of operating parameters using two different grit size diamond wheels show an increase in specific energy as the grit depth of cut (uncut chip thickness) is reduced. A plot of dimensionless specific grinding energy (specific energy divided by workpiece hardness) vs. dimensionless depth of cut (depth of cut divided by tip radius) yields a single inverse linear relationship whereby the dimensionless specific grinding energy increases steeply as the dimensionless grit depth of cut decreases below about 0.5. This would indicate that the ‘grit size effect’ is mainly due to rounding at the abrasive cutting points

Xu and Shin (2007) implemented a multi-level fuzzy control (MLFC) technique for a creep-feed grinding process. The grinding force is maintained at the maximum allowable level under varying depth of cut, so that the highest material removal rate is achieved. The control rules are generated heuristically without any analytical model of the grinding process. Experimental results show that the cycle time has been reduced by up to 25% over those without force control and by 10–20% compared with the conventional fuzzy logic controller, which indicates its effectiveness in improving the productivity of actual manufacturing processes. The effect of grinding wheel wear is also considered in the creep-feed grinding process.

Gopala Krishna and Rao (2006) proposed scatter search based optimisation approach to optimise the grinding parameters of wheel speed, work piece speed, depth of dressing and lead of dressing using a multi-objective function model with a

weighted approach for the surface grinding process. The production cost and production rate are evaluated for the optimal grinding conditions, subject to the constraints such as thermal damage, machine tool stiffness, wheel wear parameters and surface finish. The results are compared with the results obtained by the ants-colony algorithm, GA and quadratic programming techniques.

Ting et al. (2005) optimised the surface grinding process using particle swam optimisation. The optimisation based on the available model has been carried out to obtain optimum parameters for silicon carbide grinding via Particle Swarm Optimisation (PSO) based on the objective of maximising MRR with reference to surface finish and damage. Authors concluded that the results obtained by PSO are superior in comparison with Genetic Algorithm (GA) approach.

Krajnik et al. (2006) investigated the efficiency of ANN and the related metamodels (Radial basis function ANN) to simulate the centreless grinding process. They found that the quality of multimodal highly depends on prediction accuracy and concluded that ability of the multimodal is comparable to the accuracy of the response surface regression model.

Zhou and Xi (2002) developed a numerical solution for surface roughness based on the random distribution of grain protrusion height of the abrasives

Kilickap et al. (2010) focused their study on the influence of machining parameters on the surface roughness obtained in drilling of AISI 1045. The matrices of test conditions consisted of cutting speed, feed rate, and cutting environment. A mathematical predictive model of the surface roughness was developed using RSM. The effects of drilling parameters on the surface roughness were evaluated and optimum machining conditions for minimising the surface roughness were determined using RSM and GA.

Zhang et al. (2005) developed and evaluated response surface models based both on feed-forward, back-propagation neural networks as well as linear regression models for predicting the fatigue life of solder joints in area array packages. There are two physical models which are executed in sequence as part of the analysis procedure.

The first is a droplet shape prediction code developed as part of this project, which predicts the shape of the solder joint given the input pad sizes, package weight and mask definition, and the second is a commercial nonlinear finite element analysis code, which determines the inelastic dissipation for a given shape. The predicted inelastic dissipation is then used to determine the fatigue life of the joints. The response surface models developed in this study are shown to perform very well in capturing the non-linear relationship between the inputs and output. Also, using the same training data, the linear regression models are shown to be marginally better in accuracy than the neural network models.

Correia et al. (2005) compares RSM and GA techniques in the optimisation of a Gas Metal Arc Welding (GMAW) process application. The situation was to choose the best values of three control variables (reference voltage, wire feed rate and welding speed) based on four quality responses (deposition efficiency, bead width, depth of penetration and reinforcement). For the RSM, an experimental design was chosen and tests were performed in order to generate the proper models. In the GA case, the search for the optimal was carried out step by step, with the GA predicting the next experiment based on the previous, and without the knowledge of the modeling equations between the inputs and outputs of the GMAW process. Results indicate that both methods are capable of locating optimum conditions, with a relatively small number of experiments

Anjum et al. (1997) adopted the procedure of implementing RSM via neural networks. Two neural networks are trained: one for the unknown function and the other for derivatives of this function which are computed using the first neural network. These neural networks are then used iteratively to compute parameters for an equation which is ultimately used for optimising the function. The model is demonstrated with an example.

Davidson et al. (2008) applied design of experiments to study the effects of the main flow-forming parameters such as the speed of the mandrel, the longitudinal feed, and the amount of coolant used on the surface roughness of flow-formed AA6061 tube. A mathematical prediction model of the surface roughness has been developed in

terms of the above parameters. The effect of these parameters on the surface roughness has been investigated using RSM. The developed prediction equation shows that the longitudinal feed rate is the most important factor that influences the surface roughness. The surface roughness was found to increase with an increase in the longitudinal feed and it decreased with decrease in the amount of the coolant used. The verification experiment carried out to check the validity of the developed model predicted surface roughness within 6% error.

Castillo et al. (1996) demonstrated a modified version of the Derringer and Suich's desirability functions for the linear case based on polynomial approximations of the individual desirability functions at their nondifferentiable points. Then, the optimisation problem of the overall desirability function obtained from the geometric mean of the smoothed functions is solved by a generalised reduced gradient method.

Ch'ng et al. (2008) proposed a new formula to compute the overall desirability function other than the geometric mean together with a change of variables in the individual desirabilities in such a way that no nondifferentiable points occur in the functions. There are many other studies with desirability functions focusing on other drawbacks than nondifferentiability such as those in the studies of Khuri and Conlon (1980), Kim and Lin (2000) and Jeong and Kim (2008).

Bas et al. (2010) applied desirability functions in RSM and neural network approaches to study multiple response optimisation using desirability functions and artificial neural networks. The results of this study indicate that in RSM there is the potential of over-fitting the responses. Although similar arguments are also true for artificial neural networks, it can be seen that they may be a useful alternative method for multiple response optimisation

Mukherjee and Ray (2008) presented the study on application of empirical modelling technique based on direct observations, for prediction of two-stage grinding process (rough honing and finish honing) behaviour. The study proposes an integrated approach using multivariate regression, desirability function, and metaheuristic search technique. Three different metaheuristic search techniques, viz. real-coded GA, simulated annealing, and a modified Tabu search based on novel Mahalanobis

multivariate distance approach, are employed to determine near optimal path conditions for an industrial case study of two-stage CNC grinding (honing) optimisation problem. Computational study results based on different metaheuristics, and applied to the same two-stage optimisation problem, show that the modified Tabu search performs better.

Seeman et al. (2010) in their study, made an attempt to model the machinability evaluation through the RSM in the machining of homogenised 20% SiCp LM25 Al MMC manufactured through stir cast route. The combined effects of four machining parameters including cutting speed (s), feed rate (f), depth of cut (d), and machining time (t) on the basis of two performance characteristics of flank wear and surface roughness were investigated. The process parameters are optimised using desirability-based approach RSM. Cutting speed and feed rate of the regression models are found to be more significant when compared to other parameters. The proposed models for flank wear and surface roughness are found to be adequate and can be used to predict the characteristics within the experimental range.

Kodali et al. (2008) presented a truly multi-objective optimisation of the grinding process by considering both the objectives involved simultaneously. The problem involves two conflicting objectives subjected to four constraints and ten process variables. The elitist non-dominated sorting genetic algorithm (NSGA II) is used to solve this multi-objective optimisation problem. The Pareto-optimal front obtained is compared with earlier reported results, obtained using various non traditional optimisation approaches. It is observed that all solutions in the Pareto-optimal fronts obtained by NSGA II dominate those reported earlier. Also the Pareto-optimal fronts obtained provide a wide range of trade-off operating conditions from which an appropriate operating point can be selected by the decision maker. On investigation it is observed that the Pareto-optimal solutions are affected by only four of the total ten process variables considered in the optimisation study.

Xi-Ping et al. (2009) applied desirability function to achieve uniform temperature distribution on the cavity surface of the stationary mould insert. The design variables were optimised by using GA. The distances between the neighbour

heating channels were considered as the main design variables. An objective function for optimising the temperature distribution uniformity was proposed. The experiment samples for calculating the objective function were selected by using the Latin Hypercube Design experiment method. A quadric response surface equation for calculating temperature distribution uniformity was established.

Jones et al. (2004) in their work describe the application of two multiobjective optimisation techniques for high efficiency deep grinding process. The process is modelled using a fuzzy expert system. The objective is to simultaneously minimise the surface temperature and specific grinding energy. A problem constraint is represented within the fuzzy model. It forms an objective representing the degree of infeasibility of the solution. Strength Pareto Evolutionary Algorithm (SPEA) and NSGA-II are used for optimisation. NSGA-II produces a near-optimum Pareto front with good diversification in all cases. SPEA's results are generally inferior but still competitive. The codes for SPEA and NSGA-II were developed using MATLAB.

2.3 SUMMARY

From the above literature review it is evident that considerable work in the area of performance evaluation of grinding process has been done by various researchers. But studies on the grinding of Metal matrix composites have been carried out by only a few authors [Di Ilio et al. 1996, Di Ilio and Palloti 2000, Di Ilio et al. 2009, Anand Ronald 2009, Zhong 2003, and Kwak and Kim 2008] as reported. It may be due to the complex nature of the process [Malkin and Ritter 1989] and random orientation of the particulates inside the metal matrix [Hung et al. 1997]

Specific energy is the function of material removal rate and grinding force when the wheel speed is constant. It is noted by many of the authors [Di Ilio et al. 2009, Hwang et al. 1999 and Hwang and Malkin 1999] that, specific energy increases with decrease depth of grind. Hwang et al. (1999) made an attempt to develop a model for specific energy based on uncut chip thickness. But specific energy is also affected by many of the factors such as feed, the type of material to be ground etc. But, not much focus has been given to those factors so far.

The effect of grinding process parameters on performance parameters such as material removal rate, surface roughness is addressed by many of the authors [Agarwal and Rao2005, Agarwal and Rao2008, Ling Yin et al. 2005, Comley et al. 2006, Kwak 2005, Kwak and Kim 2008]. Increase in material removal rate will decrease specific energy. The multi optimisation model for material removal rate, surface roughness, surface integrity are developed for various machining process, either by RSM, ANN, or GA[Saravanan et al. 2002, Savaranan and Sachidanandam 2005, Kodali et al. 2008, VenuGopal et al. 2003]. As per the knowledge of the author, hardly any significant work is done for the simultaneous optimisation of specific energy, material removal rate and surface roughness.

Several researchers have used RSM and GA [Correia et al. 2005, Suresh et al. 2002], RSM and ANN [Bas et al. 2010] Taguchi and RSM [Davidson et al. 2008] for optimisation of the different manufacturing process including grinding and compared the results thus obtained. Many of their works reveal that GA is a better optimisation technique. But there is no evidence of using NSGA-II and RSM as the optimisation technique for surface grinding of Al6061-SiC composites.

NSGA-II is a novel method for multi-objective optimisation which is gaining a lot of importance among the researchers. Jones et al. 2004 developed codes for GA using MATLAB. Kodali et al. 2008 used two objectives (workpiece removal parameter, Total production cost) for optimisation of grinding process. Authors have used empirical relations in their work.

In the current study an attempt is made to apply RSM and a novel genetic algorithm, an improved version of elitist NSGA-II for the multi objective optimisation of three performance parameters namely, surface roughness, material removal rate and specific energy during the surface grinding of Al6061-SiC composites.

Chapter 3

EXPERIMENTAL METHODOLOGY

3.1 INTRODUCTION

Though near-net shaped products can be prepared from MMCs, they often need to be formed into the desired shapes and finished to the required dimensions and tolerances. Metal matrix composites are given their required shape by brazing, bonding, powder metallurgy techniques, casting, metal spraying and forming operations such as bending, swaging, drawing and extrusion. Although advances have been made in near-net shape technology, finishing operations are often required to obtain dimensional tolerance as well as good surface finish. Machining of these new materials requires tool materials of very high wear resistance because the reinforcement is extremely abrasive [Lin et al. 1995]. Among traditional machining processes, grinding is important for MMCs, since it could be applied also in heavy-duty machining, in addition to obtaining desired dimensional tolerances and surface quality.

Up to the present, a lot of work has been carried out to understand the mechanisms of grinding conventional materials by analysing the process as an interactive system between the surface of the wheel and the workpiece **[**Tonshoff et al. 1992, Binachi et al. 2002**].** On the contrary, there are only a few investigations on the grindability of metal matrix composites, most of them concerning the role of reinforcement and the influence of grinding wheel abrasive in the process have been discussed [Zhong and Hung 2002, Ronald et al. 2009].

This chapter deals with experimental study required for finding the effect of process variables such as volume percentage of SiC in Al6061-SiC composites, feed and depth of grind on performance parameters such as specific energy, material removal rate and surface roughness during grinding of Al-SiC composites.

First part of this chapter describes the preparation of the workpiece material. Second part is devoted to the procedure followed for grinding of workpiece material.

Measurement and calculation of performance parameters is discussed in third section. Fourth section explains the Taguchi method adopted in this study.

3.2 WORKPIECE MATERIAL

Aluminium is the most dominant matrix for MMC for both structural and electrical applications. This is because of the low cost of aluminium and its low melting point (660^0C). Al-SiC specimens having aluminum alloy 6061 as the matrix and containing 8 vol. %, 10 vol. % and 12 vol. % of silicon carbide particles of mean size 35μm were manufactured at Vikram Sarbhai Space Centre (VSSC) Trivandrum by Stir casting process. Figure 3.1 shows the schematic of rheocasting or stir casting set up for the composite processing.

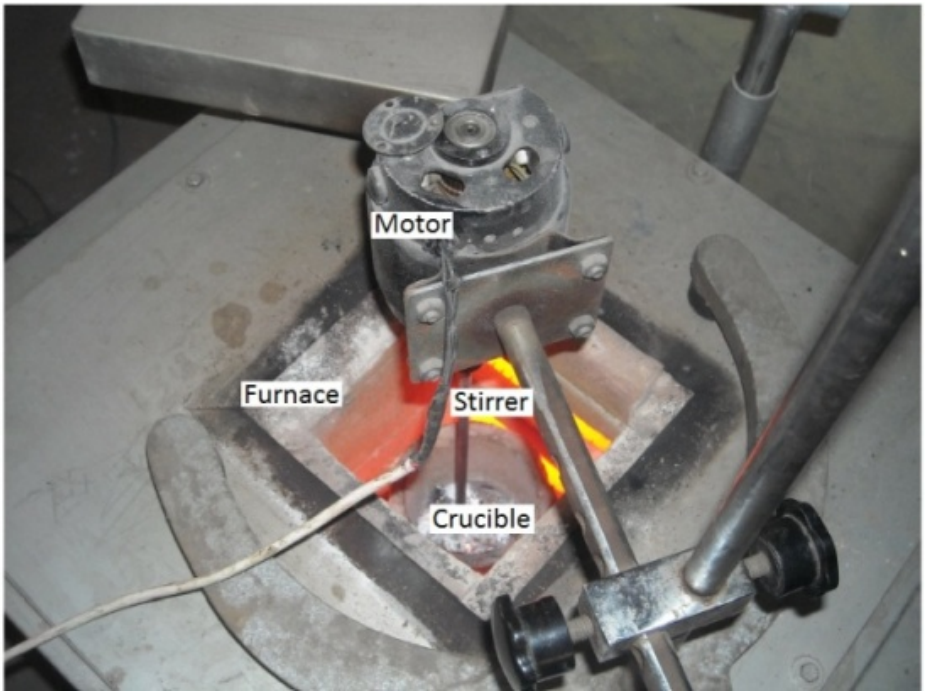

Figure 3.1 stir casting set-up

In general, stir casting of MMC involves producing a melt of selected matrix material followed by the introduction of reinforcement material into the melt and the dispersion of the reinforcing material through stirring. Stirring is carried out vigorously to form a vortex where the reinforcing particles are introduced through the

side of the vortex. The formation of the vortex will drag all the reinforcement particles into the melt, thus enhancing the proper mixture of matrix and the reinforcement.

About 2 kilograms of the Al 6061 alloy was cleaned and loaded in the silicon carbide crucible (inner dimension 200mm dia x 300 mm height with conical bottom of 50mm dia) and heated above its liquidus temperature (700-710°C) in an electrical furnace (600 x 600 x 600 mm). The heating elements of the furnace generated a temperature of 1000^0C while consuming 6kW of power. The temperature was recorded using chromel-alumel thermocouple. The specially designed mechanical graphite stirrer was introduced into the melt and stirred at 195 rpm to produce vortex motion. The depth to which the impeller was immersed is $1/3^{rd}$ of the height of the molten melt from the bottom of the crucible [Aniban et al. 2002].

The preheated (300^0C) SiC particulates of average size 35μm were added through a preheated pipe by manually tapping into the slurry, while it being stirred. Stirring produces an uniform suspension of solid particles in the melt due to the centrifugal acceleration. After addition of SiC particles the mixture was degassed by purging hexachloro ethane tablets.

A post-addition stirring time of 15 min was allowed to enhance the maximum dissolution (wetting) of particulates by the metal. Now the crucible containing the melt and SiC particles was taken out and kept on a hot refractory brick. The melt was hand stirred with graphite rod and then tapped into permanent steel mould through bottom pouring. The temperature of the slurry was raised sufficiently above the melting range of the matrix alloy before pouring.

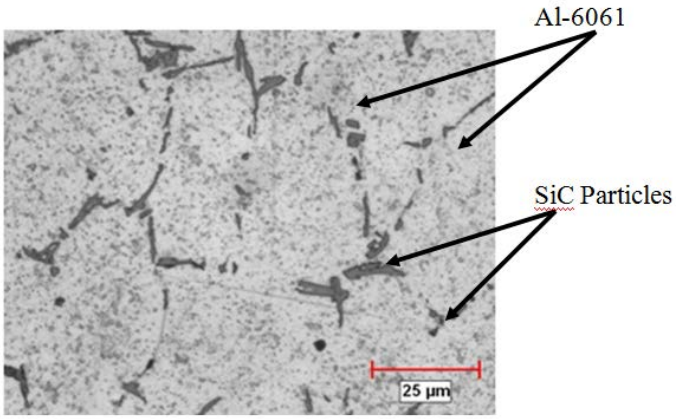

(a)

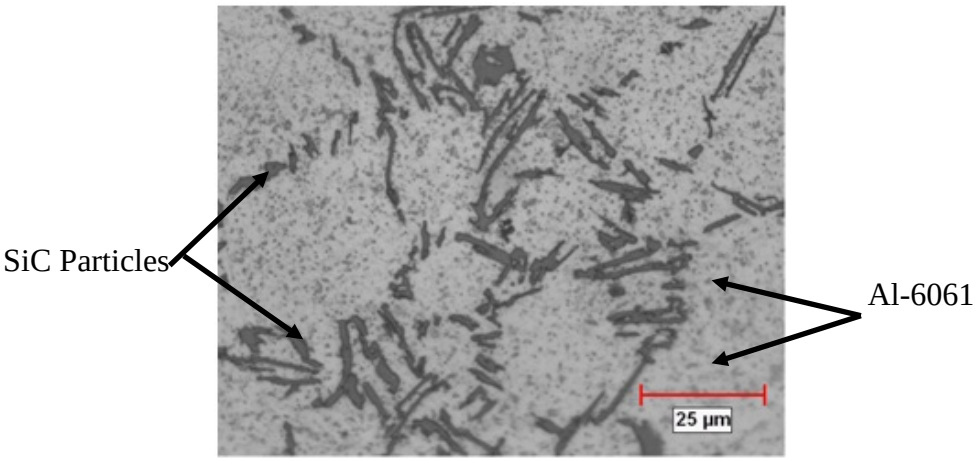

(b)

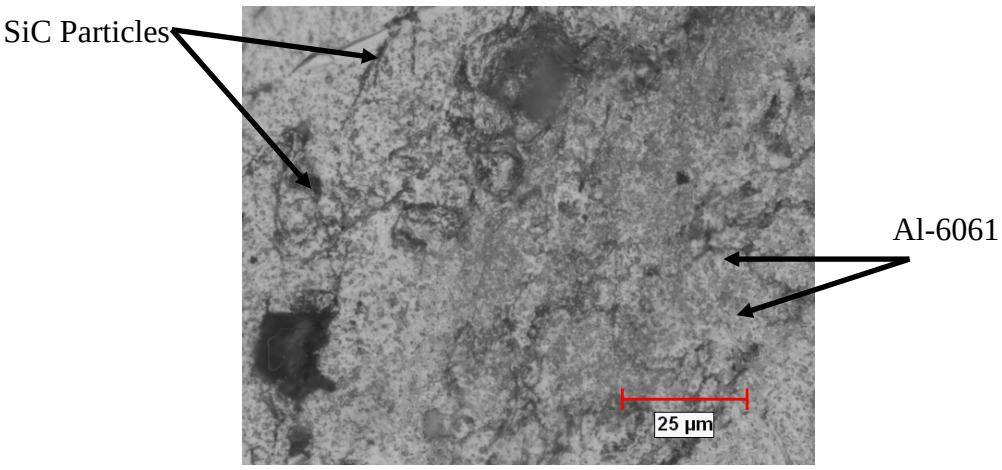

(c)

Figure 3.2 Microstructure of Al-SiC composites (a) 8 vol% (b) 10 vol % and (c) 12 vol % SiC

The specimens were extruded at 457°C, with extrusion ratio 30:1, and direct extrusion speed 6.1m/min to produce Ø22mm cylindrical bars. The machined specimens were solution treated for 2 hours at a temperature of 540^{o}C in a muffle furnace. The temperature of the furnace is kept within the accuracy of ±2^{o}C.

After solution treatment, the samples were water quenched to room temperature. Figure 3.2 shows the microstructure of Al6061 MMC specimens captured with a magnification of 500X. Chemical composition of Al 6061 alloy is given in Table 3.1. In several instances aluminium matrix reacts with the SiC reinforcement forming aluminium carbide. This reaction can be inhibited by adding silicon in the aluminium alloy.

Table 3.1 Chemical composition of Al 6061 alloy

Element	**Al**	**Cu**	**Mg**	**Si**	**Cr**	**Fe**
Weight %	97.3	0.25	1	0.6	0.25	0.2

Further the specimen was machined on conventional shaper with carbide tool to 17mm square cross-section. Figure 3.3 shows the specimen used for grinding process.

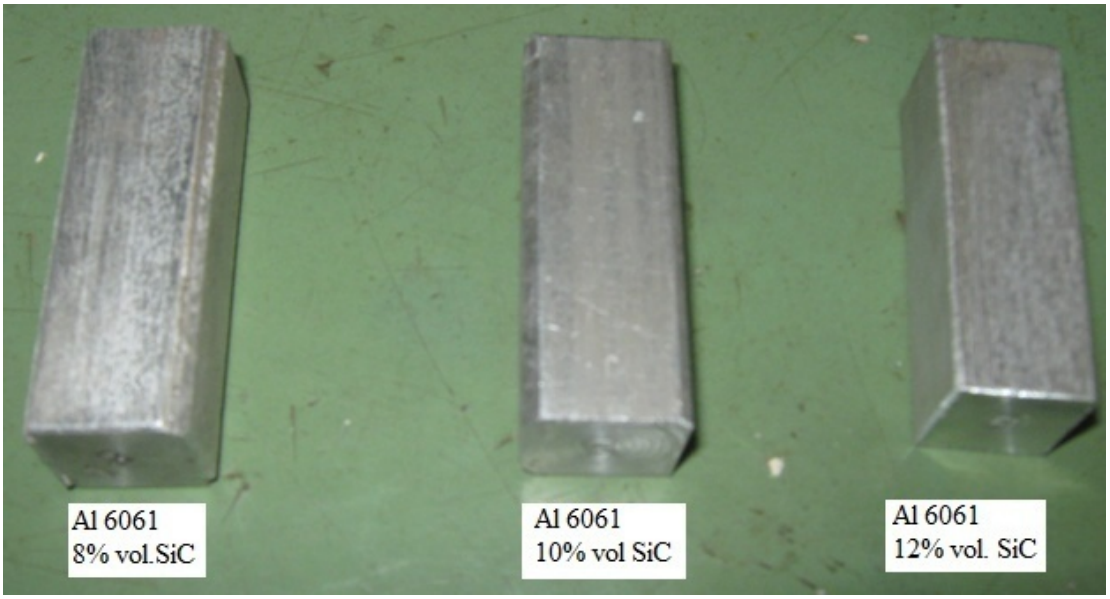

Figure 3.3 Specimen used for experimental purpose

3.3 GRINDING PROCEDURE

Down-cut surface grinding method was selected for grinding of MMCs. Experiments were conducted on 2kW, 25.6 m/s, conventional surface grinding machine 8J-1020 (Bhuraji make) with the hydraulic table feed arrangement. Figure 3.4 shows the schematic of grinding machine. The machine specifications are given in Table 3.2.

The surface grinding machine is provided with magnetic table. Al-SiC specimens being non-magnetic a special fixture is fabricated to mount the specimen on the grinding table. The fixture consists of a circular base with two holes drilled and tapped to mount it on the Kistler dynamometer. The circular base is mounted with two jaws. One of the jaws is fixed and the other is movable. The specimen is mounted between these two jaws and further located and clamped in position.

Figure 3.4 A typical grinding machine

Table 3.2 Grinding machine Specification

SPECIFICATION	**8J-1020**
Working Surface or Grinding Area	225 x 500mm
Max. Magnetic Table Travel Lx B	250 x 525mm
Max. Ground height under Wheel	240 mm
Vertical Feed Graduation	0.01 mm
Cross Feed Graduation	0.05 mm
Elevator movement with MICROFEED	0.002 mm
Grinding Speed	25.6 m/s
Grinding Wheel Size (Dia x Bore x Width)	175mm x 31.75 mm x 12.7 mm
Electric Motor Recommended	2kW-3 PHASE

The experiments were conducted with three levels and three factors. Vol % of SiC, table feed and depth of grind are the chosen independent factors. Wheel speed does not contribute significantly for surface roughness in grinding [Ling Yin et al. 2005] and Resin bonded grinding wheel is best suited for grinding MMCs. [Ronald et al. 2009, Hung et al. 1997]. Hence these two factors were not been studied in this thesis. The selected factors and their levels for the experimentation are given in Table 3.3. Selection of factors for optimisation was based on the known machine and instrument limitations.

Table 3.3 Levels of independent Factors

Factors	**Levels**		
	Low(-1)	**Medium(0)**	**High(1)**
Percentage SiC (X_1)	8	10	12
Feed (mm/s) (X_2)	60	70	80
Depth of grind(μm) (X_3)	8	12	16

3.3.1 Grinding Wheel

Diamond holds a unique place in the grinding industry. Being the hardest material known it is not only the abrasive choice for grinding the hardest, most difficult materials, but also it is the only material that can truly address all abrasive wheels effectively. Although synthetic diamond dominates in wheel manufacture, natural diamond is preferred for specific applications [Abdullah et al. 2007]. Diamond materials are also used increasingly as wear surfaces for applications such as end stops and work-rest blades on grinding machines. In these types of applications, diamond can give 20 to 50 times the life of tungsten carbide.

Metal matrix composites reinforced with carbides are better ground with diamond wheels. They come in several bond types: Resin, vitrified, metal and electro-plated. Resin is used in most tool room and production applications. Vitrified and metal bonds are newer bond types with specific applications. Electro-plated wheels are very common and are typically found in cut-off wheels and low demanding abrasive grinding such as for plastics.

Resin wheels are made much like a traditional grinding wheel with a thick bond/grit layer usually between 1/16" and 1/4". Electroplated wheels are much thinner. In both cases, the bond layer is applied to a hub which is either aluminum or steel made to the specific profile required. Like traditional grinding wheels, diamond wheels are used in a variety of processes and with a variety of materials. Typically, diamond wheels are used strictly on carbides.

Diamond wheels are classified by their shape, grit size, concentration and the bond. A typical diamond wheel specification might be D1A1-D151R100-B4 where D1A1 is the wheel shape, D151 is the average grain size in microns, 100 is the concentration, R is the resin bond and B4 is this particular manufacturer's bond.

Smaller the grain size the finer will be the wheel is. Hence for rough grinding larger mesh size is used and for finish grinding smaller mesh size is used. The concentration is, in layman's terms, simply the amount of grit in the mix. Concentrations of 75 or higher are preferred but it also depends on the specific

application. Some jobs may do better with less concentration. Generally, the higher the concentration, the longer will be the life of wheel and the more expensive it will be.

There are various types of bonds. But most common are vitrified and resin bonds. Vitrified is basically a vitreous glass much like pottery or glassware fired in a kiln. Resin wheels are plastic resins mixed and cured at lower temperatures. Vitrified wheels are commonly used for bench, surface and tool room applications while resin wheels are commonly seen in cut-off wheels, centerless wheels and superabrasive wheels (diamond & Cubic Boron Nitride). Bonds can be either weak or strong depending on the application. Exotic bonds like copper and polyamide are very expensive and are utilised in precise operations. Resin is one of the most sought after bonding material for general applications [Ronald et al. 2009].

In the current research, Norton make diamond abrasive grinding wheel having specification ASD76R100B2 with outer diameter of 175mm, width 12.5mm, thickness 5mm and inner diameter of 31.75 is chosen for the grinding purpose. In the wheel specification ASD represents synthetic diamond abrasives with Nickle coating, 76 represents the grit size R100 is the wheel concentration and B2 represents a type of resin bond. This type wheel is generally used for finishing operation.

The honing stick having specification GN0390220K7V7 is used for dressing the wheel. This product is manufactured by Grindwell Norton. In this specification G represents the series number, N represents the type of abrasive 0390220 is the manufacturers number, K is the structure, 7 is the grain size, V is the bond and 7 is the grade. The experiments conducted under dry conditions. The wheel was dressed after each test run. Truing of the wheel is done twice during the whole experimentation.

3.4 MEASUREMENT OF PERFORMANCE PARAMETERS

Dominant Performance parameters in grinding process are wheel wear, specific energy, surface finish and material removal rate. Specific energy (u) is an important performance parameter in grinding, because it defines the temperature at the wheel-work interface. Specific energy is defined as energy consumed per unit volume of metal removed. Typically, the specific energies involved in grinding are much larger

than in other metal-cutting operation. In other metal-cutting operations, shearing accounts for about 75% of the total chip formation energy, and remaining energy for chip-tool friction [Allison and Cole 1993]. But in grinding, virtually, all the energy expended is converted into heat. Since the chip-formation process in grinding is extremely rapid, owing to the high cutting velocities and large strains, the process should be nearly adiabatic. That means, there is no sufficient time for any significant amount of the heat generated by plastic flow to be conducted away during deformation. Following are the reason for high specific energy during grinding [Rowe 2009].

(i) Size effect - small chip size causes energy to remove each unit volume of material to be significantly higher
(ii) Individual grains with extremely negative rake angles result in low shear plane angles & high shear strains
(iii) Not all grits are engaged in actual cutting.

Apart from above reasons specific energy is also affected due to the change in machining parameters such as wheel speed, feed, depth of cut, type of wheel and the type of workpiece. Choudhury and Baradieb (1999) noted that the cutting force is highly affected by feed rate and slightly by cutting speed. This shows that the feed rate is a dominant parameter and it plays a very important role on the cutting force and hence the specific energy. Any plausible physical model of the grinding process should be able to quantitatively account for the magnitude of the specific grinding energy and its dependence on the operating parameters. The grinding power, which is equal to the product of the force component tangential to the wheel surface and the wheel velocity, is especially important for calculating specific energy in grinding.

Surface roughness and material removal rate are the other two important performance parameters in grinding. Any machining process demands better surface finish (R_a), higher material removal rate (MRR), lower cutting forces yet keeping the energy consumption to the minimum. It is well known fact that a high MRR and a very good surface finish while keeping the energy consumption at minimum can never be achieved simultaneously in a grinding process. This is an age-long problem and

continuous efforts are being made by different researchers all over the world to fulfill such an objective. A compromise is always sought between these performance parameters so that an optimal solution is obtained within the given range of independent variables.

3.4.1 Material Removal Rate

Material removal rate is defined as the volume of metal removed per unit time. It is specified in mm^3/s. Some time the specific material removal rate is used for calculation purpose. It is the volume of metal removed per unit width per unit time. In the present study the method followed for calculation of material removal rate is explained below.

Initially the specimen is weighed on an electronic balance having the accuracy of one mg. The grinding process is then performed on the specimen. The time required to grind the specimen is noted. The specimen is weighed in the electronic balance after the completion of the grinding process. The difference in weight divided by the time taken for grinding and the density of the material gives the material removal rate. In this study specific material removal rate, the material removal rate per unit width of the wheel is used. Hence the specific material removal rate or material removal rate (MRR) is

$$Q_w^{'} = \frac{m}{\rho_c * w * s} \ \mathrm{mm^3/mm \cdot s}$$

where m is the mass of the material removed in grams, ρ_c is the density of the composite material in g/mm^3, w is the width of the grinding wheel in mm and s is the time for grinding the specimen in seconds.

The density of the composite material is calculated using the relation [Arsenault et al. 1991]

$$\rho_c = (\rho_f * V_f + \rho_m * V_m) \ \mathrm{g/mm^3}.$$

where ρ_f is the density of the reinforcing material in g/mm^3, V_f is the volume fraction of the reinforcing material and ρ_m and V_m are the density and volume fraction of the matrix material respectively. In the current study the density of Al6061 matrix material

is taken as 0.00268g/mm^3 and density of reinforcing SiC material is taken as 0.00321g/mm^3[Clyne and Whithers 1993].

3.4.2 Specific Energy

Specific energy is defined as the energy consumed per unit volume of material removal. It is an important performance parameter to be considered for any machining process. Higher the specific energy, higher the amount of heat generated at the work tool interface which results in surface damage and hence poor surface finish on the workpiece. In the present study specific energy is measured based on the relation

$$u = \frac{F_t^{'} * v_s}{Q_w^{'} * w} \tag{3.1}$$

where $F_t^{'}$ is the specific tangential grinding force in N/mm, Q'_w is the volume of metal removed in mm^3/mm$\cdot$s and v_s is the peripheral speed of the grinding wheel in m/s. The rotational spindle speed N is 2880rpm and it is constant. The wheel diameter D is 0.175m. Hence wheel speed is calculated using the relation

$$v_s = \frac{\pi * D * N}{60}\ m/s$$

$$= \frac{\pi * 0.175 * 2800}{60} = 25.65 m/s$$

The specific tangential grinding force necessary to calculate the specific energy is measured using Kistler dynamometer type 9272. The dynamometer set up is shown in Figure 3.5 along with the axis of the dynamometer. It is a four component quartz dynamometer, which can measure four components of forces namely the tangential force (F_y), the normal force (F_z), the transverse force (F_x) and the moment about Fz. In the current experiment the grinding force in y-direction is acquired. The signals are further amplified using 8-channel charged amplifier type 5070A. The amplifier is connected to the computer through a RS-232 cable. The signals are filtered at 1MHz and stored in the computer through A/D card reader type PCIM-DA1602/16. Dynoware software type 2825A is used to read the force signal from A/D card.

Figure 3.5 Kistler dynamometer setup

A sample reading of force pattern from the dynamometer is shown in Figure 3.6. The signals were obtained while grinding Al-6061 8 vol% SiC with feed 80mm/s and depth of grind 16 μm. The negative reading of the cutting force indicates that the signals are acquired in the direction opposite to the direction of grinding force from the point of view of the safety of Kistler dynamometer. Set of force readings acquired from dynamometer are given in Appendix-I

Figure 3.6 Sample cutting force in grinding

3.4.3 Surface roughness

It is one of the important performance parameters as it will define the surface texture on the ground surface. Surface roughness is defined as the deviation of the surface waviness from the mean position. The surface roughness is measured in microns (μm) and it is desired to be maintained as minimum as possible. Higher the surface finish better will be the machining quality on the machined surface. The surface finish of machined parts plays a considerable role in the wear resistance and fatigue strength.

The surface profile traces of the ground specimen were obtained using Taylor/Hobson Surtronoic 3+ surface roughness measuring instrument with the following specifications: Traverse Speed: 1mm/sec, Cut-off values 0.25mm, 0.80mm and 2.50mm. Figure 3.7 shows the Surtronoic 3+ surface roughness measuring instrument. The device consists of a stylus stand, profile recorder and a measuring instrument that operates as follows: The stylus is allowed to slide on the ground surface. A motor and a gearbox, which control the speed of the stylus, provide the movement of the stylus. The stylus itself is mounted on an arm that is pointing at the contact limit of an "E-shaped" iron head. The outer limbs of the iron head have two induction coils. A small gap exists between the arm and the outer limbs of the head. Upon the movement of the stylus (as a result of changes in the surface topography) the air gap in the coil changes, and consequently the displacement of the stylus is recorded

as proportional to the impedance of the coil (which is proportional to the air gap). The roughness is measured at four different locations and average values are noted.

Figure 3.7 Roughness measuring Instrument

A sample result of the surface roughness obtained by using the software surftron 3^{+} is shown in Figure 3.8. This reading was taken after grinding the Al-SiC 12 vol % at 60mm/s feed and 8 µm depth of grind. The average Ra value obtained is 0.62 microns. The set of roughness profiles recorded for the present work is given in Appendix-II

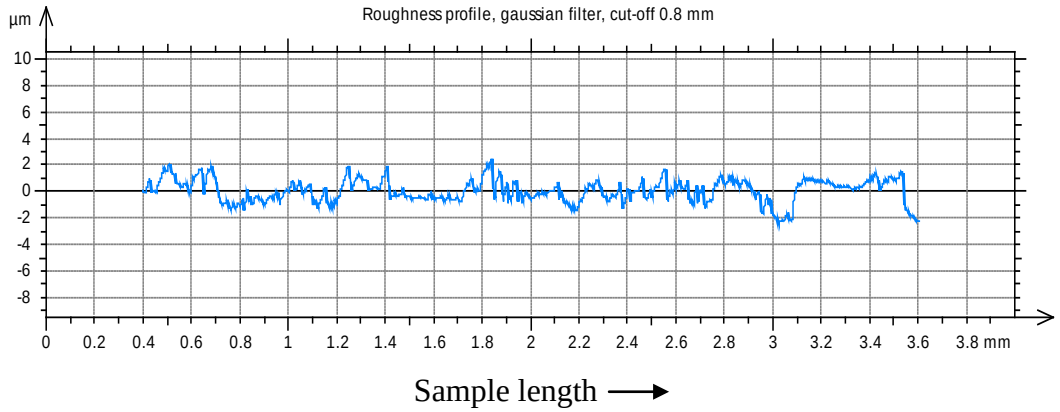

Figure 3.8 Roughness profile

3.4.4 Machined workpiece surface analysis

The workpiece damage during surface grinding process was studied using eMPower Image Analyser shown in Figure 3.9. The images were taken at a magnification of 100X. A sample image captured by the image analyser is shown in Figure 3.10.

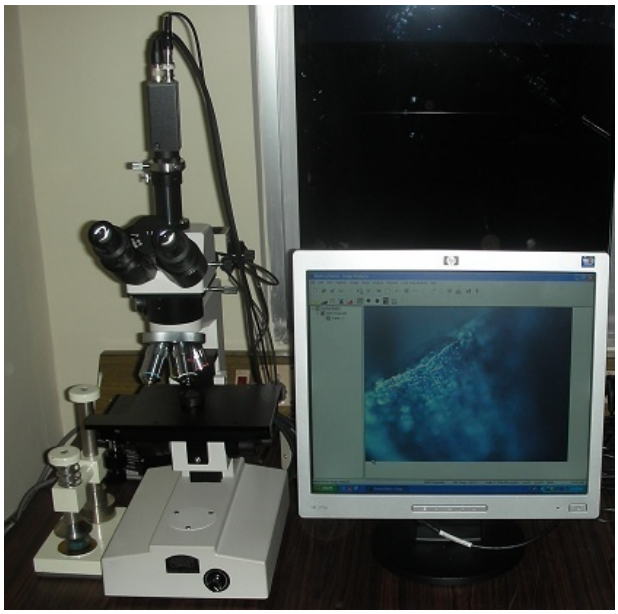

Figure 3.9 eMPower image analyser

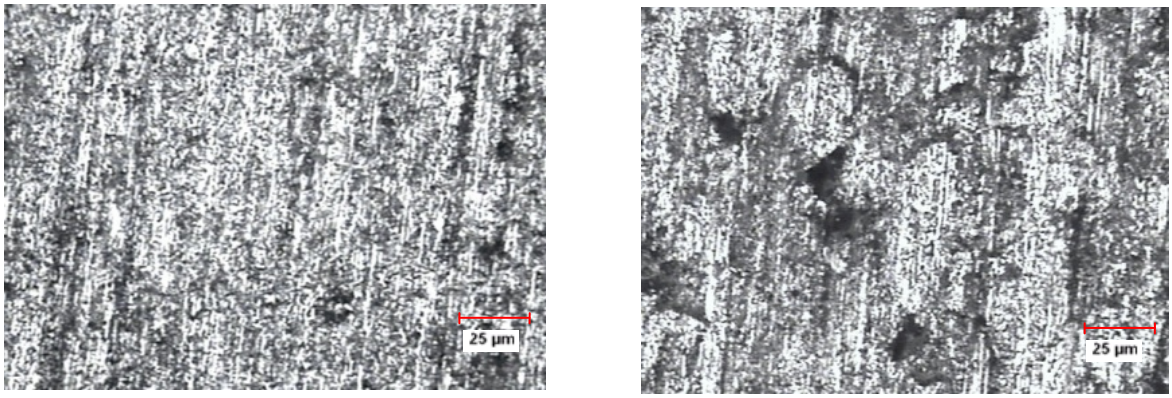

(a) (b)

Figure 3.10 (a) Optical micrograph of Al6061-SiC 12 vol % specimen with magnification factor 100 (a) depth of grind8 microns (b) depth of grind16 microns

3.5 DESIGN OF EXPERIMENTS

In manufacturing processes, it is often of primary interest to explore the relationships between the key input process variables (or factors) and the output performance characteristics (or quality characteristics). For example, in a metal cutting operation, cutting speed, feed rate, type of coolant, depth of cut, etc. can be treated as input variables and surface finish of the finished part can be considered as an output performance characteristic.

One of the common approaches employed by many engineers today in manufacturing companies is One-Variable-At-a-Time (OVAT), where one variable (factor) is varied at a time keeping all other variables in the experiment fixed. But this method does not consider the interaction effects between the main factors. Moreover, this type of experimentation requires large resources to obtain a limited amount of information about the process. OVAT experiments are often unreliable, inefficient, time consuming and may yield false optimum condition for the process.

In a designed experiment, the engineer often makes deliberate changes in the input variables (or factors) and then determines how the output functional performance varies accordingly. It is important to note that all the variables do not affect the performance in the same manner. Some may have strong influences on the output performance, some may have medium influences and some have no influence at all. Therefore, the objective of a carefully planned designed experiment is to understand which set of variables in a process affects the performance most and then determine the best levels for these variables to obtain satisfactory output functional performance of products.

Design of experiments (DOE) is an efficient procedure for planning experiments so that the data obtained can be analysed to yield valid and objective conclusions. The analysis is made using the popular software specifically used for design of experiment applications known as MINITAB 15. Before any attempt is made to use this simple model as a predictor for the measures of performance, the possible interactions between the control factors must be considered. In order to understand a concrete visualisation of the impact of various factors and their interactions, it is

desirable to develop analysis of variance (ANOVA) table to find out the order of significant factors as well as of interactions.

3.5.1 Taguchi's method

Taguchi techniques have been used widely in engineering design [Ross 2004 and Phadke, 1989]. The main thrust of the Taguchi techniques is the use of parameter design, which is an engineering method for product or process design that focuses on determining the parameter (factor) settings producing the best levels of a quality characteristic (performance measure) with a minimum variation. Taguchi designs provide a powerful and efficient method for designing processes that operate consistently and optimally over a variety of conditions. To determine the best design requires the use of a strategically designed experiment which exposes the process to various levels of design parameters.

Experimental design methods were developed in the early years of 20th century and have been extensively studied by statisticians since then, but they were not easy to use by practitioners [Phadke, 1989]. Taguchi's approach to design of experiments is easy to adopt and apply for users with limited knowledge of statistics; hence it has gained a wide popularity in the engineering and scientific community. There have been plenty of recent applications of Taguchi techniques to materials processing for process optimisation [Lin, 2002; Davim, 2003; Ghani et al. 2004; Jeyapaul et.al. 2006; Palanikumar 2008]. In particular, it is recommended for analysing metal cutting problems for finding the optimal combination of parameters [Ghani et al. 2004]. Further depending on the number of factors, interactions and their level, an orthogonal array is selected by the user. Taguchi has used Signal–Noise [S/N] ratio as the quality characteristic of choice. S/N ratio is used as measurable value instead of standard deviation due to the fact that as the mean decreases, the standard deviation also deceases and vice versa. In other words, the standard deviation cannot be minimised first and the mean brought to the target. In practice, the target mean value may change during the process development. Two of the applications in which the concept of S/N ratio is useful are the improvement of quality through variability

reduction and the improvement of measurement. The S/N ratio for continuous characteristics can be divided into three categories given by eqs. (3.2) – (3.4).

Nominal is the best characteristic $$\frac{S}{N} = 10\log\frac{\bar{y}}{s_y^2} \tag{3.2}$$

Smaller is the best characteristic $$\frac{S}{N} = -10\log\frac{1}{n}\left(\sum y^2\right) \tag{3.3}$$

And larger the better characteristic $$\frac{S}{N} = -\log\frac{1}{n}\left(\sum\frac{1}{y^2}\right) \tag{3.4}$$

where $\bar{y}$ the average of observed data, s_y^2 is the variation of y, n is the number of observations, and y is the observed data.

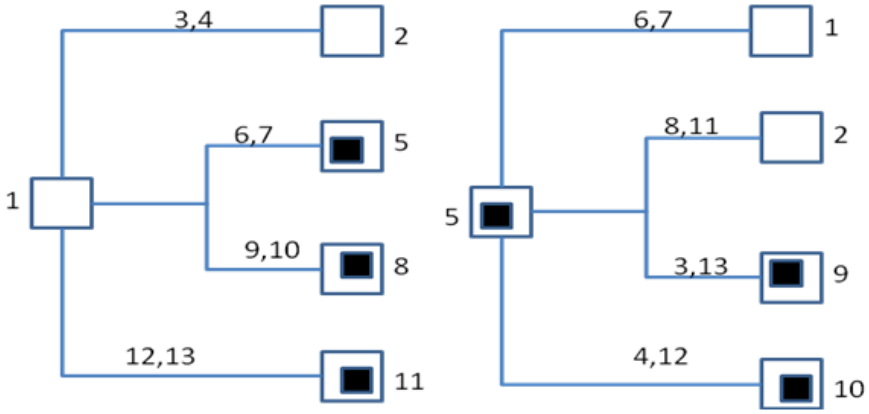

Figure 3.11 Linear graph $L_{27}(3^{13})$

For each type of the characteristics, with the above S/N ratio transformation, larger the S/N ratio better is the r. For the elaboration of experiments plan, we used the method of Taguchi for three factors at the response. By levels we mean the values taken by the factor indicates the factors to be studied and the assignment of the corresponding levels. The array chosen was the L_{27} (3^{13}) which has 27 rows corresponding to the number of tests(26 degree of freedom) with 13 columns at three levels, as shown in Table 3.4.

Table 3.4 Orthogonal array L_{27} (3^{13}) of Taguchi

L_{27} (3^{13}) Test	1	2	3	4	5	6	7	8	9	10	11	12	13
1	1	1	1	1	1	1	1	1	1	1	1	1	1
2	1	1	1	1	2	2	2	2	2	2	2	2	2
3	1	1	1	1	3	3	3	3	3	3	3	3	3
4	1	2	2	2	1	1	1	2	2	2	3	3	3
5	1	2	2	2	2	2	2	3	3	3	1	1	1
6	1	2	2	2	3	3	3	1	1	1	2	2	2
7	1	3	3	3	1	1	1	3	3	3	2	2	2
8	1	3	3	3	2	2	2	1	1	1	3	3	3
9	1	3	3	3	3	3	3	2	2	2	1	1	1
10	2	1	2	3	1	2	3	1	2	3	1	2	3
11	2	1	2	3	2	3	1	2	3	1	2	3	1
12	2	1	2	3	3	1	2	3	1	2	3	1	2
13	2	2	3	1	1	2	3	2	3	1	3	1	2
14	2	2	3	1	2	3	1	3	1	2	1	2	3
15	2	2	3	1	3	1	2	1	2	3	2	3	1
16	2	3	1	2	1	2	3	3	1	2	2	3	1
17	2	3	1	2	2	3	1	1	2	3	3	1	2
18	2	3	1	2	3	1	2	2	3	1	1	2	3
19	3	1	3	2	1	3	2	1	3	2	1	3	2
20	3	1	3	2	2	1	3	2	1	3	2	1	3
21	3	1	3	2	3	2	1	3	2	1	3	2	1
22	3	2	1	3	1	3	2	2	1	3	3	2	1
23	3	2	1	3	2	1	3	3	2	1	1	3	2
24	3	2	1	3	3	2	1	1	3	2	2	1	3
25	3	3	2	1	1	3	2	3	2	1	2	1	3
26	3	3	2	1	2	1	3	1	3	2	3	2	1
27	3	3	2	1	3	2	1	2	1	3	1	3	2

The plan of experiments is made of 27 tests (array row) in which first column was assigned to the first input parameter and the second column to be second input parameter and the fifth column to be the third input parameter and the remaining were assigned to the interaction (Figure 3.11). The response to be studied is the output parameter. In order to obtain the desired response each test for MRR and Ra were repeated three times and that for specific energy is repeated two times. The obtained results are tabulated in Appendix-III. Table 3.5 represents the design matrix containing 27 set of experiments and the average response obtained therein.

Application of Taguchi's orthogonal array to study the influence of grinding process variables on the performance parameters during the grinding of DRACs is discussed in the next chapter.

Table 3.5 Experimental Results

Sr.No	Coded Values			Actual values			Average Response		
	X_1	X_2	X_3	SiC Vol %	Feed (mm/s)	Depth of grind (a, μm)	y_1 (u, J/mm^3)	y_2 ($Q_w^{'}$, mm^3/mm·s)	y_3 (R_a, μm)
1	-1	-1	-1	8	60	8	145.585	0.498	1.08
2	-1	-1	0	8	60	12	126.052	0.581	1.09
3	-1	-1	1	8	60	16	135.641	0.675	1.14
4	-1	0	-1	8	70	8	114.220	0.431	1.13
5	-1	0	0	8	70	12	88.625	0.605	1.16
6	-1	0	1	8	70	16	84.263	0.746	1.22
7	-1	1	-1	8	80	8	95.882	0.556	1.17
8	-1	1	0	8	80	12	76.361	0.748	1.25
9	-1	1	1	8	80	16	71.530	0.870	1.30
10	0	-1	-1	10	60	8	130.266	0.498	0.86
11	0	-1	0	10	60	12	119.907	0.608	0.86
12	0	-1	1	10	60	16	115.271	0.727	0.91
13	0	0	-1	10	70	8	116.596	0.555	0.87
14	0	0	0	10	70	12	93.517	0.655	0.93

Sr.No	Coded Values			Actual values			Average Response		
	X_1	X_2	X_3	SiC Vol %	Feed (mm/s)	Depth of grind (a, μm)	y_1 (u, J/mm^3)	y_2 ($Q_w^{'}$, mm^3/mm·s)	y_3 (R_a, μm)
15	0	0	1	10	70	16	84.575	0.829	0.95
16	0	1	-1	10	80	8	86.501	0.780	0.95
17	0	1	0	10	80	12	71.379	0.926	0.98
18	0	1	1	10	80	16	70.676	1.144	1.04
19	1	-1	-1	12	60	8	124.449	0.518	0.66
20	1	-1	0	12	60	12	119.567	0.636	0.75
21	1	-1	1	12	60	16	122.177	0.772	0.81
22	1	0	-1	12	70	8	82.276	0.530	0.69
23	1	0	0	12	70	12	77.048	0.667	0.79
24	1	0	1	12	70	16	68.603	0.805	0.84
25	1	1	-1	12	80	8	78.005	0.714	0.72
26	1	1	0	12	80	12	62.848	1.007	0.78
27	1	1	1	12	80	16	65.516	1.067	0.87

Chapter 4

PERFORMANCE EVALUATION OF GRINDING PROCESS VARIABLES ON SURFACE GRINDING OF DRACs- TAGUCHI'S DESIGN OF EXPERIMENTS APPROACH

The main objective of this chapter is to study the influence of grinding process variables such as volume percentage of SiC, feed and depth of grinding on performance parameters namely specific energy, MRR and surface finish.

4.1 OVERVIEW

It is well known, the grinding process does not perform very well for soft materials due to the tendency of the chips being clog to the wheel. However, the grinding process plays an important role in secondary machining operations on MMC parts due to the free cutting tendency of these materials [Cronjager and Meister 1992]. Material removal rate (MRR) is an important aspect in productivity enhancement for grinding process. For very low values of MRR, rubbing and ploughing dominate, but as MRR increases so does the proportion of energy consumed in chip formation [Shen et al. 2002]. It is a well known fact that a high MRR and a very good surface finish can never be achieved simultaneously in a machining process. This is an age-long problem and continuous efforts are being made by different researchers all over the world to fulfill such an objective. [shen et al. 2002].

This chapter discusses the influence of process variables such as volume percentage of SiC feed and depth of grinding on specific energy, MRR and surface roughness on grinding of DRACs using Taguchi's orthogonal array. Focus of the study here is on understanding the influence of process variables on the grindability of DRACs. Specific energy, MRR and surface roughness on grinding of DRACs were studied for this purpose. The performance evaluation of the process variables on surface grinding of DRACs is proposed based on the analysis of

- Specific energy
- MRR
- Surface roughness

First part of this chapter explains the procedure for the experimental design and analysis of variance. Second part describes the effect of process variables on performance parameters namely, specific energy, MRR and surface roughness. Third part of this chapter is devoted for the results and discussions based on Taguchi design of experiments.

4.2 EXPERIMENTAL DESIGN

In general, experiments are used to study the performance of processes and systems. The process or system can be represented by the model shown in Figure 4.1. Some of the process variables $x_1,x_2,\ldots,x_k$ are controllable, whereas other variables $y_1,y_2,\ldots,y_n$ are uncontrollable.

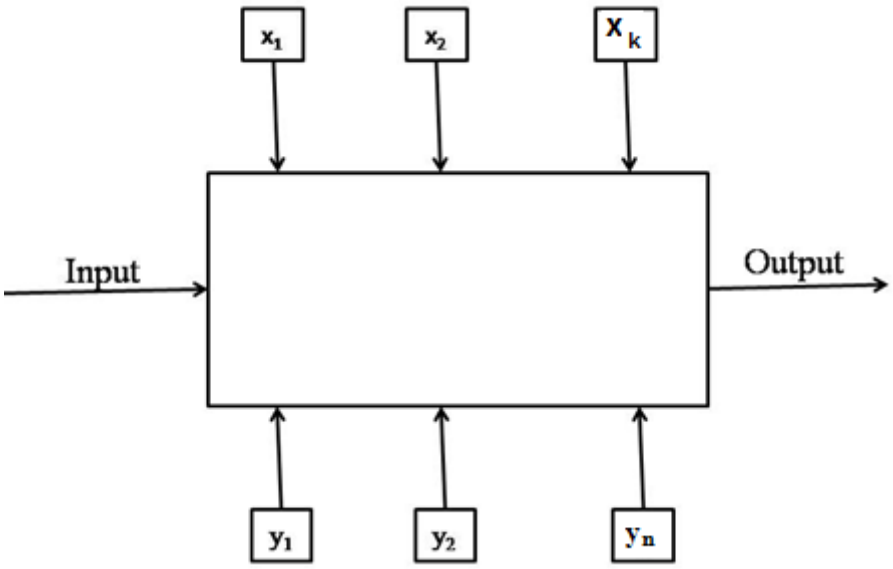

Figure 4.1 General model of process or system

The objectives of the experiment may include the following:

- Determining which variables are most influential on the response y.

- Determining where to set the influential x's so that y is almost always near the desired nominal value.
- Determining where to set the influential x's so that variability in y is small.
- Determining where to set the influential x's so that the effects of the uncontrollable variables y_1, y_2,…y_p are minimised.

4.2.1 Guidelines for designing the experiments

Following are the guidelines for designing an experiment.

- ***Recognition and statement of the problem:*** A clear statement of the problem often contributes substantially to a better understanding of the phenomena and final solution of the problem.
- ***Choice of factors, levels and ranges:*** The experimenter must choose the factors to be varied in the experiment, the ranges over which these factors will be varied and the specific levels at runs will be made. Selection of factors and their levels require the process knowledge.
- ***Selection of the response variable:*** It includes the variable to be measured which gives useful information about the process.
- ***Choice of experimental design:*** It involves the consideration of sample size, the selection of suitable run order for the experimental trials, and determination of whether or not blocking or other randomisation restrictions are involved.
- ***Performing the experiment:*** when running the experiment, it is vital to monitor the process carefully to ensure that everything is being done according to plan.
- ***Statistical analysis of the data:*** Statistical methods are used to analyse the data so that the results and conclusion are objective. Residual analysis and model adequacy checking are important analysis techniques.
- ***Conclusions and recommendations:*** Once the data have been analysed the experimenter must draw practical conclusion about the result and recommended course of action.
- ***Confirmation Test:*** Before presenting the results to the others and taking a practical course of action the experimenter needs to carry out confirmation tests to evaluate the conclusions.

4.3 INFERENCES ABOUT THE DIFFERENCES IN MEANS, RANDOMISED DESIGN

This section will explain how the data from this simple comparative experiment can be analysed using hypothesis testing and confidence interval procedures for comparing two treatment means.

Let $y_{i.}$ denote the total of all observations under the i^th^ level of factor A, y_j denote the total of all observations under the j^th^ level of factor B, y_{ij} denote the total of all observations in the ij^th^ cell, and y… denote the grand total of all the observations. Define $\bar{y}_{i..}, \bar{y}_{.j.}, \bar{y}_{ij}$, and $\bar{y}...$ as the corresponding row, column, cell, and grand averages. Expressed mathematically,

$$y_{i..} = \sum_{j=1}^{b}\sum_{k=1}^{n} y_{ijk} \qquad \bar{y}_{i..} = \frac{y_{i..}}{bn} \qquad i = 1, 2, \ldots\ldots, a$$

$$y_{.j.} = \sum_{i=1}^{a}\sum_{k=1}^{n} y_{ijk} \qquad \bar{y}_{.j.} = \frac{y_{.j.}}{an} \qquad j = 1, 2, \ldots\ldots, a$$

$$y_{ij.} = \sum_{k=1}^{n} y_{ijk} \qquad \bar{y}_{ij.} = \frac{y...}{n} \qquad i = 1, 2, \ldots\ldots, a \qquad j = 1, 2, \ldots, b \tag{4.1}$$

$$y... = \sum_{i=1}^{a}\sum_{j=1}^{b}\sum_{k=1}^{n} y_{ijk} \qquad \bar{y}... = \frac{y...}{abn}$$

where *a* and *b* are the levels of the factors A and B respectively and *n* is the number of factors in the experiment.

The total corrected sum of squares may be written as

$$\begin{aligned}\sum_{i=1}^{a}\sum_{j=1}^{b}\sum_{k=1}^{n}(y_{ijk} - \bar{y}...)^2 &= \sum_{i=1}^{a}\sum_{j=1}^{b}\sum_{k=1}^{n}[(\bar{y}_{i..} - \bar{y}_{...}) + (\bar{y}_{.j.} - \bar{y}_{...}) \\ &\quad + (\bar{y}_{ij.} - \bar{y}_{i..} - \bar{y}_{.j.} + \bar{y}_{...}) + (y_{ijk} - \bar{y}_{ij.})]^2 \\ &= bn\sum_{i=1}^{a}(\bar{y}_{i..} - \bar{y}_{...})^2 + an\sum_{j=1}^{b}(\bar{y}_{.j.} - \bar{y}_{...})^2 \\ &\quad + n\sum_{i=1}^{a}\sum_{j=1}^{b}(\bar{y}_{ij.} - \bar{y}_{i..} - \bar{y}_{.j.} + \bar{y}_{...})^2 + \sum_{i=1}^{a}\sum_{j=1}^{b}\sum_{k=1}^{n}(y_{ijk} - \bar{y}_{ij.})^2\end{aligned} \tag{4.2}$$

The total sum of squares has been portioned in to sum of squares due to "rows" or factor A, (SS_A); a sum of squares due to "columns" or factor B, (SS_B); a sum of squares due to the interaction between A and B, (SS_{AB}); and a sum of squares due to error , (SS_E).

The eq. 4.2 can be written as

$$SS_T = SS_A + SS_B + SS_{AB} + SS_E \tag{4.3}$$

The number of degrees of freedom associated with each sum of squares is depicted in Table 4.1

Table 4.1 Degrees of freedom

Effect	Degrees of Freedom
A	$a - 1$
B	$b - 1$
AB interaction	$(a-1)(b-1)$
Error	$ab(n-1)$
Total	$abn-1$

Each sum of squares divided by its degrees of freedom is a mean square.

Table 4.2 The analysis of variance for the two-factor factorial, fixed effects model

Source of Variation	Sum of Squares	Degrees of Freedom	Mean Square	F_0
A treatments	SS_A	a-1	$MS_A = \frac{SS_A}{a-1}$	$F_0 = \frac{MS_A}{MS_E}$
B treatments	SS_B	b-1	$MS_B = \frac{SS_B}{b-1}$	$F_0 = \frac{MS_B}{MS_E}$
Interaction	SS_{AB}	(a-1)(b-1)	$MS_{AB} = \frac{SS_{AB}}{(a-1)(b-1)}$	$F_0 = \frac{MS_{AB}}{MS_E}$
Error	SS_E	ab(n-1)	$MS_E = \frac{SS_E}{ab(n-1)}$	
Total		abn-1		

To test the significance of both main effects and their interaction, the corresponding mean square is divided by the error mean square. Large values of this ratio imply that the data do not support the null hypothesis.

The test procedure is usually summarised in an analysis of variance table, as shown in Table 4.2.

The total sum of squares is computed as

$$SS_T = \sum_{i=1}^{a}\sum_{j=1}^{b}\sum_{k=1}^{n} y_{ijk}^2 - \frac{y_{...}^2}{abn} \tag{4.4}$$

The sums of squares for the main effects are

$$SS_A = \frac{1}{bn}\sum_{i=1}^{a} y_{i...}^2 - \frac{y_{...}^2}{abn} \tag{4.5}$$

$$SS_B = \frac{1}{an}\sum_{j=1}^{b} y_{.j.}^2 - \frac{y_{...}^2}{abn} \tag{4.6}$$

It is convenient to obtain the SS_{AB} in two stages. First, the sum of squares is computed between the *ab* cell totals, which are called the sum of squares due to "subtotals":

$$SS_{subtotals} = \frac{1}{n}\sum_{i=1}^{a}\sum_{j=1}^{b} y_{ij.}^2 - \frac{y_{...}^2}{abn}$$

This sum of squares also contains SS_A and SS_B . Therefore, the second step is to compute SS_{AB} as

$$SS_{AB} = SS_{Subtotals} - SS_A - SS_B \tag{4.7}$$

SS_E is computed by subtraction as

$$SS_E = SS_T - SS_{AB} - SS_A - SS_B \tag{4.8}$$

or

$$SS_E = SS_T - SS_{Subtotals}$$

4.4 MODEL ADEQUACY CHECKING

Before the conclusions from the analysis of variance are adopted, the adequacy of the underlying model must be checked. As before, the primary diagnostic tool is residual analysis. The residuals for the two-factor factorials model are

$$e_{ijk} = y_{ijk} - \hat{y}_{i\,jk} \tag{4.9}$$

and since the fitted value $\hat{y}_{ijk} = \bar{y}_{ij}$. (the average of the observations in the ijth cell). Equation 4.9 becomes

$$e_{ijk} = y_{ijk} - \bar{y}_{i\,j.} \tag{4.10}$$

4.4.1 Hypothesis testing

A statistical hypothesis is a statement about a set of parameters of a population distribution. This may be stated formally as [Ross 2004]

$$H_0: \mu_1 = \mu_2$$

$$H_1: \mu_1 \neq \mu_2$$

where $\mu_1 \& \mu_2$ are the mean value of two different samples.

The statement $H_0: \mu_1 = \mu_2$ is called the null hypothesis and $H_1: \mu_1 \neq \mu_2$ is called the alternate hypothesis. We can determine whether or not to accept the null hypothesis by computing, first, the value of the test statistics and, second, the probability that a unit normal would exceed that quantity [Motorcu 2010]. This probability is called *p*-value of the test.

The *p*-value is the probability that the test statistic will take on a value that is at least as extreme as the observed value of the statistic when the null hypothesis H_0 is true and the hypothesis would be rejected at any significance level greater than equal to the test statistic. Thus, a *p*-value conveys much information about the weight of evidence against H_0, and so a decision maker can draw a conclusion at any specified level of significance.

4.4.2 Analysis of Variance (ANOVA)

ANOVA is a process concerning to hypothesis test of multiple population means. The main objective of ANOVA is to extract from the results how much variation each factor (or interaction assigned to the column) causes relative to the total variation observed in the result. The term variation is indicated by several mathematical descriptions. Perhaps, for a study with factors X_1, X_2, X_3, and so on, the total variation

in the results of experiments (all trail result) can be shown by a larger distribution and the individual factor influence distributions contained within it (Figure 4.2).

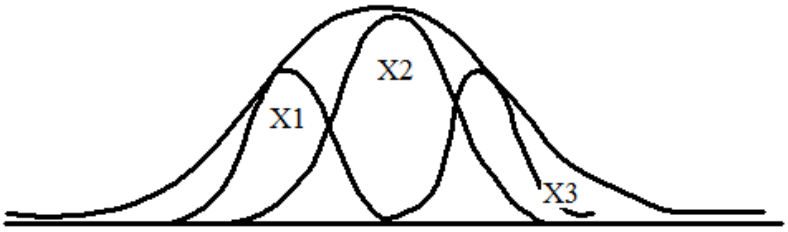

Figure 4.2 Total and individual factor influence distribution.

The assumptions needed for ANOVA are;

1) Random, independent sampling from the **k** populations;
2) Normal population distributions;
3) Equal variances within the **k** populations.

To express the influence of an individual factor to the total amount, the influence by the individual factor is expressed as a fraction (%) of the total variation. The calculation of individual factor influence is similar to finding the percentage of individual contributions in a group project when the total output is known.

For a set of data, $y_1, y_2, \ldots, y_n$ the total variation can be calculated by adding deviations of the individual data from the mean value. If the deviations were collected, as is, deviation from a data point that falls on the left of the average will be canceled by another equally away from the average on the right. To assure that all deviations are counted, the individual deviations are squared, which forces all deviation squared values to be positive (Figure 4.3).

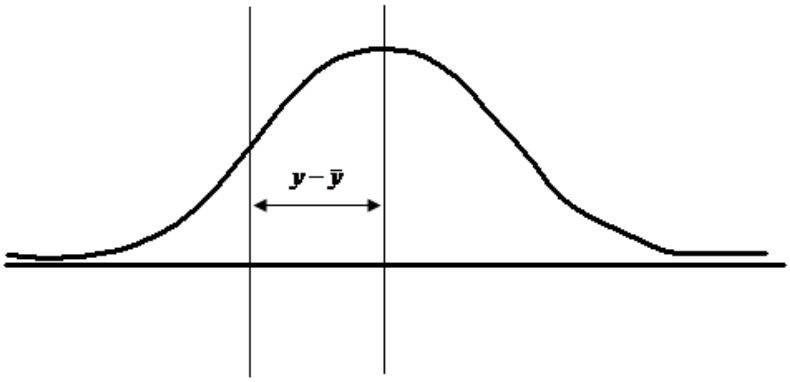

Figure 4.3 Calculation of total sum of squares

In the current study the evaluation of performance parameters is conducted using MINITAB 15 software, specifically used for design of experiment applications. Before making any conclusion regarding the effect of process variables on performance parameters, the effect of main factors and the possible interactions between them must be considered. Analysis of variance (ANOVA) is an effective method to find the variation of the process and to determine the effect of process variables on the performance parameters.

4.5 EFFECT OF GRINDING VARIABLES ON PERFORMANCE PARAMETERS

The orthogonal array for two factors at three levels was used for the elaboration of the plan of experiments the array L_{27} was selected, which has 27 rows corresponding to the number of tests (26 degrees of freedom) with 13 columns at three levels as give in Table 3.4. The factors and the interactions are assigned to the columns. The first column was assigned to the SiC volume percentage (X_1), the second column to feed in mm/s (X_2), the fifth column to the depth of grinding in μm (X_3) and remaining were assigned to interactions. The outputs to be studied were the specific energy, MRR and surface roughness. The selected levels and factors in machining of DRACs are given in Table 3.3.

Experiments are conducted with three factors at three different levels and with Taguchi L_{27} array. Experimental results for specific energy, MRR and surface roughness are shown in Table 3.5 of Chapter 3. The effect of grinding variables on specific energy, MRR and surface roughness are discussed in this section.

Figure 4.4 indicates the effect of feed on specific energy. It can be seen from the figure that specific energy decreases with increase in feed. It may be due to the reason that the energy consumed in the grinding process is spent on deforming and cutting new surfaces in the workpiece material. The new surface area produced is therefore a measure of the energy required. Increasing feed at constant depth of grinding, chip surface area decreases exponentially with increase in feed thus decreasing the specific energy [Rowe 2009].

Figure 4.5 shows that specific energy decreases with increase in depth of grind. It is because of the reason that increase in depth of grinding will increase the uncut chip thickness. Increase in uncut chip thickness results in increased material removal rate and hence there is decrease in specific energy.

From Figure 4.6, it is envisaged that material removal rate is higher at larger depth of grind. It is due to the reason that at increased depth of grind large number of grinding abrasives will assist in material removal thus increasing the MRR.

Figure 4.7 shows the effect of change in feed on MRR. From the figure, it is noted that MRR increases with increase in feed. Further, for different depth of grinding and 8vol% of SiC content, feed of 60mm/s it was observed that MRR increased up to 1.6 times.

Figure 4.8 shows the effect of depth of grinding on surface roughness at specified feed. From the figure, it is observed that surface finish is poor with increase in depth of grind. It is mainly due to the reason that, at increased depth of grind, grinding forces increase. Increase in grinding force will induce vibration of the grinding table thus resulting in poor surface finish.

Figure 4.9 shows that surface finish improves with increase in SiC vol% irrespective of feed. It is mainly due to the reason that, increase in SiC vol% will increase the hardness of the workpiece [Swamy et al. 2011] thus resulting in improved surface finish [Di Ilio et al. 1996]. It is also observed that MRR decreases with improvement in surface finish. It is mainly due to the reason that surface finish is better with low depth of grinding, which is associated with lower MRR.

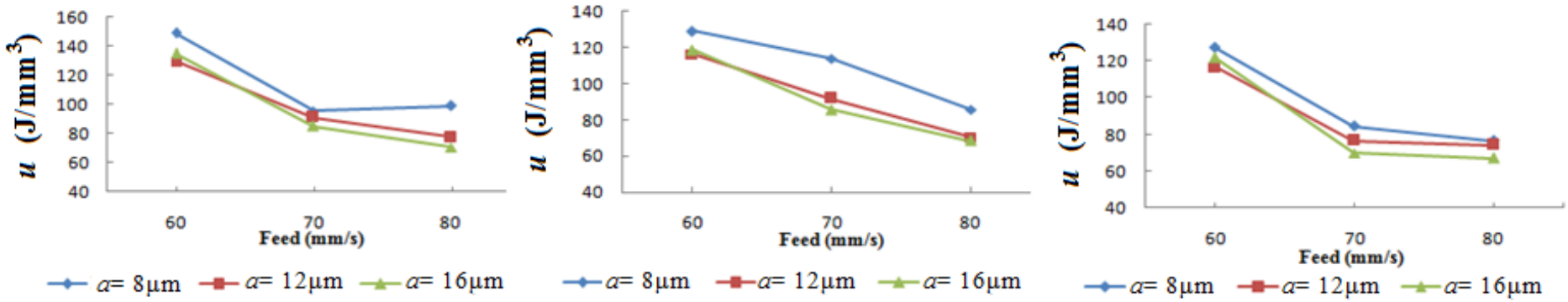

Figure 4.4. Effect feed on specific energy for different vol % of Al6061-SiC (a) 8 vol% (b) 10 vol % (c) 12 vol%

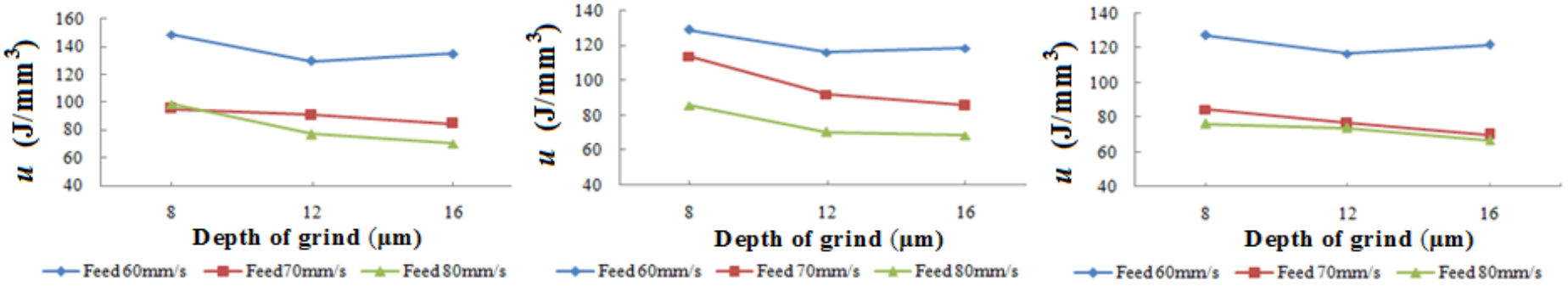

Figure 4.5 Effect depth of grind on specific energy for different vol % of Al6061-SiC (a) 8 vol% (b) 10 vol % (c) 12 vol%

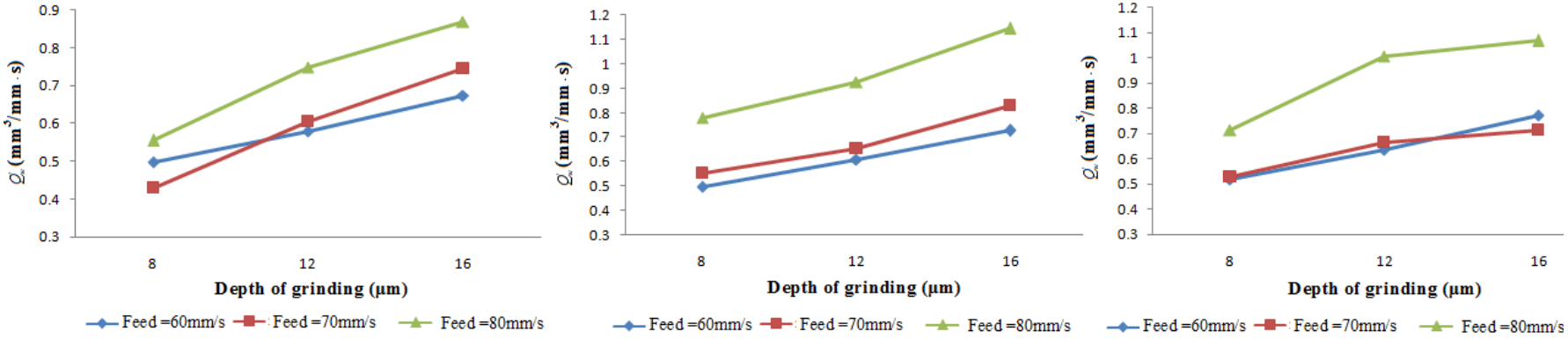

Figure 4.6 Effect of depth of grind on MRR for different vol % of Al6061-SiC (a) 8 vol% (b) 10 vol % (c) 12 vol%

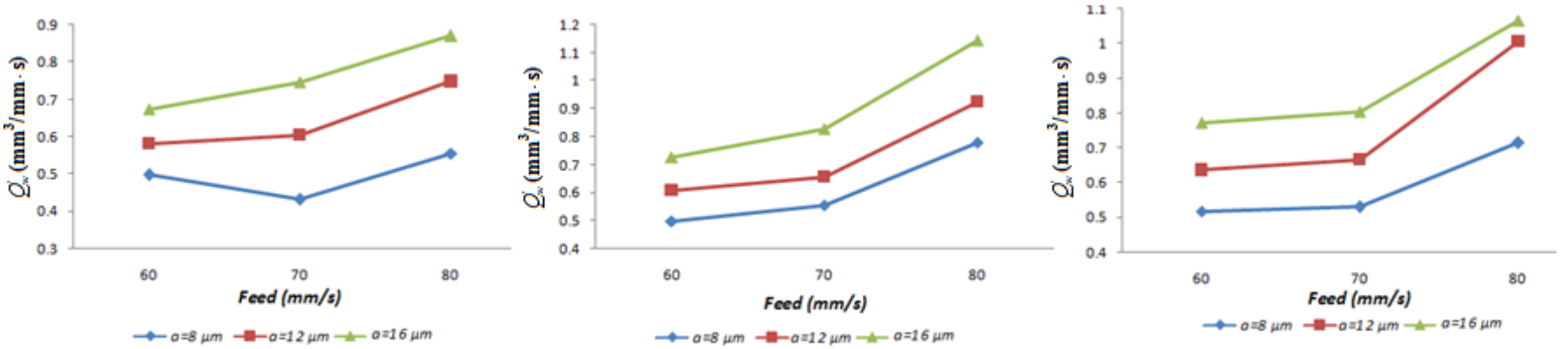

Figure 4.7 Effect of feed on MRR for different vol % of Al6061-SiC (a) 8 vol% (b) 10 vol % (c) 12 vol%

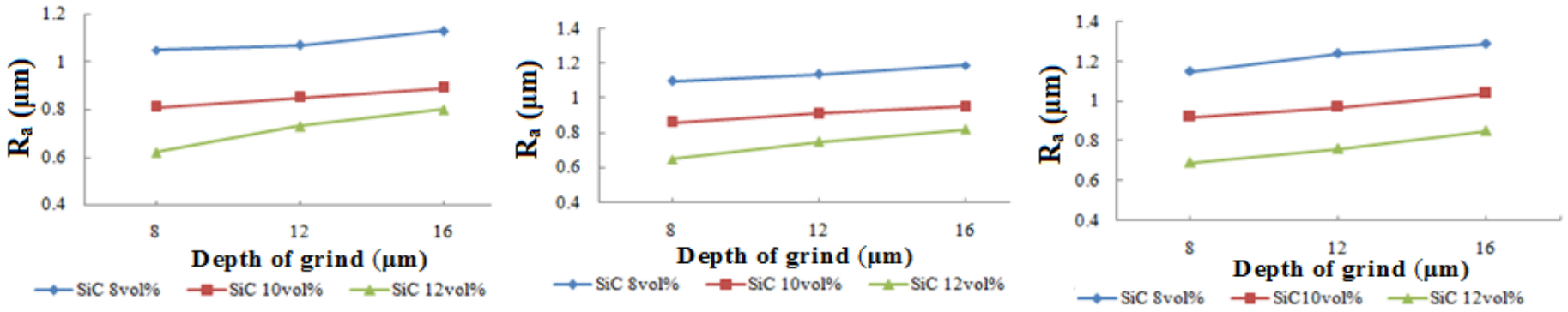

Figure 4.8 Effect of depth of grind on surface roughness for different feed (a) 60mm/s (b) 70mm/s (c) 80mm/s

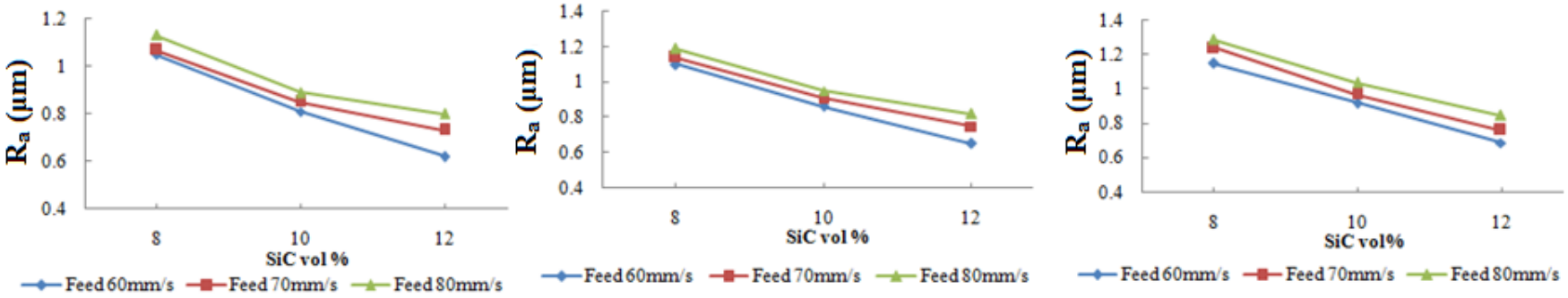

Figure 4.9 Effect of SiC vol% on surface roughness for different feed (a) 60mm/s (b) 70mm/s (c) 80mm/s

4.6 RESULT AND DISCUSSION

The Taguchi's design of experiment is applied in this work for the identification of the best levels of grinding process variables. The grinding of DRACs is performed with the factors and levels of the process variables given in Table 3.3. The performance parameters to be studied are specific energy, MRR and surface roughness.

The results of the ANOVA for Specific energy, MRR and surface roughness, are discussed in the following sections. This analysis was carried out for a significance level of $\alpha = 0.05$, i.e. for a confidence level of 95%. Tables below shows the P-values, that is, the realised significance levels, associated with the F-tests for each source of variation. The sources with a P-value less than 0.05 are considered to have a statistically significant contribution to the performance measures. Also, the last columns of the tables show the percent contribution of each source to the total variation indicating the degree of influence on the result.

4.6.1 ANOVA for specific energy

Table 4.3 shows the analysis of means for specific energy. The P-values of the feed X_2, depth of grinding X_3 and interaction of factors SiC vol % X_1 and feed X_2 are less than 0.05. The column for percentage contribution (P %) shows that factor X_2 has highest contribution (78.31%) followed by factor X_3 (11.36%) and factor X_1 (7.77%). A significant contribution (1.31%) is also found from the interaction between X_1 and X_2. In physical sense it means that, feed (X_2) is the dominant factor in analysing the specific energy for grinding Al-SiC composites. Depth of grinding (X_3), SiC vol % (X_1)and interaction of SiC vol% and feed (X_1* X_2) also contribute in analysing the specific energy. But interaction of SiC vol% and depth of grinding (X_1* X_3) and interaction of feed and depth of grinding (X_2* X_3) have the *p*-value greater than 0.05. Hence those factors neither have statistical significance, nor a percentage of physical significance of contribution to the specific energy.

Table 4.3. Analysis of variance for means of specific energy

Source	Degrees of Freedom	sum of square	Mean square	*F*-ratio	*P*-value	P%
X_1	2	9.608	4.804	85.28	0.000	7.77
X_2	2	97.414	48.707	864.71	0.000	78.31
X_3	2	14.134	7.067	125.46	0.000	11.36
$X_1 * X_2$	4	3.268	0.817	14.5	0.001	1.31
$X_1 * X_3$	4	0.853	0.213	3.79	0.052	0.34
$X_2 * X_3$	4	2.339	0.585	10.38	0.003	0.94
Residual Error	8	0.451	0.056			
Total	26	128.066				

Figure 4.10 shows the main effect plot for specific energy. It can be seen that specific energy decreases with increase in SiC vol%, (X_1), feed (X_2) and depth of grinding (X_3). Hence it can be concluded that minimum specific energy can be achieved by grinding Al-SiC specimen having 12 vol% of SiC, at feed of 80mm/s and depth of grinding of 12 μm. However the specific energy is also affected by interaction effect of different input variables as shown in Figure 4.11. The interaction is significant between SiC vol% $X_1$and feed $X_2$and feed $X_2$and depth of grinding X_3.

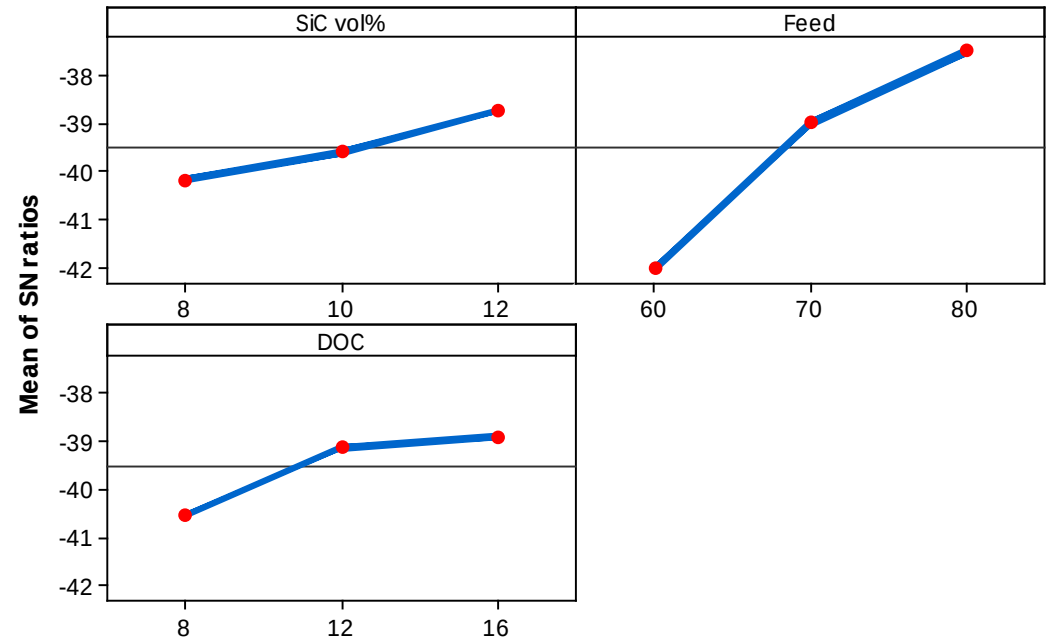

Figure 4.10 Main effect plot for specific energy

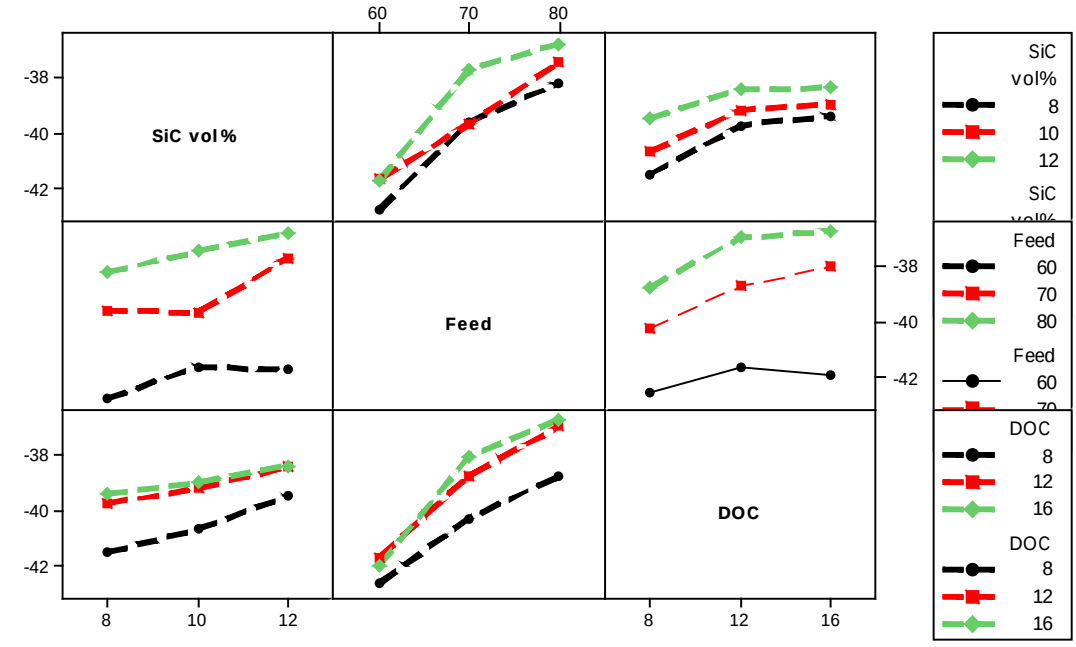

Figure 4.11 Interaction effect plot for specific energy

4.6.2 ANOVA for material removal rate

On the examination of the percentage contribution (P %) of the different factors (Table 4.4), for MRR, it can be seen that depth of grinding X_3 (P=49.33%) and feed, X_2 (P=39.26%) have the highest contribution. Thus feed and depth of grinding are the important factor to be taken into consideration while grinding DRACs. It can be seen that SiC vol % X_1 (P=9.34%) has statistical and physical significance on MRR. The interaction between the factors neither presents a statistical significance, nor a percentage of physical significance of contribution to the MRR

Table 4.4 Analysis of variance for means of MRR

Source	Degrees of Freedom	sum of square	Mean square	*F*-ratio	*P*-value	P%
X_1	2	10.844	5.422	38.96	0.000	9.34
X_2	2	45.608	22.804	163.84	0.000	39.26
X_3	2	57.297	28.647	205.83	0.000	49.33
X_1* X_2	4	3.433	0.858	6.17	0.014	1.48
X_1* X_3	4	0.571	0.143	1.02	0.450	0.24
X_2* X_3	4	0.817	0.204	1.47	0.298	0.35
Residual Error	8	1.113	0.139			
Total	26	119.683				

Figure 4.12 shows the main effect plot for MRR. It is observed for the figure that, MRR increases with increase in feed (X_2) and increase in depth of grinding (X_3). A marginal increase in MRR is observed with increase in Sic vol % (X_1). Hence it is economical to ground the Al-SiC specimen having 12 vol% of SiC with high feed and high depth of grind. The interaction effect plot for the performance variables shown in Figure 4.13 indicates that there is significant interaction between vol % of SiC and feed and feed and depth of grind.

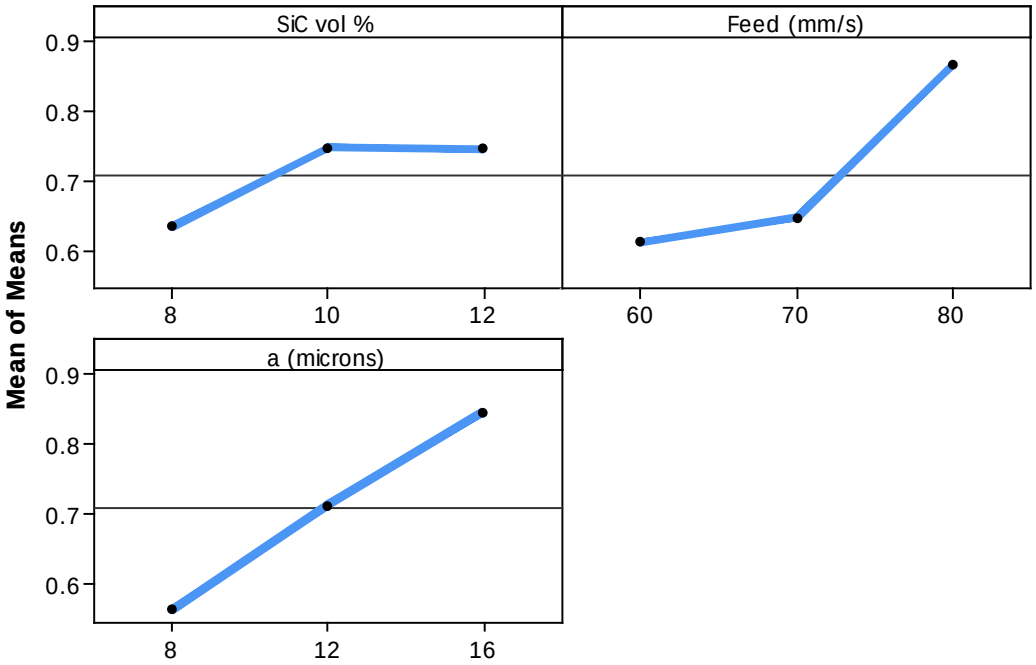

Figure 4.12 Main effect plot for MRR

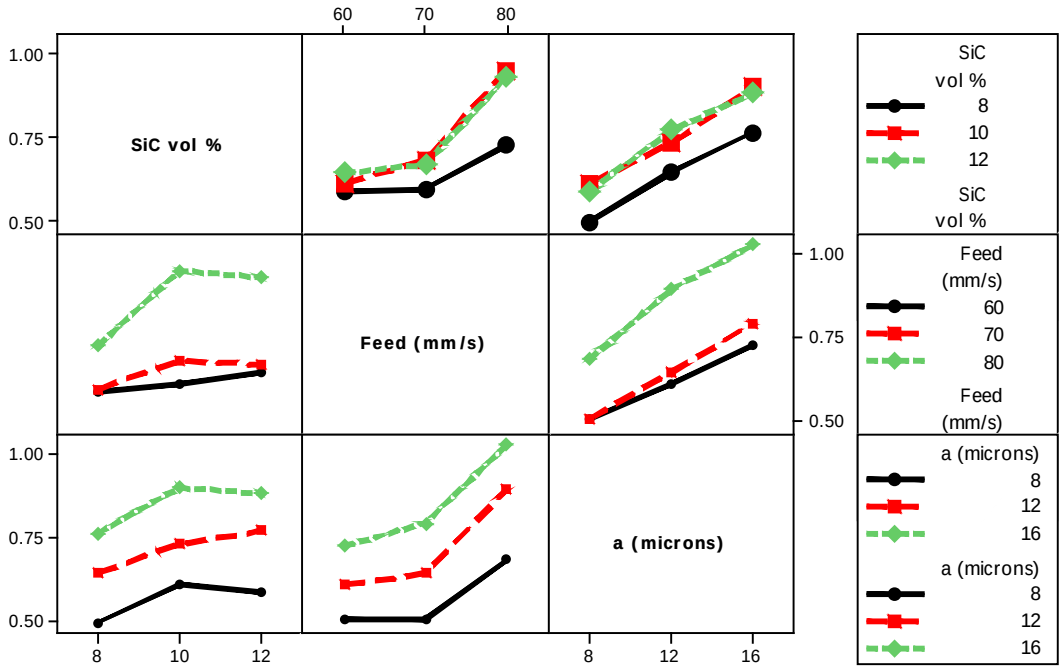

Figure 4.13 Interaction effect plot for MRR

4.6.3 ANOVA for surface roughness

The percentage contribution for surface roughness is given in Table 4.5. It can be seen from the table that, SiC vol% (X_1) has the highest contribution of 85.78%. Hence SiC vol% (X_1) is a predominant factor to be considered while grinding DRACs. It can be seen that depth of grinding X_3 (P=7.7%) feed X_2 (P=5.76%) and the interactions (X_1* X_2, X_1* X_3) have statistical and physical significance on surface roughness. The interaction (X_2* X_3) presents neither a statistical significance, nor a percentage of physical significance of contribution to the surface roughness.

Table 4.5 Analysis of variance for means of surface roughness

Source	Degrees of Freedom	sum of square	Mean square	*F*-ratio	*P*-value	P%
X_1	2	0.764	0.382	1671.1	0.000	85.78
X_2	2	0.051	0.026	112.3	0.000	5.76
X_3	2	0.069	0.034	149.99	0.000	7.70
X_1* X_2	4	0.008	0.002	8.3	0.006	0.43
X_1* X_3	4	0.005	0.001	5.6	0.019	0.29
X_2* X_3	4	0.001	0.0002	0.75	0.587	0.04
Residual	8	0.002	0.0002			
Total	26	0.899				

Figure 4.14 is the main effect plot for surface roughness. It can be concluded from the figure that surface roughness decreases with increase in SiC vol%, decrease in feed and decrease in depth of grind. The interaction between SiC vol% and feed and feed and depth of grinding is significant as shown in Figure 4.15.

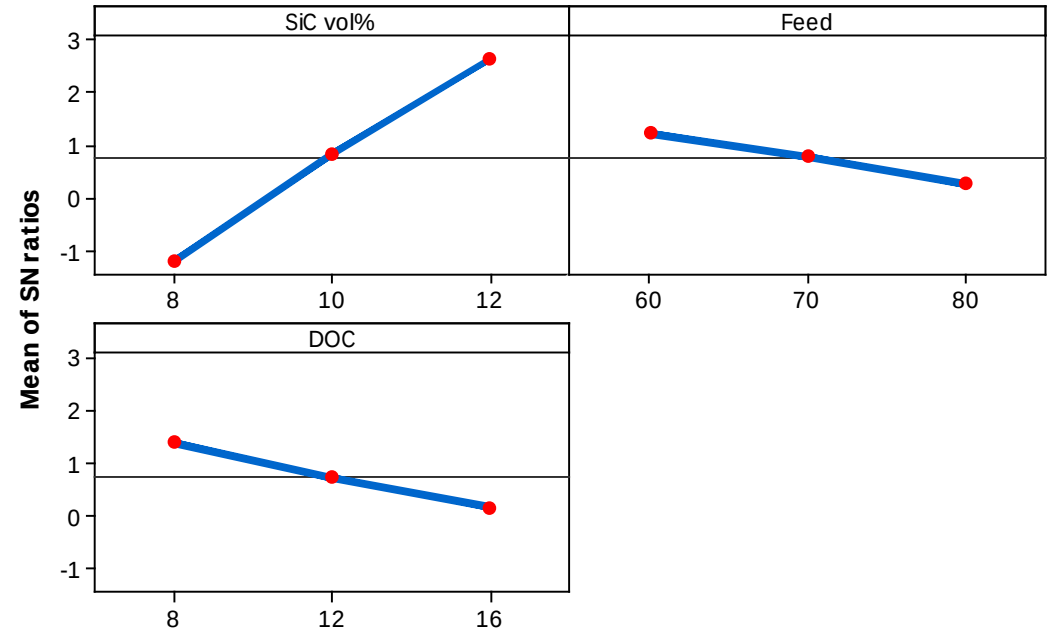

Figure 4.14 Main effect plot for surface roughness

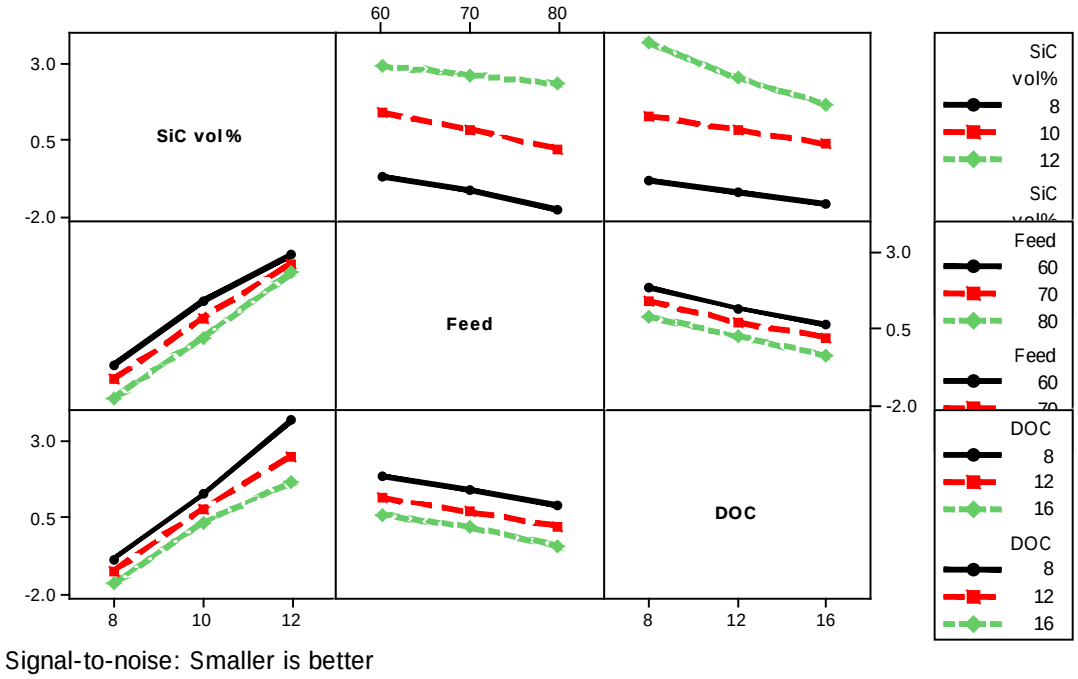

Figure 4.15 Interaction effect plot for surface roughness

In the above discussion an attempt is made to understand the effect of process parameters on grindability in surface grinding of DRACs. From the above analysis it is evident that, the grinding condition which are suitable for obtaining minimum surface roughness are not suitable for obtaining maximum material removal rate and vice versa. Similarly the grinding condition suitable for obtaining minimum specific energy is not suitable to obtain minimum surface roughness and vice versa. Hence it is necessary to strike a break even between MRR and surface finish so as to obtain the best possible setting of process variables.

The next chapter discusses on the application of response Surface Methodology for the best possible solution.

Chapter 5

RESPONSE SURFACE MODEL FOR OPTIMISATION OF SPECIFIC ENERGY, MATERIAL REMOVAL RATE AND SURFACE ROUGHNESS IN GRINDING OF DRACs

In this chapter the regression models for specific energy, material removal rate and surface roughness were developed form the principles of response surface methodology. Further, the models were optimised simultaneously from the desirability function approach.

5.1 INTRODUCTION

Response surface methodology (RSM) was originally developed by Box and Wilson in 1951 to aid the improvement of manufacturing processes in the chemical industry. The purpose was to optimise chemical reactions. In recent years, the RSM is gaining wide popularity in all the engineering and service industries. The reason for its popularity is being that the methodology is very simple and the model developed from RSM can easily be optimised quantitatively [Hood et al 2007]. Development of the RSM model is accomplished through the use of sequential experimentation involving factors affecting the process. The developed model can further be optimised either by desirability function approach, genetic algorithm or any other optimisation techniques.

The current chapter comprises of four sections. First section of the chapter explains the process of fitting the regression model and estimation of least square coefficients. An introduction to Response surface methodology is given in second section. Third section explains the desirability function approach. Results are discussed in the fourth section.

5.2 FITTING REGRESSION MODEL

In general, suppose that there is a single dependent variable or response y that depends on k independent of repressor variables, for example, x_1,x_2, . ….. x_k. The relationship between these variables is characterised by a mathematical model called a regression model. The regression model is fitted to a set of sample data. Regression models are

frequently used to analyse data from unplanned experiments. To understand the basic concepts of regression model a linear regression model is discussed in this section.

5.2.1 Linear regression models

Consider an empirical model relating the response y to factor x_1 and x_2. A model that might describe this relationship is

$$y = \beta_0 + \beta_1 x_1 + \beta_2 x_2 + \in \tag{5.1}$$

where y represents the response and x_1 and x_2 represents the variables in coded form. We often call the independent variables are often called as predictor variables or regressors.

The model describes a plane in the two-dimensional x_1, x_2 space. The parameter β_0 defines the intercept of the plane. We sometimes call β_1 and β_2 partial regression coefficients, because β_1 measures the expected change in y per unit change in x_1 when x_2 is held constant and β_2 measures the expected change in y per unit change in x_2 when x_1 is held constant.

In general, the response variable y may be related to k regressor variables. The model

$$y = \beta_0 + \beta_1 x_1 + \beta_2 x_2 + \ldots\ldots\ldots + \beta_k x_k + \varepsilon \tag{5.2}$$

is called a multiple linear regression model with k regression variables. The parameters $\beta_j, j = 0,1, \cdots, k$, are called the regression coefficient. This model describes a hyperplane in the k-dimensional space of the regressor variables $\{\mathbf{x}\}$. The parameter β_j represents the expected change in response y per unit change in x_j when all the remaining independent variables x_i $(i \neq j)$ are held constant.

5.2.2. Estimation of the parameters in linear regression models

The method of least squares is typically used to estimate the regression coefficients in a multiple linear regression model [Montgomery 2005]. Suppose that $n > k$ observations of the response variable are available, say $y_1, y_2, \ldots, y_n$. Along with each observed response y_i, we will have an observation on each regressor variable and let x_{ij} denote the i^{th} observation or level of variable x_j. The data will appear as given in Table 5.1. We assume that the error term ε in the model has E (ε) = 0 and V (ε) = σ^2 and that the $\{\varepsilon_i\}$ are uncorrelated random variables.

$$y_i = \beta_0 + \beta_1 x_{i1} + \beta_2 x_{i2} + \ldots\ldots + \beta_k x_{ik} + \in_i$$

$$= \beta_0 + \sum_{j=1}^{k} \beta_j x_{ij} + \in_i \qquad \text{i= 1,2, ... , n} \qquad (5.3)$$

We may write the model eq. 5.3 in terms of the observations as shown in Table 5.1

Table 5.1 Data for Multiple Linear regression

y	x_1	x_2	. . .	x_k
y_1	x_{11}	x_{12}	. . .	x_{1k}
y_2	x_{12}	x_{22}	. . .	x_{2k}
.	.	.	.	.
.	.	.	.	.
.	.	.	.	.
y_n	x_{n1}	x_{n2}	. . .	x_{nk}

The method of least squares chooses the β's in Eq. 5.3 so that the sum of the squares of the errors, ε_i, is minimised. The least squares function is

$$L = \sum_{i=1}^{n} \in_i^2 \qquad (5.4)$$

$$= \sum_{i=1}^{n} (y_i - \beta_0 - \sum_{j=1}^{k} \beta_j x_{ij})^2$$

The function L is to be minimised with respect to β_0, β_1, ..., β_k. The least squares estimators, say $\hat{\beta}_0, \hat{\beta}_1, \ldots, \hat{\beta}_k$, must satisfy

$$\left.\frac{\partial L}{\partial \beta_0}\right|_{\hat{\beta}_0, \hat{\beta}_1, \ldots, \hat{\beta}_k} = -2 \sum_{i=1}^{n} (y_i - \hat{\beta}_0 - \sum_{j=1}^{k} \hat{\beta}_j x_{ij}) = 0 \qquad (5.5)$$

and

$$\left.\frac{\partial L}{\partial \beta_0}\right|_{\hat{\beta}_0, \hat{\beta}_1, \ldots, \hat{\beta}_k} = -2 \sum_{i=1}^{n} (y_i - \hat{\beta}_0 - \sum_{j=1}^{k} \hat{\beta}_j x_{ij})\ x_{ij} = 0 \qquad \text{j= 1,2, ..., , k} \qquad (5.6)$$

It is simpler to solve the normal equations if they are expressed in matrix notation. The model in terms of the observations, Eq. 5.3, may be written in matrix notation as

$$y = X\beta + \in \qquad (5.7)$$

where

$$y = \begin{bmatrix} y_1 \\ y_2 \\ . \\ . \\ . \\ y_n \end{bmatrix}, \qquad X = \begin{bmatrix} 1 & x_{11} & x_{12} & . & . & . & x_{1k} \\ 1 & x_{21} & x_{22} & . & . & . & x_{2k} \\ . & . & . & . & . & . & . \\ . & . & . & . & . & . & . \\ . & . & . & . & . & . & . \\ 1 & x_{n1} & x_{n2} & . & . & . & x_{nk} \end{bmatrix},$$

$$\beta = \begin{bmatrix} \beta_0 \\ \beta_1 \\ . \\ . \\ . \\ \beta_k \end{bmatrix}, and \quad \in = \begin{bmatrix} \in_1 \\ \in_2 \\ . \\ . \\ . \\ \in_n \end{bmatrix}$$

In general, ***y*** is an (n x 1) vector of the observations; ***X*** is an (*x* X *p*) matrix of the levels of the independent variables and *p=k+1*. β is a (*p* X 1) vector of the regression coefficients, and $\in$ is an (*n* X 1) vector of random errors.

We wish to find the vector of least squares estimators, $\hat{\beta}$ that minimizes,

$$L = \sum_{i=1}^{n} \in_i^2 = \in' \in = (y - X\beta)'(y - X\beta)$$

L may be expressed as

$$\begin{aligned} L &= y'y - \beta' X' y - y' X\beta + \beta' X' X\beta \\ &= y'y - 2\beta' X' y + \beta' X' X\beta \end{aligned} \qquad (5.8)$$

Since $\beta' X' y$ is a scalar, and its transpose $(\beta' X' y) = y' X\beta$ is the same scalar. The least squares estimates must satisfy.

$$\left.\frac{\partial L}{\partial \beta}\right|_{\beta} = -2X'y + 2X'X\hat{\beta} = 0$$

which simplifies to

$$X'X\hat{\beta} = X'y \qquad (5.9)$$

Eq (5.9) is the matrix form of the least squares normal equations. To solve the normal equations multiply both sides of Eq 5.9 by the inverse of $X'X$. Thus the least squares estimators of β is

$$\hat{\beta} = (X'X)^{-1}X'y \tag{5.10}$$

In this form it is easy to see that $X'X$ is a (p X p) symmetric matrix and $X'y$ is a (p X 1) column vector. Note the special structure of the X'X matrix. The diagonal elements of $X'X$ are the sums of squares of the elements in the columns of X, and the off-diagonal elements are the sums of cross-products of the elements in the columns of X. Furthermore, note that the elements of $X'y$ are the sums of cross-products of the columns of X and the observations $\{\mathbf{y_i}\}$.

The fitted regression model is

$$\hat{y} = X\hat{\beta} \tag{5.11}$$

In scalar notation, the fitted model is

$$\hat{y}_i = \hat{\beta}_0 + \sum_{i=1}^{k} \hat{\beta}_j x_{ij} \quad \text{i= 1,2,. . . . ., n}$$

The difference between the actual observation y_i and the corresponding fitted value $\hat{y}_i$ is the residual, say $e_i = y_i - \hat{y}_i$. The (n X 1) vector of residuals is denoted by

$$e = y - \hat{y} \tag{5.12}$$

5.2.3 Estimating variance

It is also usually necessary to estimate the variance (σ^2). To develop an estimator of this parameter, consider the sum of the squares of the residuals, say

$$SS_E = \sum_{i=1}^{n} (y_i - \hat{y}_i)^2$$

$$= \sum_{i=1}^{n} e_i^2$$

$$= e'e$$

Substituting $e = y - \hat{y} = y - X\hat{\beta}$, we have

$$SS_E = (y - X\hat{\beta})'(y - X\hat{\beta})$$
$$= y'y - \hat{\beta}'X'y - y'X\hat{\beta} + \hat{\beta}'X'X\hat{\beta}$$

$$= y'y - 2\hat{\beta}'X'y + \hat{\beta}X'X\hat{\beta}$$

Because $X'X\hat{\beta} = X'y$, this last equation becomes

$$SS_E = y'y - \hat{\beta}'X'y \tag{5.13}$$

Eq.5.13 is called the error or the residual sum of squares, and it has n - p degrees of freedom associated with it. It can be shown that

$$E(SS_E) = \sigma^2(n-p)$$

so an unbiased estimator of σ^2 is given by

$$\hat{\sigma}^2 = \frac{SS_E}{n-p} \tag{5.14}$$

5.2.4 Tests for significance of regression

The test for significance of regression is a test to determine if there is a linear relationship between the response variable y and a subset of the regression variables $x_1, x_2, \ldots, x_k$. The appropriate hypotheses are

$$H_0 : \beta_1 = \beta_2 = \ldots\ldots\ldots = \beta_k = 0$$

$$H_1 : \beta_j \neq 0 \quad \text{for at least one j} \tag{5.15}$$

Rejection of H_0 in Eq. 5.15 implies that at least one of the regressor variables $x_1, x_2, \ldots, x_k$ contributes significantly to the model. The test procedure involves an analysis of variance portioning of the total sum of squares SS_T into a sum of squares due to the model (or to regression) and a sum of squares due to residual (or error), say

$$SS_T = SS_R + SS_E \tag{5.16}$$

Now if the null hypothesis $H_0 : \beta_1 = \beta_2 = \ldots\ldots\ldots = \beta_k = 0$ is true, then SS_R/σ^2 is distributed as X_k^2 where the number of degrees of freedom for X^2 is equal to the number of regressor variables in the model. The test procedure for $H_0 : \beta_1 = \beta_2 = \ldots\ldots\ldots = \beta_k = 0$ is to compute

$$F_0 = \frac{SS_R/k}{SS_E/(n-k-1)} = \frac{MS_R}{MS_E} \tag{5.17}$$

and to reject H_0 if F_0 exceeds $F_{\alpha,k,n-k-1}$. Alternatively, we could use the *p*-value approach to hypothesis testing and thus, reject H_0 if the *p*-value for the statistic F_0 is less than α.

A computational formula for regression sum of square (SS_R) may be found easily. We have derived a computational formula for SS_E in Eq. 5.16 that is,

$$SS_E = y'y - \hat{\beta}'X'y$$

where $\hat{\beta}'X'y$ is SS_R

The coefficient of multiple determination R^2 is defined as

$$R^2 = \frac{SS_R}{SS_T}$$

Coefficient of multiple determination (R^2) is a measure of the amount of reduction in the variability of y obtained by using the regression variables $x_1, x_2, \ldots\ldots\ldots x_k$ in the model. R^2 varies between 0 and 1. The value of R^2 should be nearer to 1 for the best fit of the model. However larger a value of R^2 does not necessarily imply that regression model is a good one. Adding a variable to the model always increases the R^2, regardless whether the additional variable is significant or not. Hence many a times it is preferred to use adjusted R^2, defined as

$$R^2_{adj} = 1 - \left(\frac{n-1}{n-p}\right)\left(1 - R^2\right) \qquad (5.18)$$

5.3 RESPONSE SURFACE METHODOLOGY

Response surface methodology (RSM) is a collection of mathematical and statistical techniques that are useful for the modelling and analysis of problems in which a response of interest is influenced by several variables and the objective is to optimise this response [Montgomery 2005].

In many engineering fields, there is a relationship between an output variable of interest 'y' and a set of controllable variables $\{x_1, x_2 \ldots . x_n\}$. In some systems, the

nature of the relationship between *y* and *x* values might be known. Then, a model can be written in the form [Puri and Bhattacharya 2005]

$$y = f(x_1, x_2, ..., x_n) + \varepsilon \tag{5.19}$$

where ε represents noise or error observed in the response *y*. If we denote the expected response be

$$E(y) = f(x_1, x_2, ..., x_n) = \hat{y} \tag{5.20}$$

then the surface represented by

$$\hat{y} = f(x_1, x_2, ..., x_n) \tag{5.21}$$

is called response surface. In most of the RSM problems, the form of relationship between the response and the independent variable is unknown. Thus the first step in RSM is to find a suitable approximation for the true functional relationship between *y* and a set of independent variables employed. Usually a second order model is utilised in response surface methodology [Li et al 2009, Kwak 2005, Montgomery 2005].

$$\hat{y} = \beta_o + \sum_{i=1}^{k} \beta_i x_i + \sum_{i=1}^{k} \beta_{ii} x_i^2 + \sum_{i} \sum_{j} \beta_{ij} x_i x_j + \varepsilon \tag{5.22}$$

The β coefficients, used in eq. 5.22 can be calculated by least square method. The second-order model is normally used when the response function is not known or nonlinear.

The necessary data for building the response models are generally collected by the experimental design. In this study, the collections of experimental data were adopted using central composite design (CCD). The factorial portion of CCD is a full factorial design with all combinations of the factors at two levels (high, +1 and low, −1) and composed of the six axial points and six central points (coded level 0) which is the midpoint between the high and low levels[Montgomery 2005]. The star points are at the face of the cubic portion on the design which corresponds to a value of α =1 and this type of design is commonly called the face-centered CCD. A total 20 different combinations (including six replicates of centre point each sighed the coded

value 0) were chose in random order according to a CCD configuration for three factors. The coded values of independent variables were found from equation

$$X_1 = \frac{x_1 - 10}{4}$$

$$X_2 = \frac{x_2 - 70}{20}$$

$$X_3 = \frac{x_3 - 12}{8}$$

Face-centred central composite design is a useful variation of the central composite design, in which the axial distance α=1. This type of design is used when the ranges of design variables are specified and these ranges are strict. The obvious region for the design is a cube. The experiment includes three controllable process factors (k = 3), whose levels are presented in Table3.3. Here, we follow the convention of coding the factor levels so the design points have coded levels for each factor. The region of interest, coded {−1, 1}, is a region determined by lower and upper limits on factor level setting combinations that are of major interest.

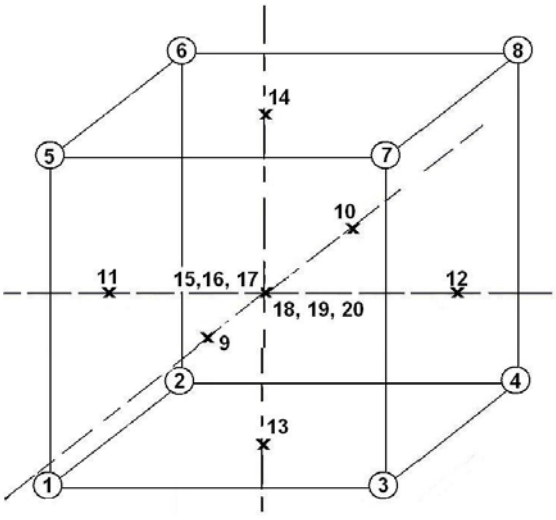

Figure 5.1 Representation of a 2^3 central composite design.

In this proposed work, face centered composite design (CCD) having 20 sets of experiments are sorted using the standard ordering and are carried out according to

experimental design matrix. The design is shown schematically in Figure 5.1. It is a two-level full factorial design with 8 factorial points (1-8), augmented with additional 6 centre (15-20) and 6 axial points (9-14) as shown in Figure 5.1.

5.4 DESIRABILITY FUNCTION

Until a few years ago, several objective functions were combined into a single scalar objective function, using arbitrary weightage factors, so that the problem could become computationally tractable. This 'scalarisation' of a vector objective function suffers from several drawbacks. One is that the results are sensitive to the values of the weighting factors used, which are difficult to assign on a-*priori* basis. What is even more important is that there is a risk of losing some optimal solutions. The desirability function approach [Derringer and Suich 1980; Deming, 1991] is a most widely used methods in the industry for the optimisation of multiple response processes. It is based on the idea that the "quality" of a product or process that has the multiple quality characteristics, with one of them outside of some "desired" limits, is completely unacceptable. The method finds operating conditions that provide the "most desirable" response values.

The desirability function approach is based on the idea that when one of the quality characteristics of an industrial process or product with many characteristics are not in the desired limits, then the overall quality of the industrial process or the product is not desirable. By this approach the process (and/or product) variables which yield the most desirable responses are found. The desirability function approach for the optimisation of the multi response problems was originally introduced by Harrington [1965]. Then another version was developed by Derringer and Suich [1980] which has been the one widely used in the literature. In their study, the overall desirability function, delivered as the geometric mean of linear individual desirability functions, is optimised by a univariate search technique which does not use any derivative information of the function. The desirability functions continue to be a commonly preferred method because it easily converts a multi response problem into a single response one.

A product performance is a function of responses associated with multiple quality characteristics. Each response has its own effect on the performance where one response may have a stronger influence on product performance than another [Raissi and Farsani 2009]. Also each response may be measured in different units. Hence it becomes difficult to combine all the different types of responses into a single entity that would indicate the level of product performance. The desirability function achieves this task by transforming the responses into dimensionless variables called as desirability index d_i. The range of a desirability index falls in the closed interval [0, 1]. A higher value of the desirability index for a response implies a higher contribution to the product performance by the particular response. The overall assessment of product performance is accomplished by multiplying all desirability indices to yield an aggregate desirability index D.

The desirability functions considered in this study are of Derringer and Suich's type. In a multi response optimisation problem each response can be expressed as

$$Y_j(\mathbf{x}) : \boldsymbol{R}^n \rightarrow \boldsymbol{R} \ (j = 1,2,....m) ,$$

where $\mathbf{x} \in \boldsymbol{R}^n$ ($\boldsymbol{R}$ denoting the real numbers) are the decision variables or controllable factors. An individual desirability function d_j (Y_j ($\mathbf{x}$)) : $\boldsymbol{R} \rightarrow \boldsymbol{R}$ assigns a number between 0 and 1; 0 being a completely undesirable and 1 being a completely desirable or ideal response value. One or two-sided desirability functions are used, depending on whether each of the n responses has to be maximised or minimised, or has an allotted target value.

For maximisation of the response d_i can be defined as[Derringer and Suich 1980]

$$\begin{aligned} \hat{d}(\hat{y}) &= \left[\frac{\hat{y} - L}{T - L} \right]^{wt} \rightarrow L < \hat{y} < T \\ 1 &\rightarrow \hat{y} > T \\ 0 &\rightarrow \hat{y} < L \end{aligned} \tag{5.23}$$

and for minimisation d_i is

$$d(\hat{y}) = \left[\frac{\hat{y} - H}{T - H}\right]^{wt} \rightarrow T < \hat{y} < H$$

$$1 \rightarrow \hat{y} < T \qquad (5.24)$$

$$0 \rightarrow \hat{y} > H$$

In Eq.-5.23 and 5.24, L, H and T are respectively the lowest, highest and the target values and wt is the weight. The value of weight wt can be varied between 0.1 and 10. The value of one creates a linear ramp function between the low value, goal and the high value. Increased weight moves the result towards the goal or its decrease creates the opposite effect [Jing et al. 2008]. The partial desirability function d_i ranges between 0, (for a completely undesired response), and 1, (for a fully desired response).

The partial desirability functions are then combined into a single composite response, the global desirability function D, defined as the geometric mean of the different d_i-values [Nguyen et al. 2009]:

$$D = (d_1^{v_1} * d_2^{v_2} * d_n^{v_n})^{\frac{1}{\sum v_n}} \qquad (5.25)$$

In eq (5.25) v_1, v_2, etc., are the relative importance assigned to the response 1, 2, etc. respectively and n is the number of response. The relative importance is a comparative scale for weighting each of the resulting d_i in the overall desirability product and it varies from the least important (v_i = 1) to the most important (v_i = 5). It is noteworthy that the outcome of the overall desirability D depends on the importance value that offers users flexibility in the definition of desirability functions

In this formulation of desirability functions, possible correlations between the responses are not taken into account [Islam et al. 2010].

5.4.1 Optimisation of desirability functions

The optimisation of overall desirability function becomes a complicated task when there are two sided individual desirability functions in the problem. In the two-sided desirability function formulation, the target value is a non-differentiable point and

hence the function is not smooth at this point. To optimise the overall desirability function given in eq-(5.25) involving two-sided desirabilities, one way is to use the optimisation techniques that do not employ the derivative information to find the optimum. Another way is to modify the individual desirability functions by approximation approaches to smooth it and then use the gradient based methods.

In the study of Derringer and Suich [1980], firstly second degree polynomials are fit by regression to some data collected through experimentation to model the relations between the responses and the factors. Then, the individual desirabilities of these responses are calculated and used to calculate the overall desirability. Hence, for each set of factor levels, an overall desirability value is obtained. Then, all factor levels are searched to find the optimal *D* by a direct search method similar to that of Hooke and Jeeves [1960].

5.5 RESULTS AND DISCUSSIONS

5.5.1 Response surface model

Experiments were conducted on Al-SiC composites with SiC volume percentage, feed and depth of cut as the factors in the experimentation. Each of factor was studied at two different levels to analyse the response of the desired output. In the present study specific energy, MRR and surface roughness have been selected as the responses to be optimised. A response surface model is developed for each of the response based on the full factorial experimentation. It is observed that the use of full factorial experimentation guarantees a uniform data distribution over the entire design space but is practical only when the number of variables is small. In the underlying study, full factorial, Face-centered central composite design (CCD) in which $\alpha=1$ is adopted. The design is a two-level full factorial with 8 factorial points, augmented with additional 6 centre and 6 axial points. Table 5.2 shows the design matrix along with experimental results. These experiments are the subset of experiments depicted in Table 3-5 with 6 cente point experiments performed at random.

The development and the analysis of response surface model are carried out using MINITAB15 software. Eq. (5.26) –eq. (5.28) represents the response surface

model developed for specific energy, specific material removal rate and surface roughness respectively.

Table 5.2 Experimental Results

Test No	SiC Vol %	Feed (mm/s)	*a* (µm)	*u* (J/mm^3)	$Q_w^{'}$ (mm^3/mm·s)	R_a (µm)
1	8	60	8	145.585	0.498	1.04
2	12	60	8	124.449	0.518	0.66
3	8	80	8	95.881	0.556	1.17
4	12	80	8	78.005	0.714	0.72
5	8	60	16	135.640	0.675	1.14
6	12	60	16	122.177	0.772	0.81
7	8	80	16	71.529	0.870	1.30
8	12	80	16	65.516	1.067	0.87
9	8	70	12	88.625	0.605	1.16
10	12	70	12	77.047	0.667	0.79
11	10	60	12	119.907	0.608	0.86
12	10	80	12	71.379	0.926	0.98
13	10	70	8	116.596	0.555	0.87
14	10	70	16	84.575	0.829	0.95
15	10	70	12	91.937	0.655	0.91
16	10	70	12	95.097	0.708	0.95
17	10	70	12	84.498	0.660	0.89
18	10	70	12	94.436	0.708	0.91
19	10	70	12	88.498	0.659	0.92
20	10	70	12	95.543	0.707	0.93

The regression equation for specific energy is

$$\hat{y}_1 = 683.819 + 15.727X_1 - 12.608X_2 - 18.043X_3 - 1.379X_1^2 + 0.0729X_2^2 + 0.765X_3^2 + 0.067X_1X_2 + 0.305X_1X_3 - 0.077X_2X_3 \quad (5.26)$$

The regression equation for specific material removal rate is

$$\hat{y}_2 = 3.555 + 0.173X_1 - 0.120X_2 - 0.380X_3 - 0.016X_1^2 + 0.00007X_2^2 + 0.0001X_3^2 + 0.015X_1X_2 + 0.002X_1X_3 + 0.0007X_2X_3 \quad (5.27)$$

The regression equation for surface roughness is

$$\hat{y}_3 = 2.096 - 0.311X_1 + 0.015X_2 + 0.013X_3 + 0.014X_1^2 - 1.1E-09X_2^2 - 6.25E-04X_3^2 - 0.001X_1X_2 + 0.001X_1X_3 + 9.38E-05X_2X_3 \quad (5.28)$$

where $\hat{y}_{1,}\hat{y}_2$ *and* $\hat{y}_3$ are the predicted responses for specific energy, specific material removal rate and surface roughness respectively and X_1, X_2 and X_3 are the volume percentage of SiC, feed and depth of grind respectively.

5.5.2 Model adequacy checking

Before the conclusions from the analysis of variance are adopted, the adequacy of the underlying model should be checked. Proceeding with exploration and optimisation of a fitted response surface will likely give poor or misleading results unless the model has an adequate fit. Residual analysis is one of the techniques for checking the model adequacy.

A check of the normality assumption can be made by constructing a normal probability plot of the residuals. If the residuals plot is approximately along a straight line, then the normality assumption is satisfied. In the residual plot if the residuals are randomly scattered, then it suggests that the variance of original observations is constant for all values of *y*.

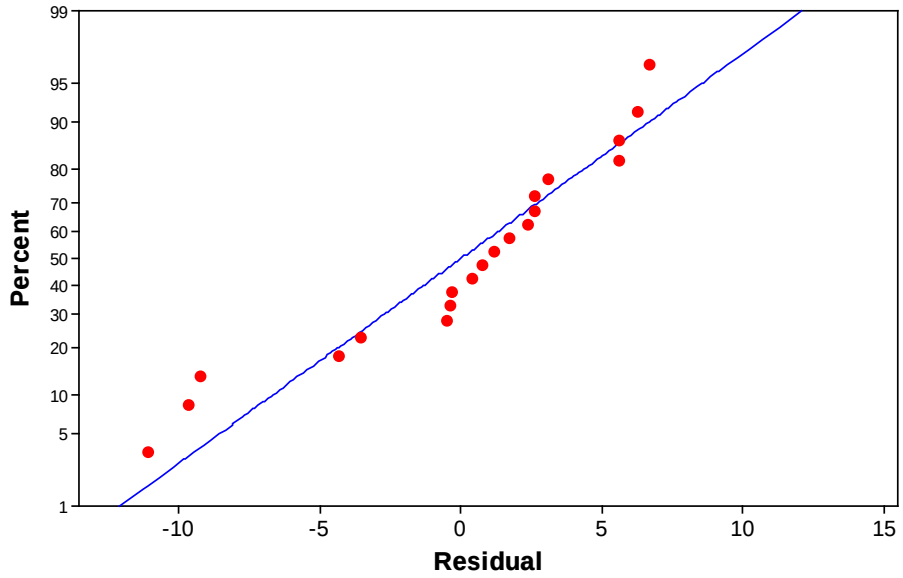

(a)

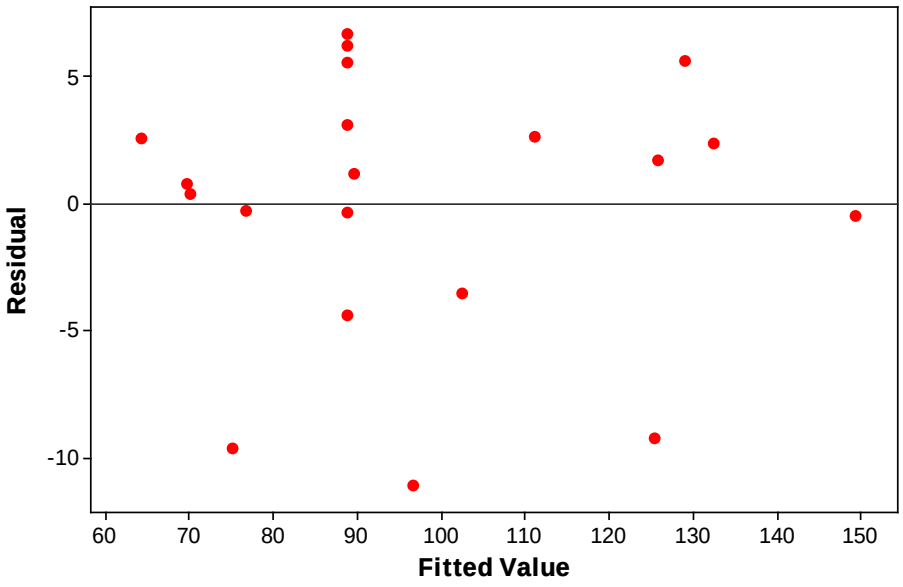

(b)

Figure 5.2 (a) Normal probability plot and (b) Residual plot for specific energy.

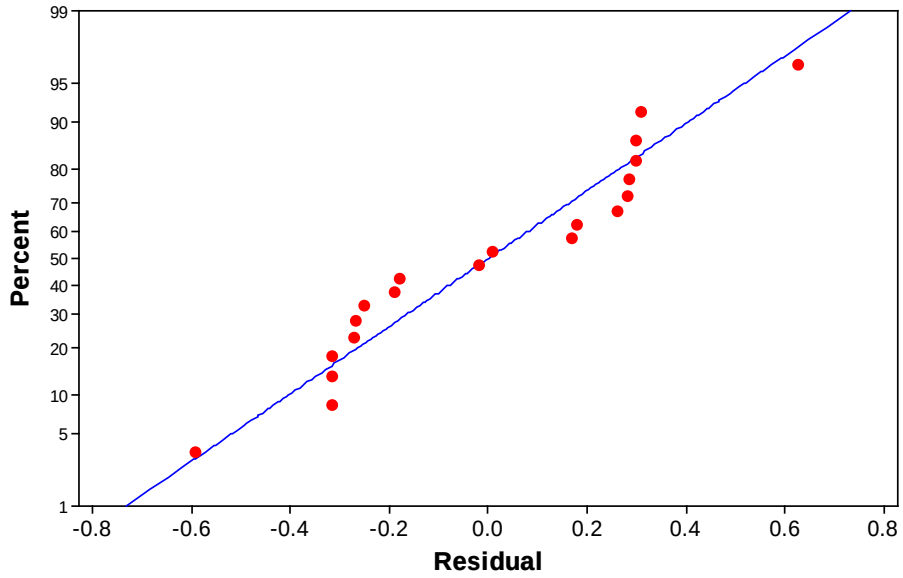

(a)

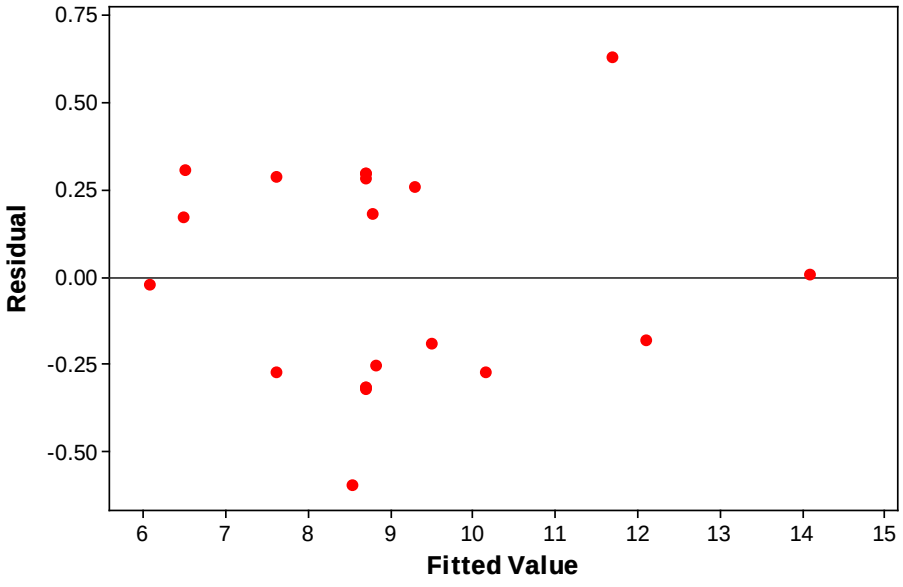

(b)

Figure 5.3 (a) Normal probability plot (b) Residual plot for MRR.

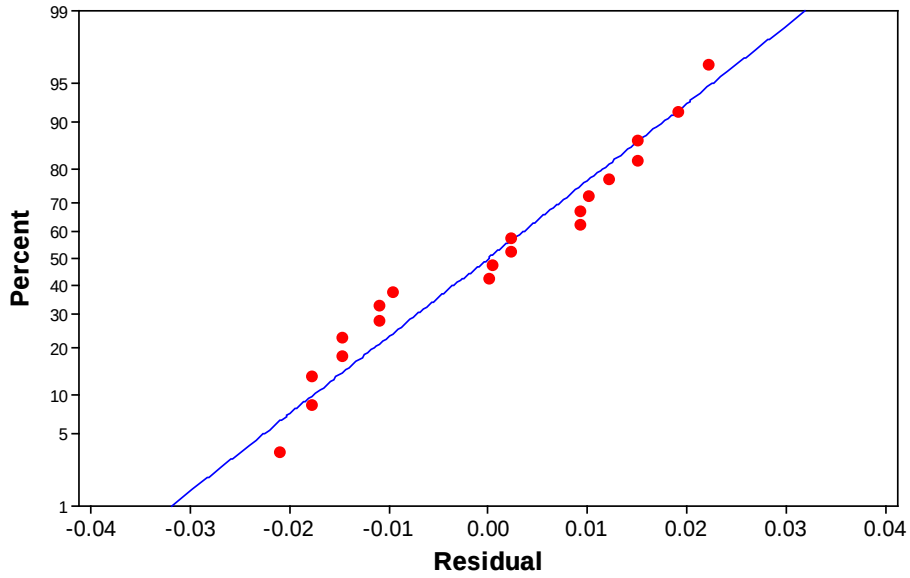

(a)

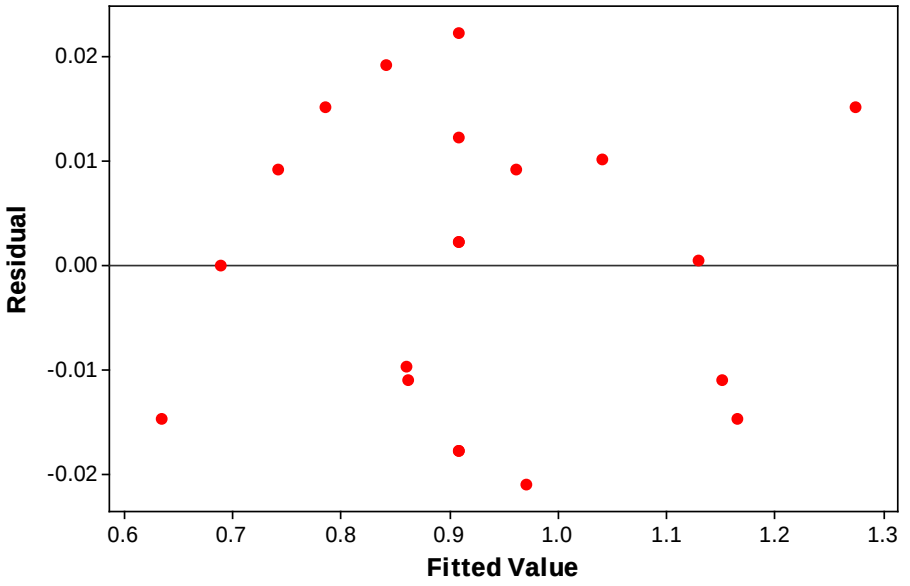

(b)

Figure 5.4 (a) Normal probability plot (b) Residual plot for surface roughness.

The normal probability plot, histogram plot and residual plot of residuals are the means of checking the adequacy of the developed model. Figure 5.2-5.4 shows the

normal probability and residual plot for the specific energy, MRR and surface roughness respectively. The residual plot for all the three responses does not reveal anything particularly troublesome as the residual plot for each of the response does not follow any particular pattern.

5.5.3 Analysis of variance for regression

Analysis of Variance (ANOVA) is a statistical technique to compare two or more means. By performing ANOVA on the available experimental data it is possible to understand a concrete visualisation of the impact of various factors and their interactions on the response. That is, ANOVA will signify the relative importance of each factor on the response.

In the present study ANOVA is performed to find the lack of fit in the developed model. ANOVA is also performed to identify the significant factors and their interaction which affects the performance parameters namely, specific energy, MRR and surface roughness. Table 5.3- Table 5.5 shows the results of ANOVA for Specific energy, MRR and surface roughness respectively.

Table 5.3 ANOVA for specific energy

Source	**Degrees of Freedom**	**Seq Sum of Square**	**Adj Mean Square**	**F-value**	**P-value**
Regression	9	9387.67	1043.07	33.94	0.000
Linear	3	8194.64	2731.55	88.89	0.000
Square	3	1055.2	351.73	11.45	0.001
Interaction	3	137.83	45.94	1.5	0.275
Residual Error	10	307.3	30.73		
Lack-of-Fit	5	211.34	42.27	2.2	0.203
Pure Error	5	95.97	19.19		
Total	19	9694.97	1043.07	33.94	

R^2=96.83% R^2_{adj} =93.98%

Table 5.4 ANOVA for material removal rate

Source	Degrees of Freedom	Seq Sum of Square	Adj Mean Square	F-value	P-value
Regression	9	0.365	0.041	32.75	0.000
Linear	3	0.330	0.110	88.8	0.000
Square	3	0.019	0.006	5.22	0.020
Interaction	3	0.016	0.005	4.24	0.035
Residual Error	10	0.012	0.001		
Lack-of-Fit	5	0.009	0.002	2.31	0.190
Pure Error	5	0.004	0.001		
Total	19	0.378	0.041		

R^2 = 96.78% R^2_{adj} =93.88%

Table 5.5 ANOVA for surface roughness

Source	Degrees of Freedom	Seq Sum of Square	Adj Mean Square	F-value	P-value
Regression	9	0.466	0.0518	138.76	0.000
Linear	3	0.449	0.1498	401.39	0.000
Square	3	0.012	0.0041	11.01	0.002
Interaction	3	0.004	0.0014	3.87	0.045
Residual Error	10	0.004	0.0004		
Lack-of-Fit	5	0.002	0.0003	0.79	0.598
Pure Error	5	0.002	0.0004		
Total	19	0.470			

R^2= 99.21% R^2_{adj} = 98.49%

5.5.4 Test for lack of fit

A first-order design allows the experimenter to determine, when the first-order model is no longer adequate, provided that there are more design points than first-order

model parameters, and the design includes replication at one or more points. There is said to be model lack-of-fit when the model does not adequately represent the mean response as a function of the factor levels. Lack of fit of the first-order model occurs when the local response surface is no longer a plane. Hence the designer will go for higher order model adequacy checking. The ratio of sum of square of lack of fit to sum of square of pure error is used to check the lack of fit. The null hypothesis is rejected at confidence level α if this ratio exceeds $F_{\alpha, n_d - p - 1, n - n_d}$ where n is the total number of trreatments, p is the number of design factor and n_d is the number of distinct coded treatment combinations [Dean and Voss 1999]

It can be observed from Table 5.3-5.5 that, F-test value for lack-of-fit of the model developed for specific energy, MRR and surface roughness are respectively 2.2, 2.31 and 0.79. The F-value for lack-of-fit ($F_{0.05, 5, 5}$) from standard F-distribution is 5.05. Since the F-value of lack-of-fit for the developed model is less than the theoretical value, it indicates that lack-of fit is insignificant and developed model is adequate [Seeman et al. 2010]. Further, ANOVA for the regression reveals that, R^2 value for all the model is greater than 95%. It indicates that the developed model fits very well with the experimental results.

5.5.5 Response surface plots

Response surface plots such as contour and surface plots are useful for establishing desirable response values and operating conditions. In a contour plot, the response surface is viewed as a two-dimensional plane where all points that have the same response are connected to produce contour lines of constant responses. A surface plot generally displays a three-dimensional view that may provide a clearer picture of the response. If the regression model (i.e. first-order model) contains only the main effects and no interaction effect, the fitted response surface will be a plane (i.e. contour lines will be straight). If the model contains interaction effects, the contour lines will be curved and not straight. Both contour and surface plots help experimenters to understand the nature of the relationship between the two factors and the response.

Based on the model developed in Eq-(5.26) – eq-(5.28) for the responses namely specific energy, MRR and surface roughness, the contour plots and surface plots were drawn to visualise the effect of process variables on the response. Figure 5.5-5.7 shows the contour plots and surface plot for specific energy, MRR and surface roughness respectively.

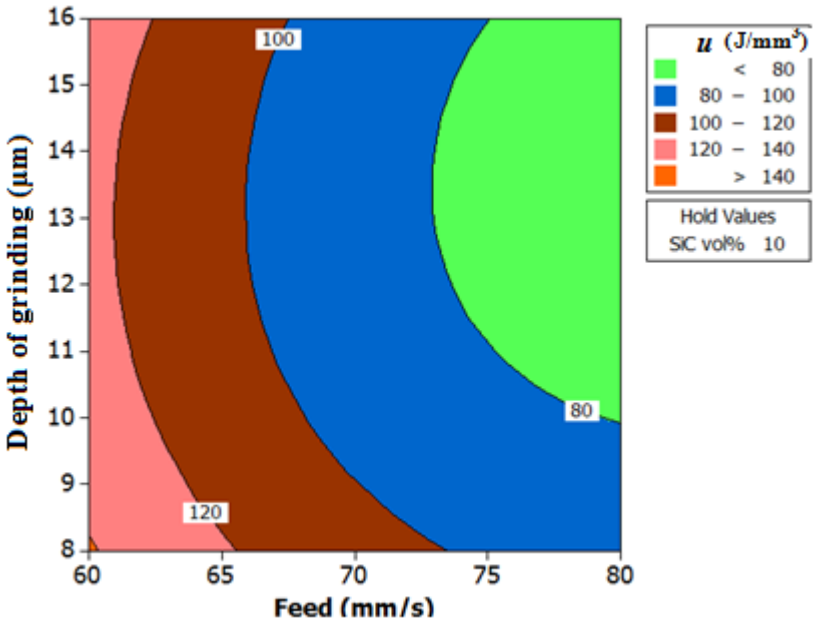

(a)

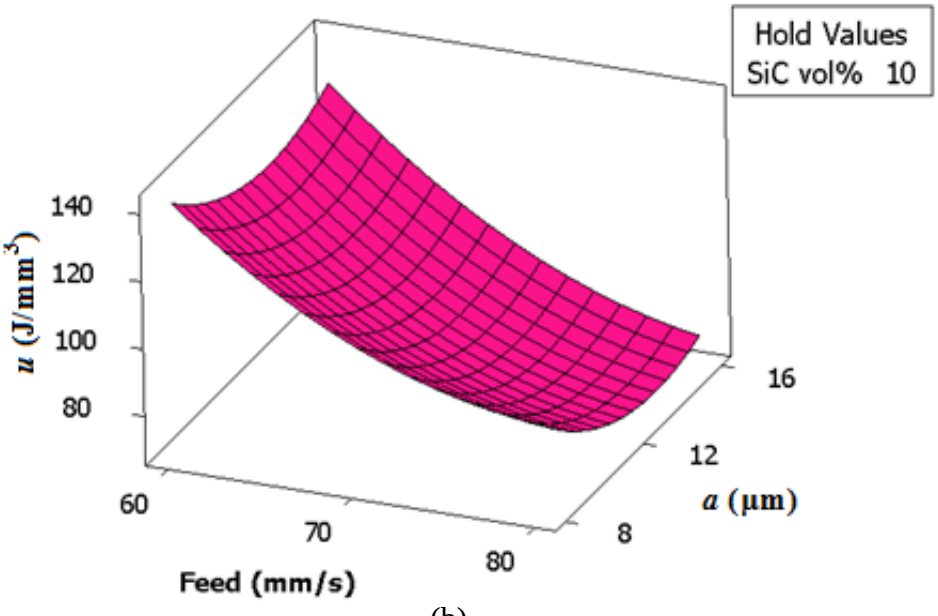

(b)

Figure 5.5 (a) Contour plot for specific energy (b) surface plot for specific energy

Contour plot for specific energy from Figure 5.5 reveals that specific energy decrease with increase in feed. It is also observed that specific energy decrease gradually with increase in depth of cut and further increases.

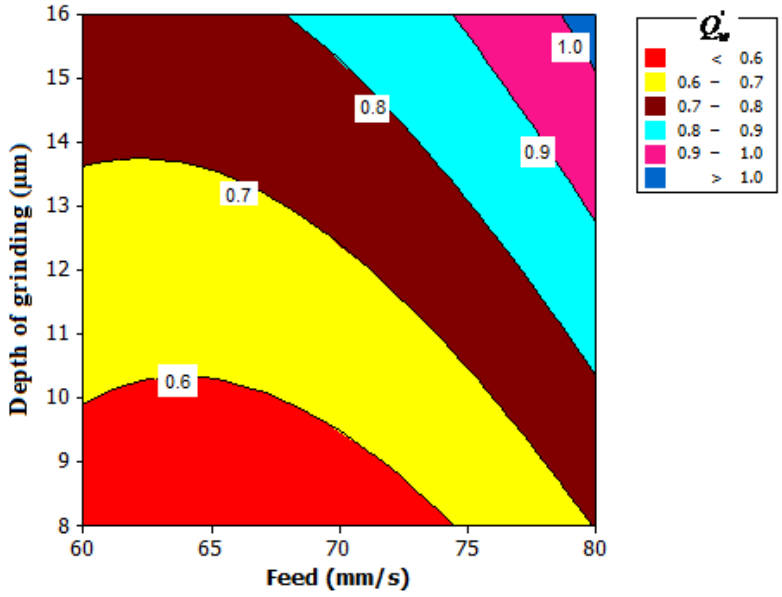

(a)

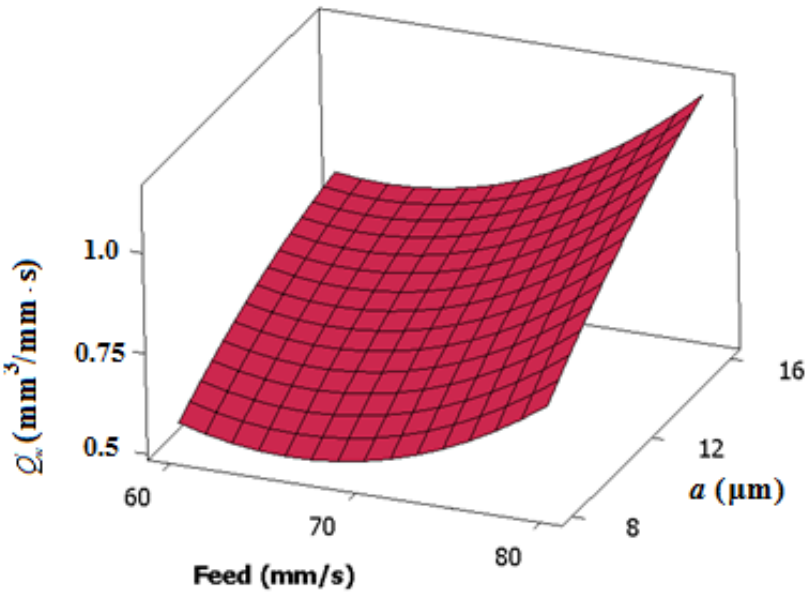

(b)

Figure 5.6 (a) Contour plot for MRR (b) Surface plot for MRR

Figure 5.6 shows the contour plot for MRR. It is observed that, MRR increases with increase in feed and depth of cut.

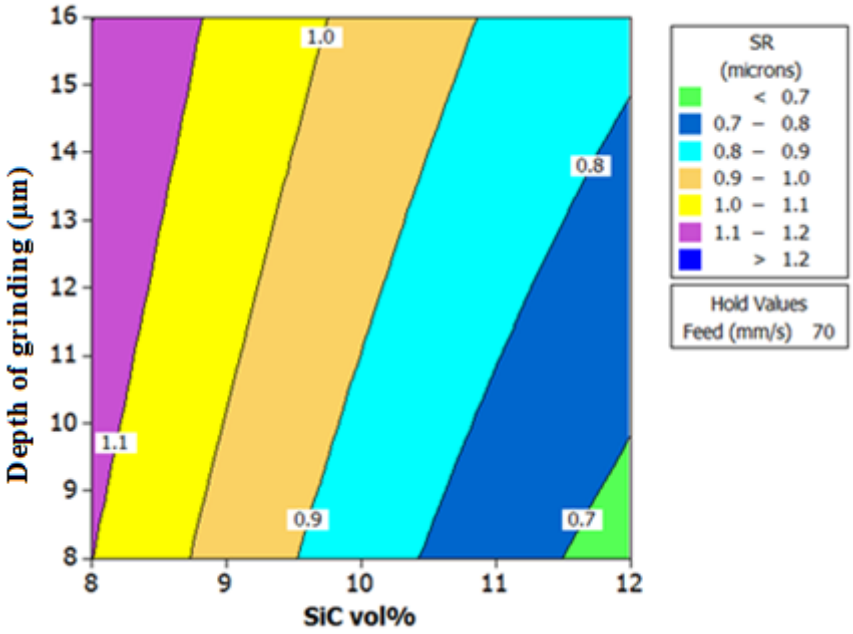

(a)

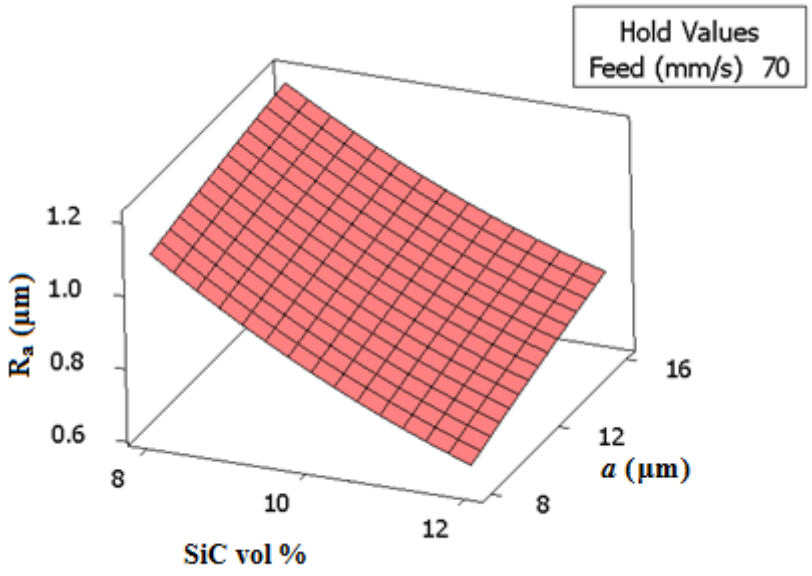

(b)

Figure 5.7 (a) Contour plot for surface roughness. (b) Surface plot for surface roughness

Figure 5.7 shows the contour and surface plot for surface roughness. It is observed from the plot that, surface finish improves with increase in SiC vol % and

deteriorates with increase in dept of cut. Hardness of the MMCs increases with increase in reinforcing material [Swamy et al. 2011]. In MMCs grinding, the morphology of the ground surfaces is characterised by the presence of side flow ploughing marks and scratches and by areas which evidence high plastic deformation and lack of ridges. It has been noted that the zones with high plastic deformation decrease for materials which exhibit higher hardness values thus improving the surface finish [Di Ilio et al. 2009].

It is evident from the micrograph (Fig. 5.8) that, ploughing is more significant on the specimen with less SiC volume content which results in poor surface finish [Di Ilio et al. 2009].

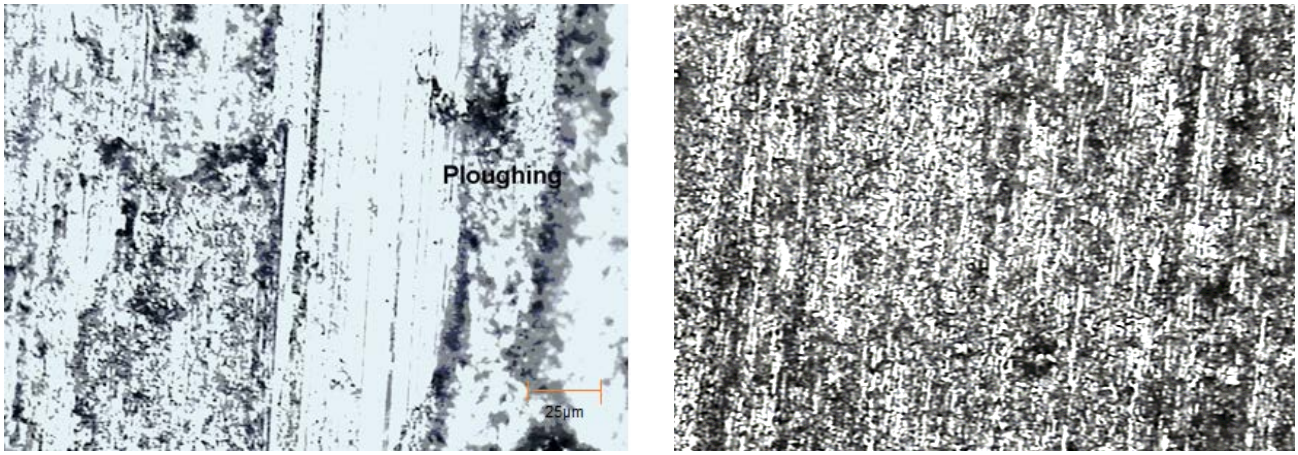

(a) (b)

Figure 5.8 Ground surface of (a) 8 vol% SiC and (b) 12 vol% SiC at 60mm/s feed and 12µm depth of grinding at 100X magnification.

5.5.6 Process Optimisation

The regression model developed for the specific energy, material removal rate and surface roughness is given in eq. (5.26) - eq (5.28). The optimisation process was performed using desirability function, the option available in MINITAB 15 software. A prediction profile for the performance parameters consists of a series of graphs, one for each process variable, of the performance parameters at different levels of one process variable, holding the levels of the other process variables constant at specified values, called target values. If appropriate target values for the independent variables have been selected, inspecting the prediction profile it is possible to explain which

levels of the process variables produce the most desirable predicted response on the performance variable. In the current study, the objective is to minimize the specific energy, maximize the material removal rate and to minimize the surface roughness.

As mentioned in eq. (5.23) and eq. (5.24) it is necessary to specify the lower limit and target value of the response for the maximisation problem and target value and minimum value for the minimisation problem. The CCD design matrix results represent maximum specific energy (145.785 J/mm^3), minimum material removal rate (0.45 mm^3/mm·s) and maximum surface roughness (1.3 µm). The target values for Specific energy, MRR, and surface roughness were assigned as 60 J/mm^3, 0.95 mm^3/mm·s and 0.7 µm respectively. These target values were assigned based on the goal to achieve the desirability score of 1.0. Afterwards, the predicted responses at each level of each factor, holding all other factors constant at their current setting are calculated, and the individual desirability scores for the predicted values for each performance parameters are then combined by computing their geometric mean according to eq.(5.25).

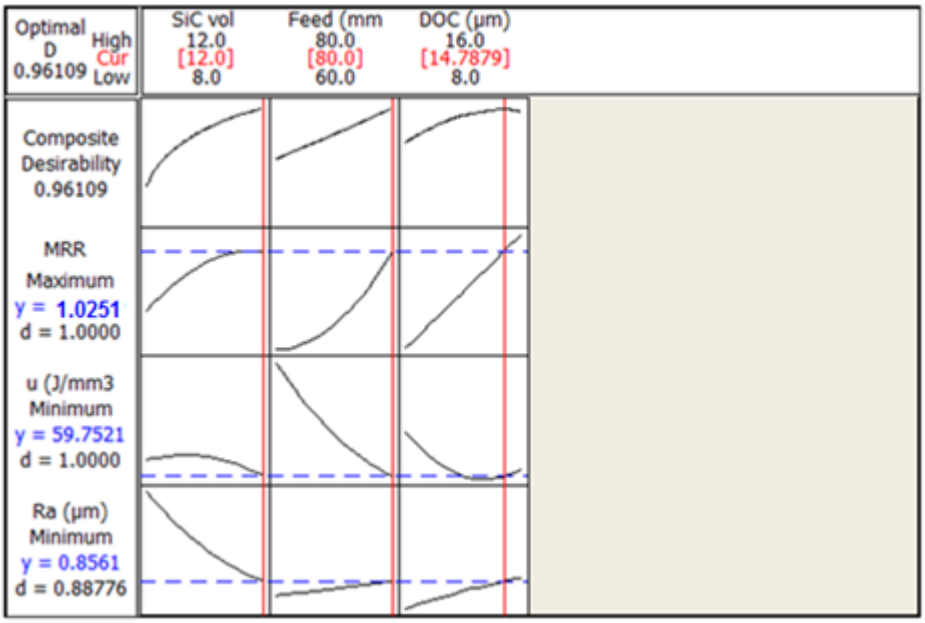

Figure 5.9 Desirability function plot

On the basis of the above calculations the optimal conditions were found to be specific energy of 59.752 J/mm^3, surface roughness of 0.86 µm and MRR of 1.025

$mm^3/mm \cdot s$. The respective individual desirability function values are 1.000, 1.000 and 0.887. The composite desirability is 0.961. The details are shown in Figure 5.9.

5.6 VALIDATION OF RESULTS

Experiments were conducted to validate the results obtained from the developed statistical optimisation model. The response surface models given by eq. 5.26 –5.28 were validated by the set of test runs. Table 5.6 gives the results obtained from experimental test, and the predicted results obtained from the developed response surface model. Test No. 1 refers to the comparison of the results obtained from experiment, and RSM for the factors (process variables) listed in Table 5.2. Test No.2-test no 5 refers to the process variables other than listed in Table 5.2 and test no. 6 and 7 is performed at the optimal conditions obtained from the desirability function approach.

The percentage error between the experimental results and developed model is calculated as

$$Percentage \quad error = \frac{Experimental \;\; value - Predicted \;\; value}{Experimental \;\; value} * 100$$

It can be observed from the Table 5.6 that the experimental results and the predicted results are in close agreement. Fig. 5.10 shows the plot of error between the predicted and experimental results of specific energy, MRR and surface roughness. The percentage error for specific energy is within 8.0%, for MRR is within 7.0% and for surface roughness the error is within 6.0%. Hence it can be concluded that, RSM can effectively be used for predicting the performance parameters of the surface grinding process.

Table 5.6 Validation of experimental results

Test No.	Process variables			Method	Performance Parameters			Percentage error		
	SiC vol %	Feed (mm/s)	*a* (μm)		*u* (J/mm^3)	MRR (mm^3/mm·s)	R_a (μm)	*u*	MRR	R_a
1	10	70	8	Experimental	116.596	0.555	0.87	5.06	0.79	2.3
				RSM	110.686	0.550	0.85			
2	8	80	12	Experimental	77.173	0.784	1.19	7.77	6.73	4.2
				RSM	71.172	0.731	1.24			
3	10	80	10	Experimental	82.338	0.806	0.89	3.15	2.43	-5.6
				RSM	79.742	0.786	0.94			
4	8	80	14	Experimental	68.740	0.846	1.31	1.82	4.47	3.05
				RSM	67.488	0.808	1.27			
5	12	70	10	Experimental	89.11	0.579	0.77	6.05	-5.3	3.89
				RSM	83.713	0.610	0.74			
6	12	80	14	Experimental	55.443	1.052	0.87	-5.68	6.03	3.45
				RSM	58.593	0.989	0.84			
7	12	80	14	Experimental	63.296	1.058	0.89	7.43	6.5	5.61
				RSM	58.593	0.989	0.84			

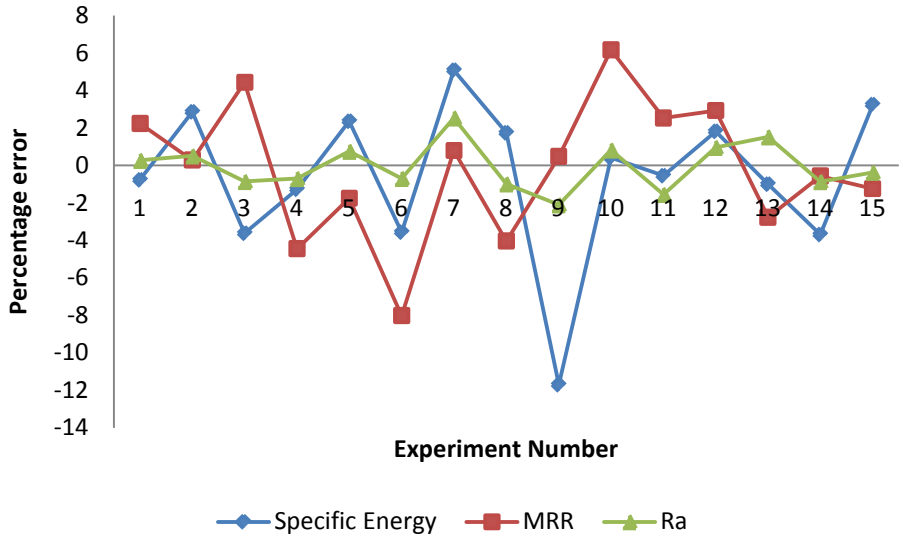

Figure 5.10 Percentage error plot

Figure 5.11 shows the ground surface of the specimen Al 6061 SiC 12 vol% ground at feed 80mm/s and depth of grinding 14 µm. The micrograph was taken with eMpower optical microscope with 100X magnification. The surface roughness obtained for this ground condition is 0.82µm. The feed mark observed in the micrograph is a natural defect because of infeed. Additionally, a ground surface may be characterized by clean cutting paths and ploughed materials to the sideway [Hecker and Liang 2003].

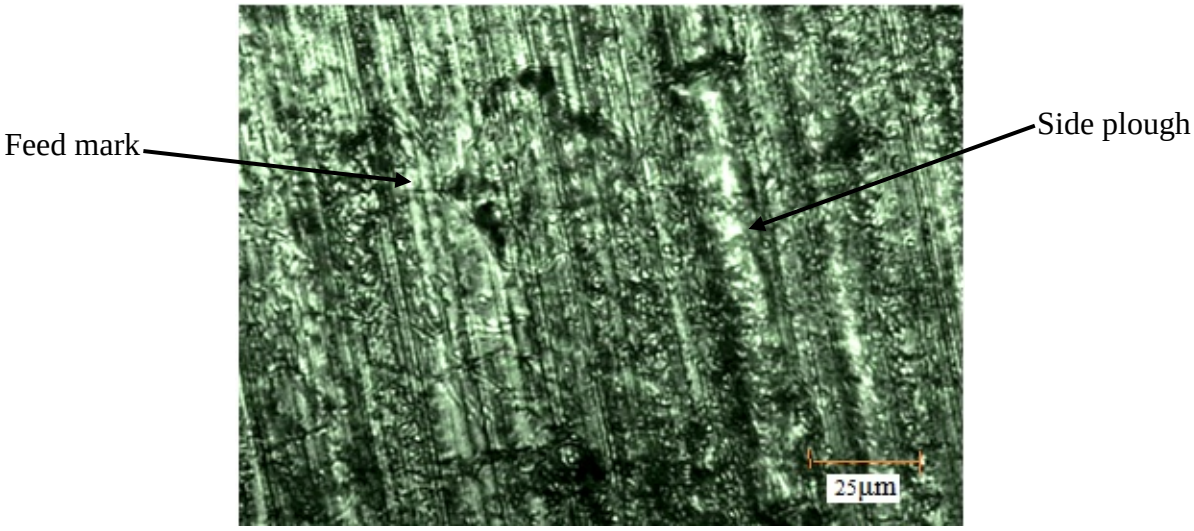

Figure 5.11 Optical micrograph of ground surface Al 6061 SiC 12 vol% ground at feed 80mm/s and depth of grinding 14 µm and magnification 100X.

In the next chapter, the regression models obtained through RSM for specific energy, material removal rate and surface roughness in surface grinding of DRACs were simultaneously optimized by novel genetic algorithm approach.

Chapter 6

MULTI OBJECTIVE OPTIMISATION OF SURFACE GRINDING PROCESS BY NOVEL GENETIC ALGORITHM

This chapter discusses the multi objective optimisation strategy for finding the optimal solution for the performance parameters in surface grinding of DRACs. A novel and time saving method of non-dominated sorting genetic algorithm called enhanced non-dominated sorting genetic algorithm-II is employed for the study.

6.1 INTRODUCTION

A multi objective optimisation problem arises when two or more objective functions are simultaneously optimised. Generally such problems consist of conflicting objectives so that it is not possible to obtain a single solution which is optimum in all the objectives. Instead of a single optimum solution, a set of optimum solutions exists in such cases. Members of the solution set are such that there exist no solution in the set which is better than the others in all the objectives; neither does a solution exist in the set which is worse than the others in all the objectives.

Since the pioneering work of Schaffer (1985) in the field of vector evaluated genetic algorithm, multi-objective genetic algorithms have been attracting increased interest. These algorithms process a set of solutions, the population, in parallel which makes them particularly suited to this task. They naturally generate a set of solutions approximating the Pareto front.

Multi objective optimisation problems can prove very difficult. Objectives can be conflicting and incomparable [Hwang et al. 1980]. This prohibits the use of aggregation methods[Jones 2004]. In such situations a single optimum can rarely be identified. Instead, a set of non-dominated or efficient solutions are required. These sets are also known as the Pareto optimal set.

In the first part of this chapter, a brief study of basics of genetic algorithms and non-dominated sorting genetic algorithms (NSGA-I and NSGA-II) are discussed.

Second part discusses the novel genetic algorithm adopted in the thesis. Final part of the chapter is devoted for results and discussion.

6.2 ALGORITHMS FOR MULTI OBJECTIVE OPTIMISATION

Extensive research has been reported on the algorithms used for generating the multi objective optimisation. The algorithms include: vector evaluated GA (VEGA), [Schaffer, 1985], vector-optimised evolution strategy (VOES), weight-based GA, multiple-objective GA [Fonseca and Fleming, 1993], distance-based Pareto GA [Osyczka and Kundu, 1995], non-dominated sorting genetic algorithm-I (NSGA-I), [Srinivas and Deb, 1993], random-weighted GA [Ishibuchi and Murata 1996], strength Pareto evolutionary algorithm (SPEA), [Zitzler et al. 1998], Pareto-archived evolution strategy [Knowles and Corne, 2000] and NSGA-II [Deb et al. 2002]. These algorithms have been extensively reviewed in the recent books by Deb (2008) and the advantages and disadvantages of the different algorithms have been pointed out, using simple examples.

Process modeling and optimisation are two important issues in grinding. The grinding process is characterised by a multiplicity of dynamically interacting process variables. Surface finish, material removal rate and specific energy are considered to be the important factors in predicting performance of grinding process. Several authors have developed the mathematical model for grinding process using RSM [Kwak, 2005, Shetty et al. 2008, Seeman et al. 2010]. Wen et al. (1992) applied quadratic programming (QP) to solve the problem by formulating the problem as a multi objective function model. The optimisation problem has also been solved applying various non-traditional optimisation methods including genetic algorithms (GA) [Saravanan et.al. 2002], particle swarm optimisation (PSO) [Asokan(2005)], scatter search (SS) [Bhaskar et. al. 2001], and differential evolution (DE) [Gopala Krishna 2007]. However, the classical multi objective optimisation technique, the method of weighted sum has been used in all these earlier works reported. Suresh et.al (2002) applied genetic algorithm for optimisation of surface roughness while machining mild steel using TiN-coated tungsten carbide tool. Saravanan et.al (2001) applied multi objective GA approach for optimisation of grinding process and compared the results with quadratic programming and observed that improved results were obtained by GA

approach. Hsu (2004) demonstrated the superiority of GAs over other network capability in terms of its optimised search.

6.3 BASIC GENETIC ALGORITHM

Genetic Algorithms are a family of computational models inspired by evolution. These algorithms encode a potential solution to a specific problem on a simple chromosome like data structure and apply recombination operators to these structures so as to preserve critical information. Genetic algorithms are often viewed as function optimisers, although the range of problems to which genetic algorithms have been applied is quite broad.

The genetic algorithm (GA), inspired by concepts of natural selection and evolutionary processes [Goldberg, 1989], is a derivative-free, population-based optimisation method.

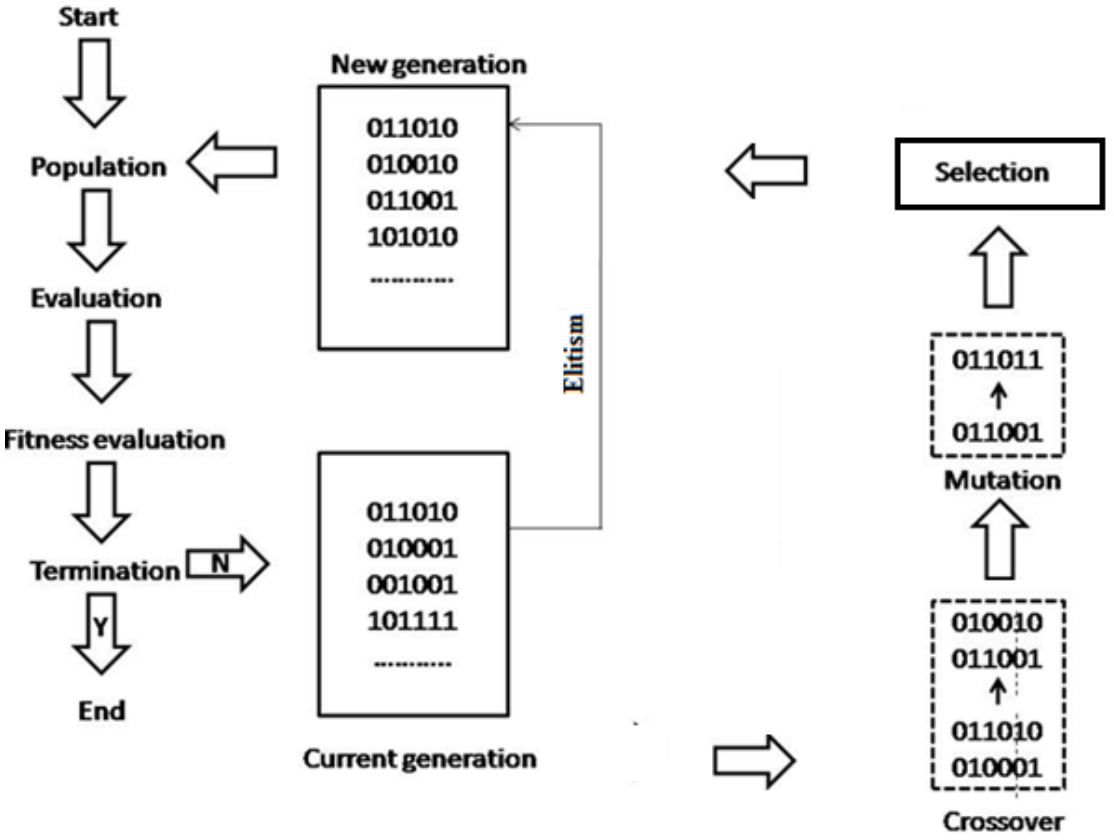

Figure 6.1 Overview of genetic algorithm evolution

The problem-specific knowledge is translated into the GA framework by the encoding scheme, which transforms points in the solution space into binary bit strings or chromosomes. Each chromosome is associated with fitness values. The GA stores a set of points as a population, representing the gene pool for the solution. A group of randomly generated chromosome forms the first generation, from which successive generations are repeatedly evolved through genetic operators – namely selection, crossover, mutation and elitism – towards populations with better fitness values (Figure 6.1).

In GA terminology, a solution vector is called an individual or a chromosome. Chromosomes are made of discrete units called genes. Each gene controls one or more features of the chromosome. In the original implementation of GA, genes are assumed to be binary numbers.

6.3.1 Genetic algorithm operators

GA operates with a collection of chromosomes, called a population. The population is normally randomly initialised. GA uses two operators to generate new solutions from existing ones: crossover and mutation [Konak et al., 2006].

6.3.1.1 Crossover: The crossover operator is the most important operator of GA. It is a genetic operator used to vary the coding of chromosomes from one generation to the next. In crossover, two parent chromosomes, are combined together to form new chromosomes, called offspring. The parents are selected among existing chromosomes in the population with reference towards fitness so that offspring is expected to inherit good genes which make the parents fitter. By iteratively applying the crossover operator, genes of good chromosomes are expected to appear more frequently in the population, eventually leading to convergence to an overall good solution. The mutation operator introduces random changes into characteristics of chromosomes.

6.3.1.2 Mutation: Mutation is generally applied at the gene level. It is a genetic operator used to maintain genetic diversity by triggering small random changes in the bits of a chromosome. The prime purpose of mutation is to allow the algorithm to avoid local minima by preventing the population of chromosomes from becoming too similar to each other, thus slowing or even stopping evolution. In typical GA

implementations, the mutation rate is very small, typically less than 1%. However, the mutation plays a critical role in GA. As discussed earlier, crossover leads the population to converge by making the chromosomes in the population alike. Mutation reintroduces genetic diversity back into the population and assists the search escape from local optima. Reproduction involves selection of chromosomes for the next generation. In the most general case, the fitness of an individual determines the probability of its survival for the next generation.

There are different selection procedures in GA depending on how the fitness values are used. Roulette wheel selection, proportional selection, ranking, and tournament selection are the most popular selection procedures.

6.3.2 Procedure for basic genetic algorithm

The procedure for genetic algorithm is shown in Fig 6.1 and the same is explained the following section:

1. Initialisation: Randomly generate the initial population of size N and set i = 0.

2. Fitness Evaluation: Evaluate the fitness value for each population based on its objective function value.

*3. Termination criteria***:** If the stopping criterion is satisfied, terminate the search and display the result else, go to Step 4.

4. (i) Crossover: To generate the offspring using crossover, randomly select two parents solution from the initial population and then generate the two offspring using crossover operator.

*(ii) Mutation***:** This operator randomly **s**elects one parent solution from the initial population and applies the mutation operator to generate a single offspring.

5. Selection: Select N solutions from generated population and the old population, based on their fitness. Set generation i = i+1. Go to step 2.

6.4 MULTI OBJECTIVE OPTIMISATION USING GENETIC ALGORITHM

Being a population based approach, GAs are well suited to solve multi objective optimisation problems. A generic single-objective GA can be easily modified to find a set of multiple non-dominated solutions in a single run. The ability of GA to simultaneously search the different regions of a solution space makes it possible to find a diverse set of solutions for difficult problems with non-convex, discontinuous, and multi-modal solutions spaces [Carlos et al. 2002].

As there is rarely a case that a single point in solution space simultaneously optimises all objective functions, trade-off solutions are instead sought after. For example if objective functions are to be minimised, a vector of decision variable $x_i \in F$ is Pareto optimal if $f_j(x_i^*) \leq f_j(x_i)$ for all j and

$$f_j(x_i^*) < f_j(x_i) \text{ in at least one j.}$$

This concept gives a set of solutions called Pareto optimal set. The x_i^* corresponding to the solution in the Pareto optimal set is named non-dominated vectors. The plot of the objective functions of the non-dominated vectors is called the Pareto front.

The crossover operator of GA may exploit structures of good solutions with respect to different objectives to create new non-dominated solutions in unexplored parts of the Pareto front. In addition, most multi objective GA do not require the user to prioritise, scale, or weight objectives. Therefore, GA has been the most popular heuristic approach to multi objective design and optimisation problems. Jones et al. (2002) reported that 90% of the approaches to multi objective optimisation aimed to approximate the true Pareto front for the underlying problem. A majority of these used a meta-heuristic technique, and 70% of all meta-heuristics approaches were based on evolutionary approaches.

Mainly there are four approaches for multi objective optimisation in genetic algorithm [Ishibuchi and Murata 1996]: plain aggregating approaches, population-

based non-Pareto approaches, niched induction approaches, and Pareto-based approaches.

i) **Plain aggregating approaches** apply a weighted aggregating method to convert the multi objective optimisation problem into a single objective problem, and then use the single function genetic algorithm to get solutions. Aggregation methods combine multiple objectives into a higher scalar function that are used for fitness calculation. An aggregation approaches have the advantage of producing one single solution. On the contrary, defining the goal function in this way requires profound domain knowledge that is often not available. Popular aggregation methods are the weighted-sum approach, target vector optimisation, and the method of goal attainment.

ii) **Population-based non-Pareto approaches** are able to evolve multiple non-dominated solutions because the population is monitored for non-dominated solutions concurrently in a single simulation run by changing the selection criterion during the reproduction phase. The search is guided in several directions at the same time then they cannot make direct use of the concept of Pareto dominance or Pareto optimality. A vector evaluated genetic algorithm (VEGA) [Schaffer, 1985] is a population-based non-Pareto approache.

iii) **Niching approach** is suggested to keep GA from convergence to the single point on the front and a niching mechanism such as fitness sharing that allows GA to maintain individuals along the non-dominated frontier. The use of fitness sharing was proposed to prevent the genetic drift and to promote the sampling of the Pareto set [Schaffer, 1985].

iv) **Pareto-based fitness assignment** uses the non-dominated ranking and selection to move a population to the Pareto front in multi objective optimisation problems (MOOP). The basic idea is to find a set of individuals that are the non-dominated solutions to the rest of the population. These individuals are assigned the highest rank and eliminated from further contention. Another set of Pareto non-dominated individuals are determined from the remaining individuals and are assigned the next highest rank. This process continues until the individuals are suitably ranked.

6.4.1 Non-Dominated Sorting Genetic Algorithm-I (NSGA-I)

The Non-dominated Sorting Genetic Algorithm-I (NSGA-I) was proposed by Srinivas and Deb (1993), and is based on the front which is obtained from several layers of individual sorting. Before the selection is performed, the population is sorted on the basis of Pareto ranking domination: all non-dominated individuals are classified into one category called rank 1 and all these ranks are assigned front 1. To maintain the diversity of the population, these classified individuals are shared with their dummy fitness values. Then this group of classified individuals are removed from the population and another layer of non-dominated individuals from the remainder of the population are obtained and assigned the next front. The process continues until all individuals in the population are classified. Figure 6.2 shows the flow chart for member classification by front.

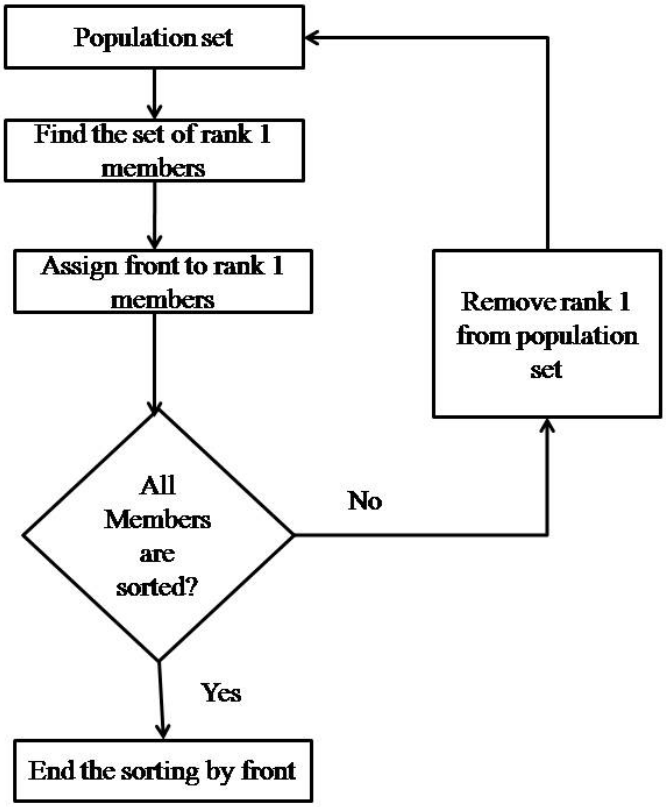

Figure 6.2 Flow chart of Member classification by front

Since individuals in the first front have the maximum fitness value, they always get more copies than the rest of the population. This allows searching for non-

dominated regions, and results in quick convergence of the population toward such regions. Sharing by its part helps to distribute it over this region. The efficiency of NSGA lies in the way in which multiple objectives are reduced to a dummy fitness function using a non-dominated sorting procedure. With this approach, any number of objectives can be solved, and both maximisation and minimisation problems can be handled.

The main strength of this technique is that, it can handle any number of objectives and does the sharing in the parameter value space instead of the objective value space, which ensures a better distribution of individuals, and allows multiple equivalent solutions exist. Its main weakness is that it is more inefficient (both computationally and in terms of quality of the Pareto fronts produced) than MOGA, and more sensitive to the value of the sharing factor σ_{share}. NSGA uses non dominated sorting procedure, which compare each solution in population with every other to find the first non dominated front.

6.4.2 Non-Dominated Sorting Genetic Algorithm-II (NSGA-II)

Multi objective evolutionary algorithms which use non-dominated sorting and sharing (NSGA-I) have been mainly criticised for the following reasons [Deb et al. 2008]:

i) **High computational complexity of non-dominated sorting:** The non-dominated sorting algorithm in use uptill now is $O(mN^3)$ computations, where m is the number of objective functions and N is the population size. In case of large population sizes the computation is very expensive, especially since the population needs to be sorted in every generation.
ii) **Lack of elitism:** Recent results show clearly that elitism can speed up the performance of the GA significantly; also it helps to prevent the loss of good solutions once they have been found.
iii) **Need for specifying the sharing parameter σ_{share}.:** Traditional mechanisms of insuring diversity in a population so as to get a wide variety of equivalent solutions have relied heavily on the concept of sharing. The main problem with sharing is that it requires the specification of a sharing parameter (σ_{share}.).

Though there has been some work on dynamic sizing of the sharing parameter, a parameter less diversity preservation mechanism is desirable.

The solution set in NSGA-II is based on their crowding distances and no niching parameter is required here, as needed in the MOEA, NSGAs & NPGAs. In the absence of the crowding comparison operator, this algorithm also exhibits a convergence proof to the Pareto-optimal solution set, but the population size would grow with the generation counter. The elitism mechanism does not allow an already found Pareto-optimal solution to be deleted. However, when the crowded comparison is used to restrict the population size, the algorithm loses its convergence properly.

6.4.2.1 Description of NSGA-II: Two distinct entities are calculated in the NSGA-II to validate the quality of a given solution. The first is a domination-count where the numbers of solutions that dominate a given solution are tracked. The second keeps track of how many sets of solutions a given solution dominates. In the process, all the solutions in the first non dominated front will have their domination count set to zero. The next step is to select each solution in which the non-domination count is set to zero and visit all other solutions in the solution set and reduce the domination count by one. In doing so, if the domination count of any other solution becomes zero, this solution is grouped in a separate list. This list is flagged as the second non- dominated front. This process is then continued with each member of the second list until the next non-dominated front is identified. The process is continued until all fronts are identified. Based on the non-domination count given to a solution, a non-domination level will be assigned. Those solutions that have higher non-domination levels are flagged as non-optimal and will never be visited again.

One of the key requirements of a successful solution method is ensuring that a good representative sample from all possible solutions is chosen. Introduction of a density estimation process and a crowded-comparison operator has helped NSGA- II to address the above need.

The crowding-distance computation requires sorting of a given population according to each objective function value in ascending order of magnitude. Once this is done, the two boundary solutions with the largest and smallest objective value are

assigned distance values of infinity. All other solutions lying in between these two solutions are then assigned a distance value calculated by the absolute normalised distance between each pair of adjacent solutions. After each population member is assigned a crowding distance value, a crowded-comparison operator is used to compare each solution with the others. This operator considers two attributes associated with every solution which is the non-domination rank and the crowding-distance. Every solution is rated with others based on the non-domination rank. Solutions with lower ranks are deemed better in this attribute. Once solutions that belong to the best front are chosen based on the non-domination rank, the solution that is located in a lesser-crowded region is considered better and forms the basis of the NSGA-II algorithm.

In this approach, the sharing function approach is replaced with a crowded comparison. Initially, an offspring population Q_t is created from the parent population P_t at the t^{th} generation. After, a combined population R_t is formed.

$$R_t = P_t \cup Q_t$$

R_t is sorted into different non domination levels F_j as shown in the NSGA approach. So, we can write:

$$R_t = P_t \bigcup_{j=1}^{r} F_j$$

The main objective of NSGA-II is to find multiple Pareto-optimal solutions in one single simulation run. Since NSGA-II work with a population of solutions [Deb, et al. 2002], a simple multi objective genetic algorithm (MOGA) can be extended to maintain a diverse set of solution. Elitism helps to keep the best solution of the current population and does not allow it to deteriorate in the next generation. Major advantages of using NSGA-II technique are given below:

- It uses non dominated sorting techniques to provide the solution as close to the Pareto-optimal solution as possible.
- It uses crowding distance techniques to provide diversity in solution.
- It also uses elitist techniques to preserve the best solution of current population in next generation.

6.4.2.2 Procedure for Non-Dominated Sorting Genetic Algorithm-II (NSGA-II): A brief procedure for NSGA-II is given below.

1) Population Initialisation: The population contains a set of chromosomes. Each chromosome is initialised randomly with binary bits having length same as the code length.

2) Non-Dominated sort: The initialised population is sorted based on non-domination

- for each individual p in main population P perform the following
  - **–** Initialise the set of individuals dominated by p
  - $S_p = \varphi$
  - **–** Initialise the number of individuals that dominate p i.e. $n_p = 0$.
  - **–** for each individual q in P
  - * if p dominates q then
    - $S_p = S_p \cup \{q\}$
  - * else if q dominates p then
    - $n_p = n_p + 1$
  - **–** if $n_p = 0$ then p belongs to the first front and rank of individual p i.e. $p_{rank} = 1$. Update the first front F_1 by adding p to front one i.e. $F_1 = F_1 \cup \{p\}$
- This is carried out for all the individuals in main population P.
- Initialise the front counter i = 1
- perform the following if i^{th} front is nonempty i.e. $F_i \neq \varphi$
  - **–** Q = φ. The set Q is used to store the members of the next front.
  - **–** for each individual p in front F_i
  - *for each individual q in S_p
    - $n_q = n_q - 1$
    - decreament the domination count for individual q
    - if $n_q = 0$, set $q_{rank} = i + 1$. Update Q i.e. $Q = Q \cup q$
  - **–** i = i + 1.
  - **–** set Q is the next front and hence $F_i = Q$.

3) Crowding Distance Assignment: Once the non dominated sorting is complete, the crowding distance is assigned. Since the individuals are selected based on rank and

crowding distance, all the individuals in the population are assigned a crowding distance value, front wise.

4) Selection: The individuals are selected using a binary tournament selection. The selection is carried out as follows.

a) An individual is selected if its non domination rank is smaller than the other.

b) If both the individuals belong to the same front i.e both has same non domination rank then the individual having higher crowding distance is selected

5) Genetic Operators: Single point crossover and mutation operations as used in GA [Srinivas and Deb1993] are also employed in NSGA-II.

6) Recombination and Selection: The offspring population is combined with the current generation population and the total population is sorted based on nondomination.

The new generation is filled by chromosomes from each front subsequently until the population size exceeds the current population size N. If by adding all the individuals in front F_j the population exceeds N then individuals in front F_j are selected based on their crowding distance sorted in the descending order until the population size is N

In NSGA-II, first the offspring population Q_t (of size N) is created using the parent population P_t (of size N), as shown in Figure 6.3. The usual genetic operators such as single-point crossover and bit-wise mutation operators are used in this process. Next, the two populations are combined to form an intermediate population R_t of size 2N. Thereafter, the fitness of each offspring in the 2N population is evaluated using the multiple objective functions

At this stage, the non-dominated sorting procedure is carried out over the 2N population to rank and divide the individuals into different non-dominated fronts. Thereafter, the new parent population P_{t+1} is created by choosing individuals of the non-dominated fronts, one at a time. The individuals of best ranked fronts are chosen first, followed by the next-best and so on, till N individuals are obtained.

Since the intermediate population R_t has a size of 2N, those fronts which could not be accommodated are discarded. In case there is space only for a part of a front in the new population, the individuals as per existing order are selected, so as to complete the new parent population.

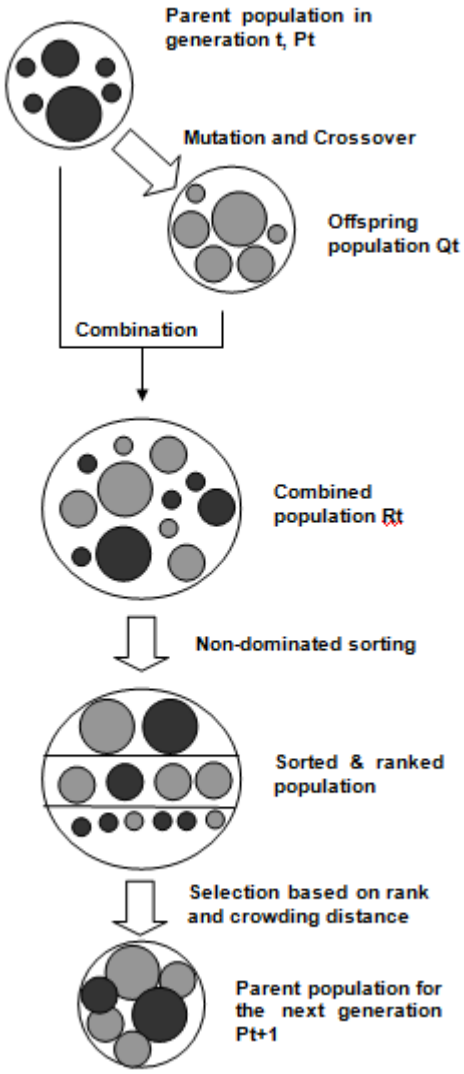

Figure 6.3 Working principle of NSGA-II

The complete NSGA-II procedure can be written in condensed form as explained below:

BEGIN

While generation count is not reached

Begin Loop

- Apply selection, crossover and mutation to new parent population P_{t+1} and obtain the new offspring population Q_{t+1}.
- Combine parent P_t and offspring population Q_t to obtain population R_t of size

$$2N. R_t = P_t \bigcup Q_t$$

- Perform Non-dominated Sorting on R_t and assign ranks to each Pareto front with fitness F_i.
- Starting from the Pareto front with fitness F_1, add each Parato-front F_i to the new parent population P_{t+1} until a complete front F_i cannot be included.
- From the current Pareto-front F_i, add individual members to new parent population P_{t+1} until it reaches the size N.
- Increment generation count.

End Loop

END.

6.4.3 Novel Genetic Algorithm

In the current enhanced version of genetic algorithm [D'souza et al. 2010], sorting of individuals based on each of the objectives is performed, one after the other, till all objectives are considered. During this sort, the index of each individual is tracked so that the position value of any given individual in each sorted array is known. This information is critical since it helps in ranking the fronts in the next step.

Each individual is ranked by summing up the position value of that individual in all the objectives. Since similar position values were assigned to individuals having similar objective values, the sum of the position values becomes equivalent to the rank which the individual would have obtained through non-dominated comparison. Hence the non-dominated sort is completed in a single iteration of the sorted individuals, thereby reducing the time required for processing each generation.

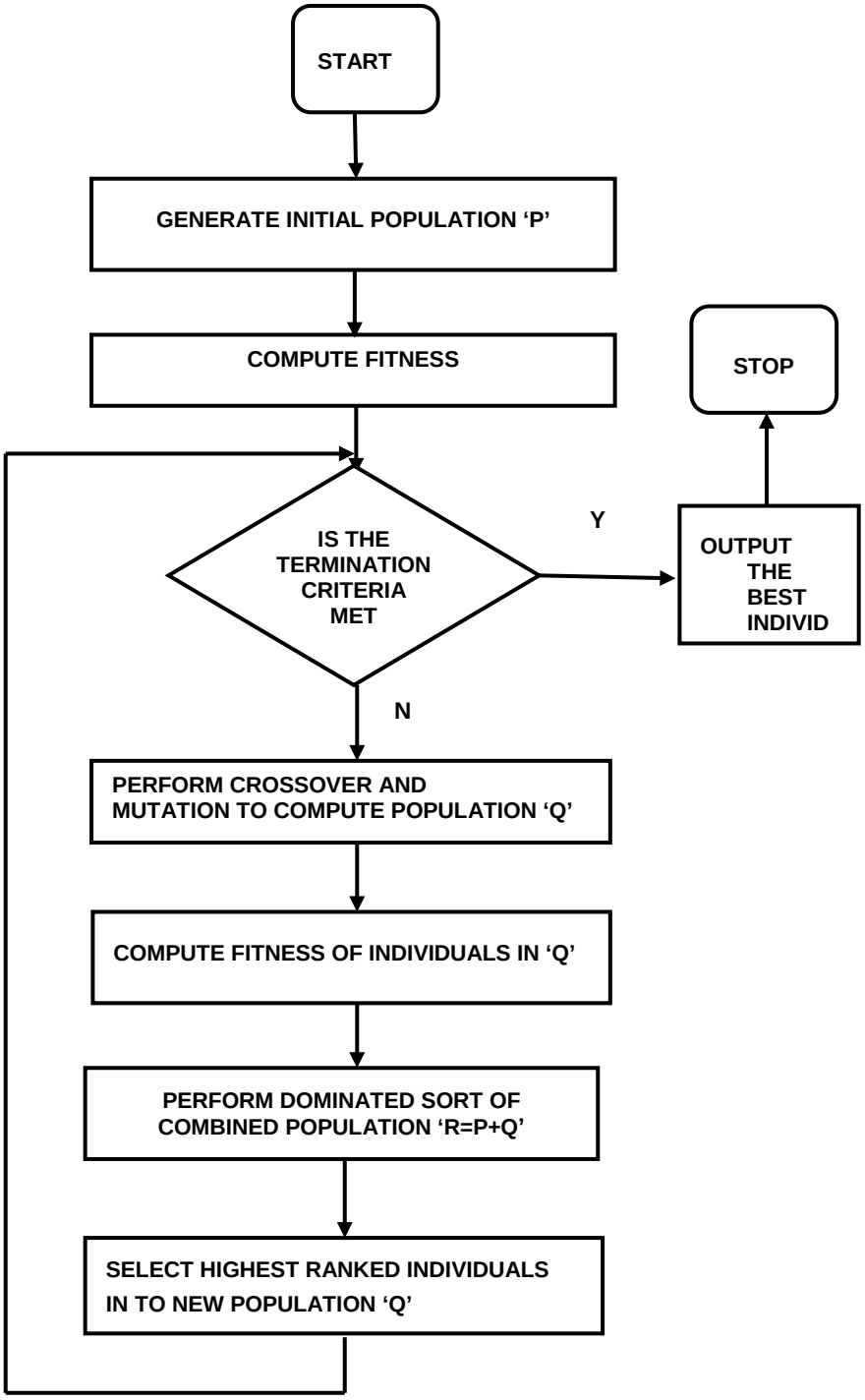

Figure 6.4 Flowchart for novel genetic algorithm

The flow chart for optimisation of the grinding of MMC using novel genetic algorithm is shown in Figure 6.4. In this figure, generate initial population means the possible solutions of the optimisation problem, and each possible solution is called an individual. The possible solution is formed by binary strings of Vol % of SiC, feed and depth of cut. Later these binary strings are converted in to decimals to obtain the

output. Thus generated population is selected based on roulette wheel selection and they are arranged depending on the dominance of one solution over the other.

The crossover and mutation genetic operators are applied on the selected population in a manner similar to that used during single objective GA. For real parameter implementations, binary crossover and mutation operator are used. Further an elitist recombination strategy is used by combining the current population and the offspring population. For an initial population size of N, the combined population contains 2N members. The new population is obtained by picking members from each front successively until the size exceeds N. The members from the last added front are then sorted in descending order of crowding distance. A suitable number of members from this front are then picked so that a total of N members are obtained. All the steps starting from non–dominated sorting are repeated until the desired number of generations is completed.

6.5 RESULTS AND DISCUSSION

Although several conventional optimization methods have been applied to solve grinding optimization problems, their application is often limited because of getting struck at a local optima and lack of robustness. Since the problem of grinding optimization is complex involving highly nonlinear multiple objectives and many constraints, the application of meta-heuristic techniques seems to be very useful. The single optimal solution reported in earlier works is not of much use to the decision maker, considering the fact that the two objectives involved are conflicting.

Hence in the present study, the objective is to minimse specific energy, maximise material removal rate and to minimise the surface roughness during surface grinding DRACs. The objective functions were developed based on the planned set of experiments as explained in section 5.4.1. The regression equations developed by response surface model thus developed as given by eq. (5.26) –eq. (5.28) along with the constraints is as given below.

The regression equation for specific energy is

$$\hat{y}_1 = 683.819 + 15.727X_1 - 12.608X_2 - 18.043X_3 - 1.379X_1^2 + 0.0729X_2^2 + 0.765X_3^2 + 0.067X_1X_2 + 0.305X_1X_3 - 0.077X_2X_3 \quad (6.1)$$

The regression equation for material removal rate is

$$\hat{y}_2 = 3.555 + 0.173X_1 - 0.120X_2 - 0.380X_3 - 0.016X_1^2 + 0.00007X_2^2 + 0.0001X_3^2 + 0.015X_1X_2 + 0.002X_1X_3 + 0.0007X_2X_3 \quad (6.2)$$

The regression equation for surface roughness is

$$\hat{y}_3 = 2.096 - 0.311X_1 + 0.015X_2 + 0.013X_3 + 0.014X_1^2 - 1.1E-09X_2^2 - 6.25E-04X_3^2 - 0.001X_1X_2 + 0.001X_1X_3 + 9.38E-05X_2X_3 \quad (6.3)$$

Subject to the constraints

$$\begin{aligned} 8 \le X_1 \le 12 \\ 60 \le X_2 \le 80 \\ 8 \le X_3 \le 16 \end{aligned} \quad (6.4)$$

A multi objective algorithm was implemented using novel genetic algorithm for performing the evolutionary optimisation. Java (Version 2.0) programming language was used to code the algorithm. The developed algorithm is given in Appendix-IV.

Each of the objective function was coded along with the parameters used for RSM Optimisation. The constraints on each parameter were also specified in the program. As described in the novel genetic algorithm algorithm in the previous section, a population of 100 individuals was generated with various initial values of parameters which were initialised randomly, keeping appropriate minimum and maximum ranges in view. Thereafter the program was allowed to iterate over 500 generations and the final optimised parameter values of the non-dominated solutions resulting from this run were noted. After several such runs, results were tabulated and analysed. A sample result obtained from novel genetic algorithm is given in Table 6.1.

Table 6.1 The Sample result of novel genetic algorithm

Solution No	SiC (vol %)	Feed (mm/s)	a (µm)	Q'_w (mm^3/mm·s)	u (J/mm^3)	R_a (µm)
Sol 44	>> SIC: 8	F: 69	DOC: 11	>> MRR: 0.546	SE: 98.33	RA: 1.14
Sol 45	>> SIC: 8	F: 77	DOC: 15	>> MRR: 0.782	SE: 73.57	RA: 1.25
Sol 46	>> SIC: 11	F: 71	DOC: 15	>> MRR: 0.831	SE: 84.68	RA: 0.87
Sol 47	>> SIC: 8	F: 73	DOC: 8	>> MRR: 0.482	SE: 108.24	RA: 1.12
Sol 48	>> SIC: 11	F: 66	DOC: 9	>> MRR: 0.571	SE: 108.41	RA: 0.75
Sol 49	>> SIC: 12	F: 80	DOC: 14	>> MRR: 0.997	SE: 58.98	RA: 0.82
Sol 50	>> SIC: 9	F: 69	DOC: 11	>> MRR: 0.611	SE: 98.59	RA: 1.0
Sol 51	>> SIC: 11	F: 70	DOC: 12	>> MRR: 0.706	SE: 85.76	RA: 0.82
Sol 52	>> SIC: 12	F: 77	DOC: 13	>> MRR: 0.869	SE: 62.93	RA: 0.8
Sol 53	>> SIC: 12	F: 68	DOC: 13	>> MRR: 0.706	SE: 82.91	RA: 0.77
Sol 54	>> SIC: 11	F: 71	DOC: 11	>> MRR: 0.683	SE: 85.84	RA: 0.81
Sol 55	>> SIC: 9	F: 78	DOC: 14	>> MRR: 0.850	SE: 72.89	RA: 1.1
Sol 56	>> SIC: 8	F: 79	DOC: 11	>> MRR: 0.676	SE: 77.18	RA: 1.21
Sol 57	>> SIC: 8	F: 75	DOC: 13	>> MRR: 0.674	SE: 77.8	RA: 1.21
Sol 58	>> SIC: 8	F: 78	DOC: 11	>> MRR: 0.656	SE: 78.63	RA: 1.2
Sol 59	>> SIC: 9	F: 67	DOC: 14	>> MRR: 0.691	SE: 100.37	RA: 1.03
Sol 60	>> SIC: 10	F: 69	DOC: 13	>> MRR: 0.716	SE: 92.15	RA: 0.92
Sol 61	>> SIC: 11	F: 67	DOC: 10	>> MRR: 0.609	SE: 100.22	RA: 0.77
Sol 62	>> SIC: 8	F: 77	DOC: 9	>> MRR: 0.566	SE: 92.74	RA: 1.16
Sol 63	>> SIC: 8	F: 70	DOC: 15	>> MRR: 0.676	SE: 91.04	RA: 1.19

The novel genetic algorithm generates a set of multiple optimal points. The best solution among the multiple solutions is chosen as the optimal solution. Figure 6.5-figure 6.7 shows the result of novel genetic algorithm developed from java for specific energy, material removal rate and surface roughness respectively. It can be observed that novel genetic algorithm gives multiple optimum results as marked by ♦ and subsequently tabulated in Table 6.2.

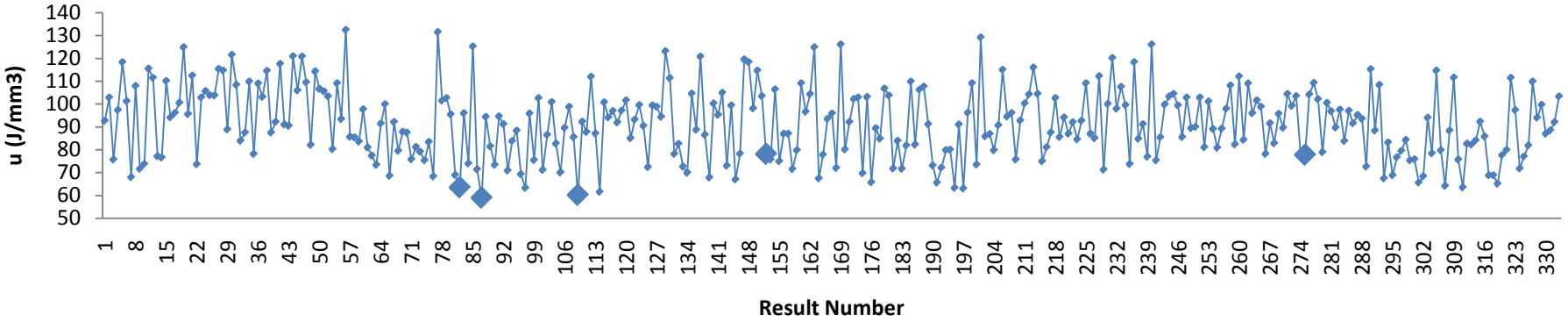

Figure 6.5 Result of novel genetic algorithm for specific energy

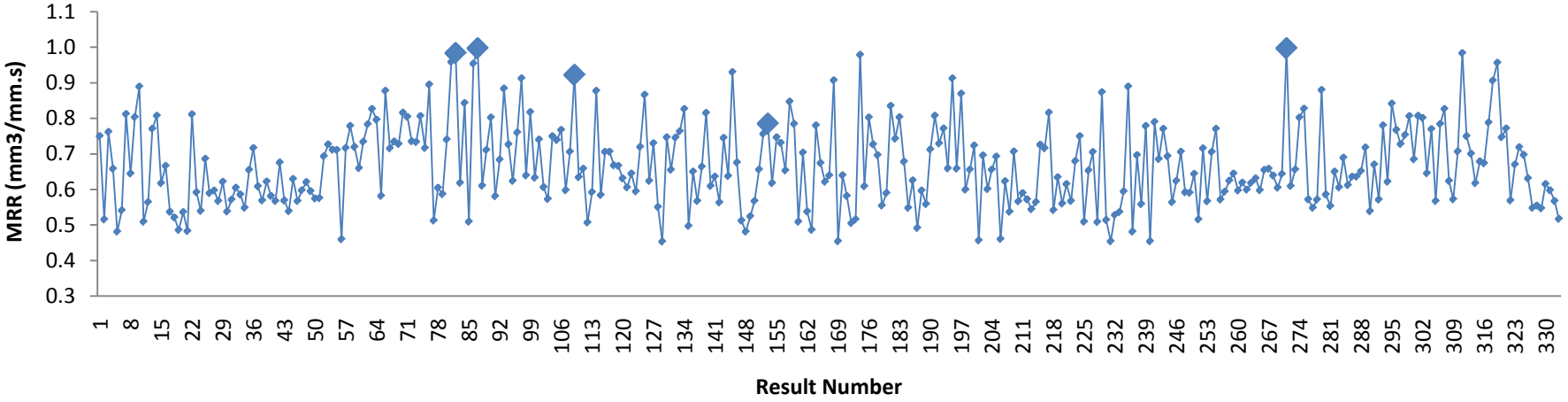

Figure 6.6 Result of novel genetic algorithm for material removal rate

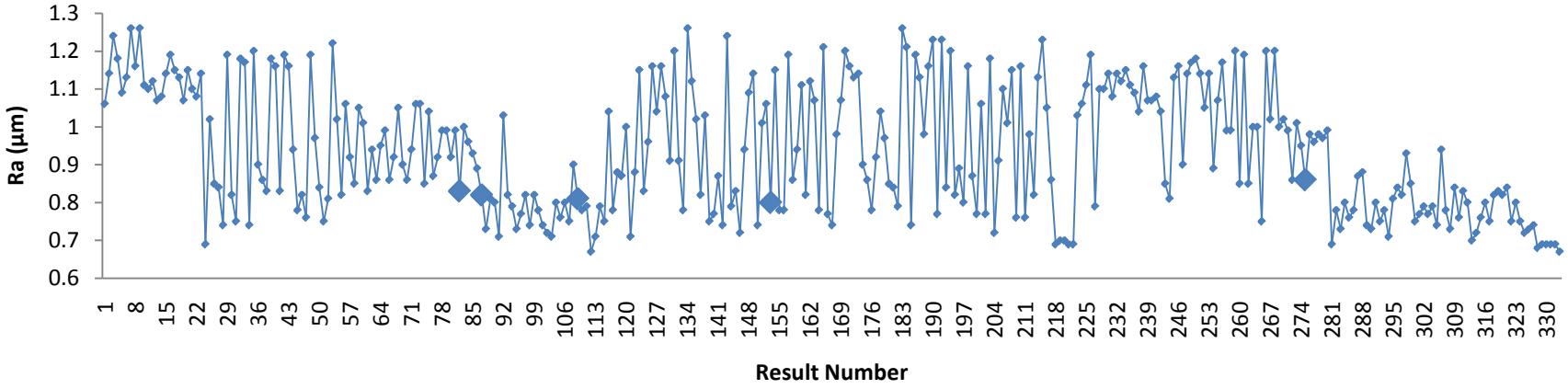

Figure 6.7 Result of novel genetic algorithm for surface roughness

Table 6.2 Multiple Optimal Results from Novel Genetic Algorithm

Result Number	Process Variables			Novel Genetic Algorithm Results		
	SiC vol %	Feed (mm/s)	Dept of grinding	u (J/mm^3)	MRR ($mm^3/mm \cdot s$)	Ra (µm)
82	12	79	15	61.95	1.012	0.84
87	12	80	15	60.60	1.043	0.85
109	12	79	13	60.10	0.922	0.81
152	12	71	14	78.11	0.785	0.80
275	11	73	14	77.80	0.992	0.86
271	12	80	14	58.98	1.013	0.82

6.5.1 Validation of results

The response surface models given in Eq. (6.1) –Eq. (6.3) were validated by the set of test runs. Table 6.3 gives the results obtained from experimental test and the results obtained by novel genetic algorithm.

In Table 6.3 the results shown from the first row to the seventh row are the test results that are compared with response surface table of chapter 5 (Table 5.2) and the novel genetic algorithm results. It is observed from the results that the maximum deviation of the RSM and novel genetic algorithm results are within 6%. The remaining results of Table 6.3 are compared with experimental results of chapter 3 (Table 3.5). The maximum deviation between the results of specific energy obtained from novel genetic algorithm and form the experiments are limited to 14.5%. However the average deviations for material removal rate and surface roughness are within 6%. Process variables in the last row of Table 6.3 reefer to the optimal results obtained from the desirability function approach of chapter 5. The experimental results are in

close agreement with the predicted results of novel genetic algorithm. It is also observed that the deviation of the predicted results of RSM and the results obtained from novel genetic algorithm are limited to ±0.5%. The percentage error between predicted RSM results for the set of experiment from Table 5.2 and the novel genetic algorithm results are shown in Fig.6.8.

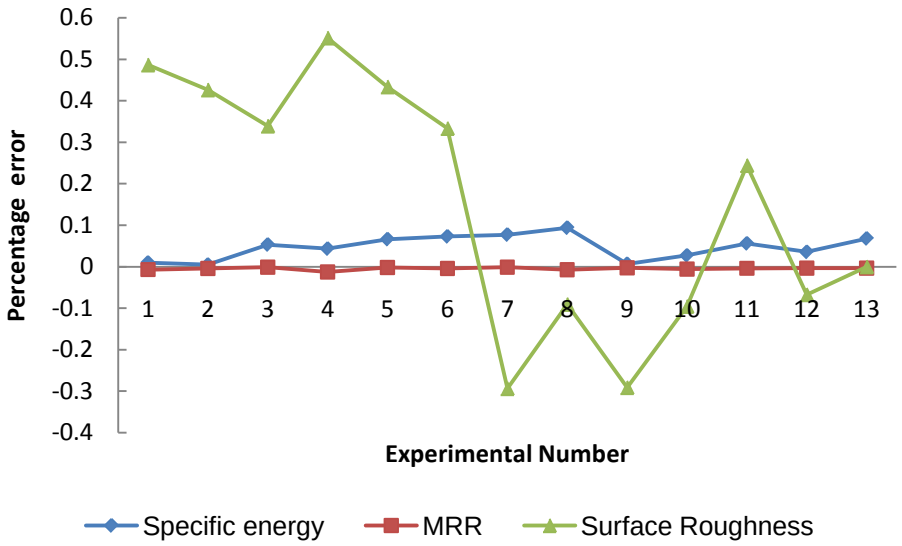

Figure 6.8 Comparison between RSM and novel genetic algorithm results

The novel genetic algorithm approach for multi objective optimisation of grinding process parameters is flexible, more accurate and adaptive. Hence the developed RSM model and novel genetic algorithm model can effectively be used to predict the specific energy, MRR and surface roughness.

The developed novel genetic algorithm programme could be helpful for a manufacturing engineer to obtain machining conditions for optimal machining performance of a product. This approach, used to optimize using the mathematical model, was found to be the most useful technique for research.

The methodology of optimization of regression models using novel genetic algorithm can be used in computer- aided process planning (CAPP), and computer aided manufacturing (CAM) to obtain optimum surface grinding conditions. The predictive capability of novel genetic algorithm could also be incorporated for

automatic process monitoring. With the known boundaries of input variables, the surface grinding process could be performed with relatively higher productivity.

Table 6.3 Validation of experimental results

Sr. No	Process Variables			Experimental Results			Novel genetic algorithm Results			Percentage Error		
	SiC (Vol %)	Feed (mm/s)	a (µm)	u (J/mm^3)	Q_w (mm^3/mm·s)	R_a (µm)	u (J/mm^3)	Q_w (mm^3/mm·s)	R_a (µm)	u	Q_w	R_a
1	>> SIC: 10	F: 70	DOC: 8	106.596	0.513	0.86	SE:107.24	>>MRR: 0.511	RA: 0.85	-0.60	-0.39	1.16
2	>> SIC: 10	F: 80	DOC: 12	71.379	0.926	0.98	SE:71.79	>>MRR: 0.920	RA: 0.97	-0.58	-0.69	1.02
3	>> SIC: 12	F: 60	DOC: 8	124.449	0.518	0.66	SE: 125.39	>>MRR: 0.513	RA: 0.66	-0.76	-1.05	0.00
4	>> SIC: 8	F: 60	DOC: 8	145.585	0.498	1.04	SE: 146.97	>>MRR: 0.491	RA: 1.03	-0.95	-1.52	0.96
5	>> SIC: 8	F: 70	DOC: 12	88.625	0.605	1.16	SE:92.13	>>MRR: 0.582	RA:1.16	-3.95	-3.97	0.00
6	>> SIC: 10	F: 70	DOC: 12	91.937	0.660	0.91	SE:90.64	>>MRR: 0.692	RA:0.91	1.41	4.64	0.00
7	>> SIC: 12	F: 70	DOC: 12	77.047	0.667	0.79	SE:78.12	>>MRR: 0.693	RA:0.76	-1.39	3.74	3.80
8	>> SIC: 12	F: 60	DOC: 12	119.567	0.636	0.75	SE: 110.5	>>MRR: 0.633	RA: 0.73	7.58	-0.46	2.67
9	>> SIC: 8	F: 70	DOC: 8	114.22	0.431	1.13	SE:114.99	>>MRR: 0.461	RA:1.1	-0.67	6.43	2.65
10	>> SIC: 8	F: 80	DOC: 12	76.361	0.748	1.25	SE: 71.67	>>MRR: 0.735	RA: 1.23	6.14	-1.82	1.60
11	>> SIC: 8	F: 60	DOC: 12	126.052	0.581	1.09	SE: 127.19	>>MRR: 0.583	RA: 1.09	-0.90	0.29	0.00
12	>> SIC: 12	F: 70	DOC: 8	82.276	0.530	0.69	SE:94.09	>>MRR: 0.543	RA:0.68	-14.36	2.31	1.45
13	>> SIC: 12	F: 80	DOC: 12	62.848	1.007	0.78	SE:63.31	>>MRR: 0.959	RA:0.77	-0.74	-5.01	1.28
14	>> SIC: 12	F: 80	DOC: 14	63.296	1.058	0.89	SE:58.98	>>MRR: 0.997	RA:0.82	6.82	-6.13	5.62

Chapter 7

CONCLUSION AND FUTURE SCOPE

7.1 CONCLUSION

Experiments were conducted with three factors at three levels. Taguchi's L_{27} array is used for the experimentation. Following conclusions can be drawn from the analysis of the experiments.

- Specific energy decreases with increase in vol % of SiC, increase in feed and increase in depth of grinding. This phenomenon is attributed to the fact that specific grinding energy associated with the ductile material removal process is much higher than that with a brittle removal mode.
- It is observed that specific energy decreases gradually from average value of 145 J/mm^3 to 59 J/mm^3 with increase in depth of grind from 8μm to 14μm and further increases to an average value of 65 J/mm^3 for a depth of grind of 16μm. This may happen because of blunt grains on the wheel surface which result in higher sliding friction and ploughing forces and accentuate the increase in specific energy. A solution for the same can be attained by continuous dressing of the grinding wheel.[Rowe 2009]
- Decrease in specific energy with increase in feed may be due to the reason that the energy consumed in the grinding process is spent on deforming and grinding new surfaces in the workpiece material. The new surface area produced is therefore a measure of the energy required. Increasing feed at constant depth of cut, ground surface area decreases exponentially with increase in feed thus decreasing the specific energy [Rowe 2009].

- MRR increases with increase in depth of grind and increase in feed. Increase in depth of grind will increase the uncut chip thickness thus increasing the material removal rate.

- Surface roughness decreases from average value of 1.30μm to 0.69μm with increase in vol % of SiC from 8 vol% to 12 vol%. It is primarily due to the reason that, with increase in vol % of SiC, hardness of the workpiece will increase thus resulting in improved surface finish [D Ilio et al. 2009]. It is also observed that surface roughness increase with increase in depth of grinding. It may be due to the reason that increase in dept of grinding will result in increased cutting forces and vibrations thus resulting in poor surface finish.

- Response surface methodology is applied for analysing specific energy, MRR and surface roughness in the surface grinding of DRACs. Face central composite design is used for the analysis.

- Second order regression model for specific energy, MRR and surface roughness in terms of the process variables were developed form response surface methodology. It is observed that fitted value is very close to the experimental value. ($R^2 > 0.95$)
- From the analysis of the response surface plots it can be observed that
  - Specific energy is largely affected by feed followed by depth of grinding.
  - MRR is predominantly affected by feed followed by depth of grinding and volume % of SiC.
  - Surface roughness is more dependent on volume % of SiC, followed by depth of grinding and feed.

- Multi objective optimisation based on desirability function approach is performed to find the desired process variables such as SiC vol%, feed and depth of grinding so as to obtain optimal values of specific energy, material remival rate and surface roughness.

- From Desirability function approach, optimal cutting conditions were determined for obtaining maximum MRR, minimum surface roughness and minimum specific energy. The optimal conditions were obtained while grinding Al6061-12vol %SiC under constant feed of 80mm/s and depth of grinding 14μm.

- Second order model developed from RSM were used for optimisation based on novel genetic algorithm. Java codes were written for maximisation of MRR, minimisation of specific energy and surface roughness. A population of size 100, with cross-over probability of 0.8, mutation probability of 0.02, were adopted. It was observed during the analysis that this combination of population, cross-over and mutation gives better results. Further the parato front is obtained for 500 generations. Larger the number of generations more the number of parato fronts and better the results. It is observed that largest deviation of the results obtained by genetic algorithm and those obtained by RSM are within 2%. It indicates that the results obtained by NSGA-II are in conformance with the results obtained by RSM.
- Confirmation tests were conducted to validate the second order response surface model for specific energy, material remival rate and surface roughness. The predicted test results are in conformance to the experimental test results. Maximum deviation of 7% is observed between experimental results for RSM and predicted response. But a maximum deviation of 14% is obtained between the experimental results of Table 3.5 and predicted response. However the average deviation for all other experiments is within 6%. An error of 12% between RSM and experimental results is acceptable [Krajnik et 2005].

- Therefore, from this study, it may be concluded that the novel genetic algorithm can effectively be used to optimise the model developed from RSM.

7.2 SCOPE FOR FUTURE WORK

To begin with, only few variables were selected for the design of experiments. In order to investigate the effects of other variables, further study is required. Though the values and methods recommended in the literature were selected, some of the important factors such as wheel speed, grinding wheel and coolant were treated as constant input factors in the design of experiments. An experiment designed to investigate the influence of these parameters, would be ideal. Research work investigating the effect of these variables on DRACs would be very informative. This

would result in many test runs, which was not possible in the present study due to the cost of the material and time involved in the process. With more replicates for each test condition, comprehensive knowledge about the grinding of DRACs can be achieved.

In the present study the MMCs were prepared by stir casting method. In order to accomplish the better distribution of reinforcement material in to the matrix, novel method of manufacturing MMCs such as powder metallurgy can be used.

In this investigation the study on specific energy material remival rate and surface roughness during machining of DRACs did not include the effects of cutting fluids, dressing conditions and infeed. A good extension of this research work could be used by taking all these factors into account.

The mathematical model developed in this investigation can further be used to develop a mechanistic model so that the predicted results are for a wider range of workpiece material, cutting conditions and will include other factors such as machine dynamics and tool geometry.

The optimisation process adopted in this investigation was limited to desirability function approach and novel genetic algorithm. The same can be extended to ant colony optimisation, simulated annealing and tabu search and also for prediction of the responses using artificial neural network.

The research conducted and the methodology developed in the present work is limited to Al-SiC composites. But it can be extended for different advanced materials and different machining processes such as milling, drilling, cylindrical grinding and un-conventional machining processes. Further, the novel genetic algorithm being time efficient, could conveniently be adopted in adaptive control system for real-time operations.

APPENDIX-1

CUTTING FORCE MEASUREMENT

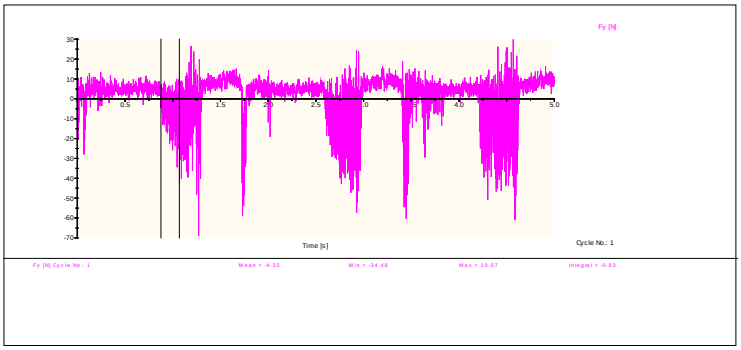

Test-1

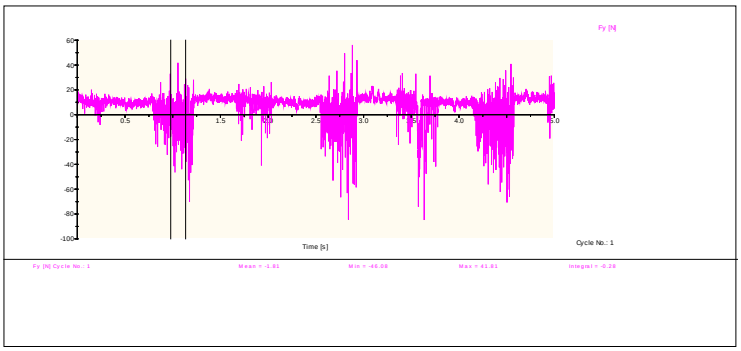

Test 3

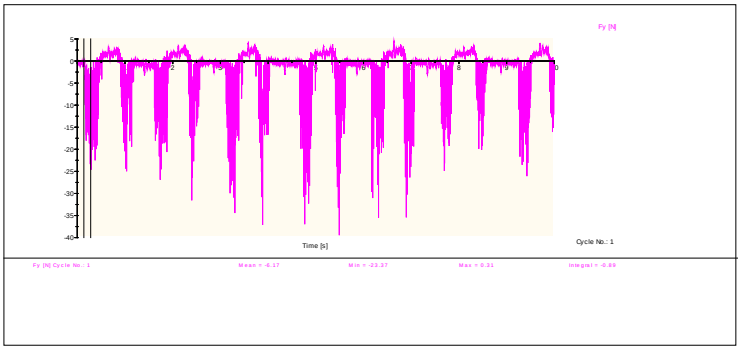

Test 4

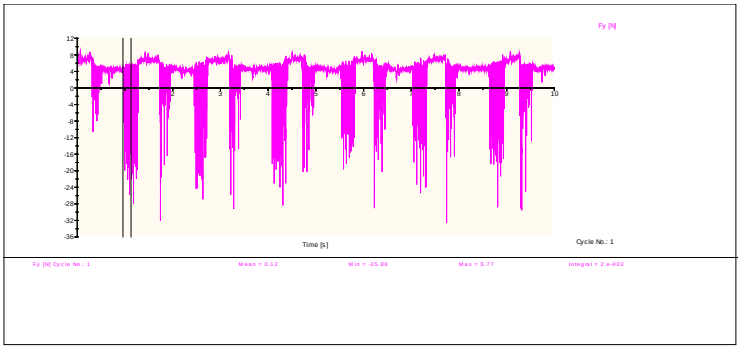

Test 7

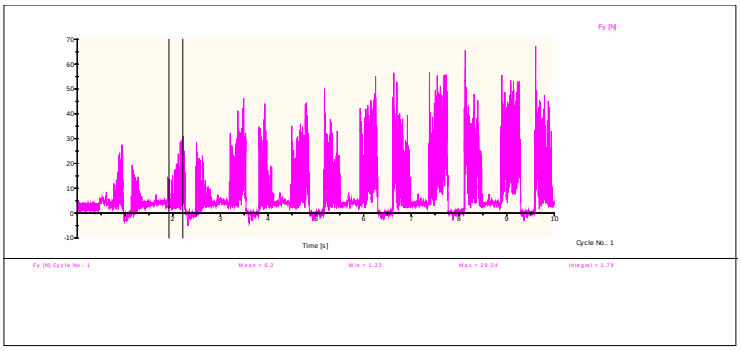

Test 8

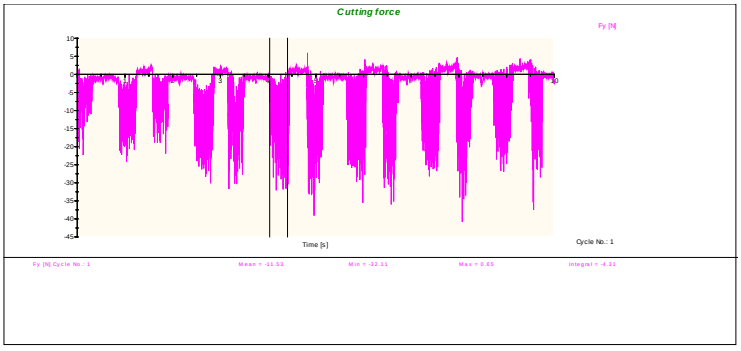

Test 9

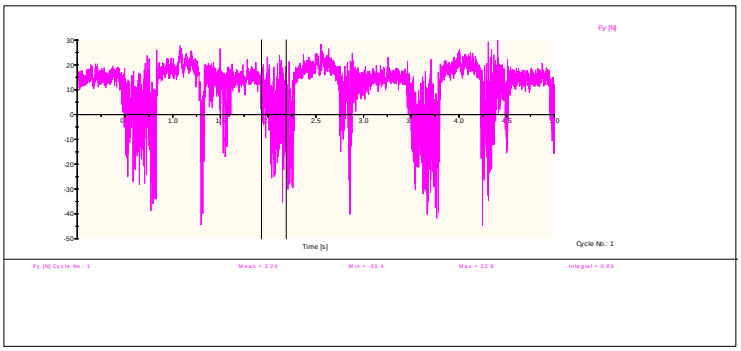

Test 11

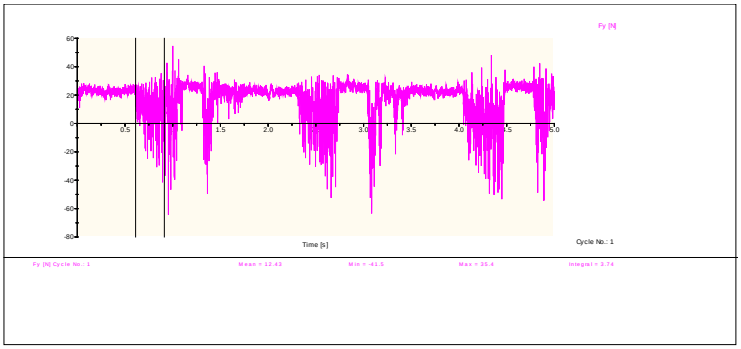

Test 12

Test 13

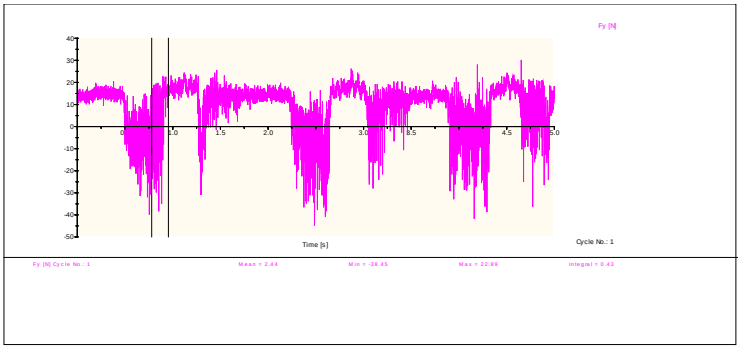

Test 18

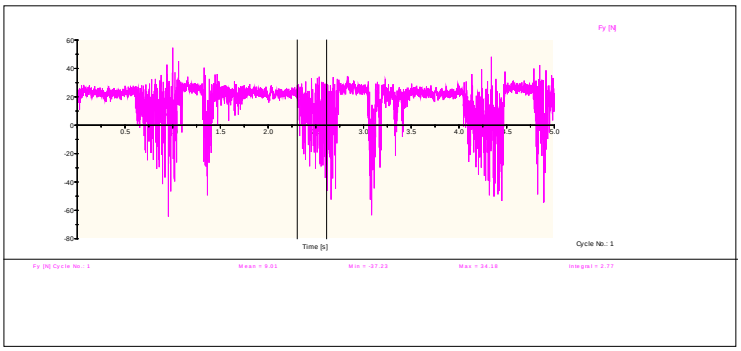

Test 20

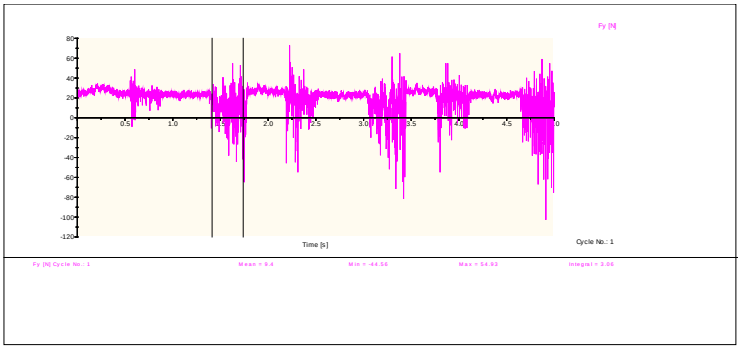

Test 21

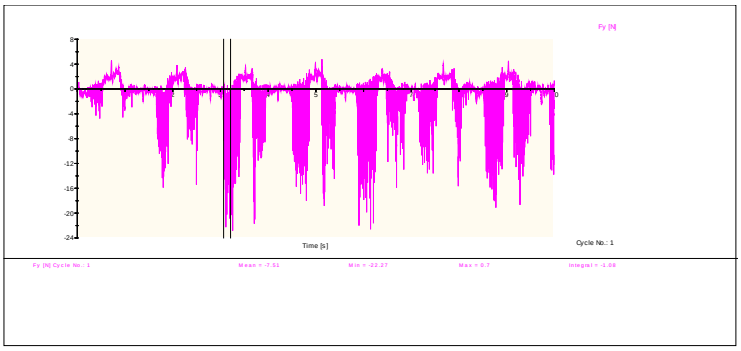

Test 22

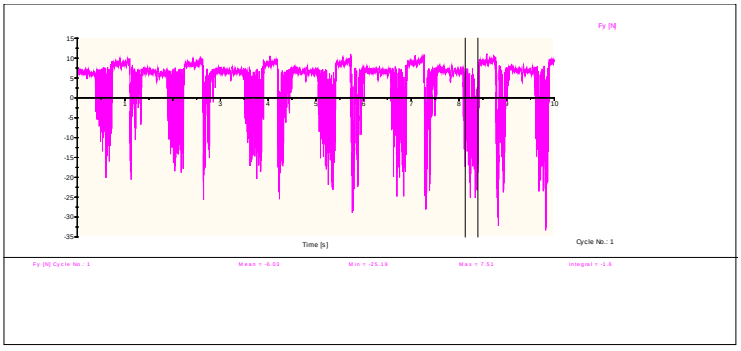

Test 23

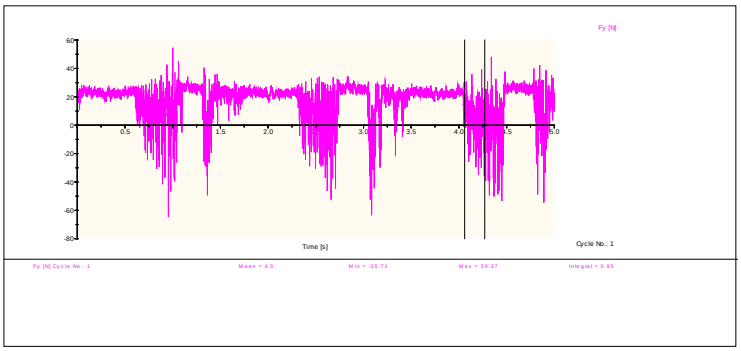

Test 27

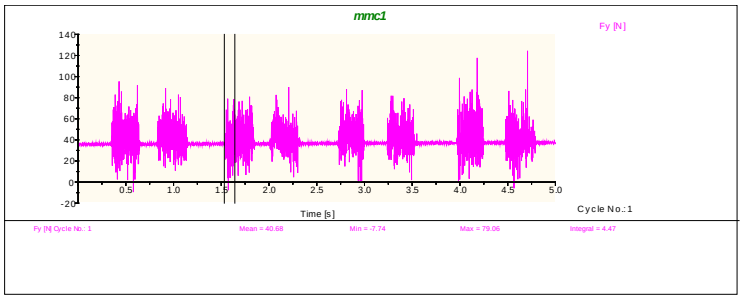

Validation test result Table 5.6, Test No.3

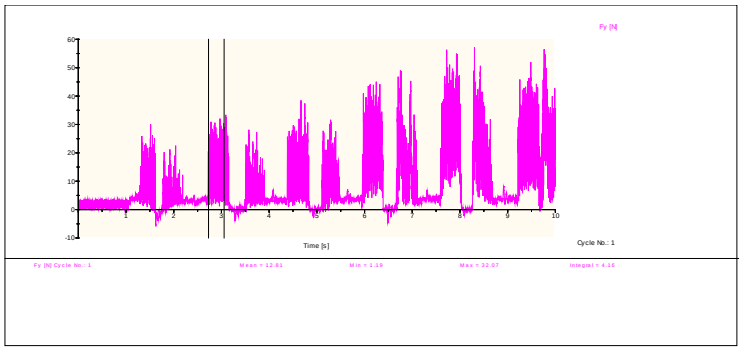

Validation test result Table 5.6, Test No.6.

APPENDIX-2

SURFACE ROUGHNESS PROFILE OF THE RTEST SPECIMEN

1. Test No. 4

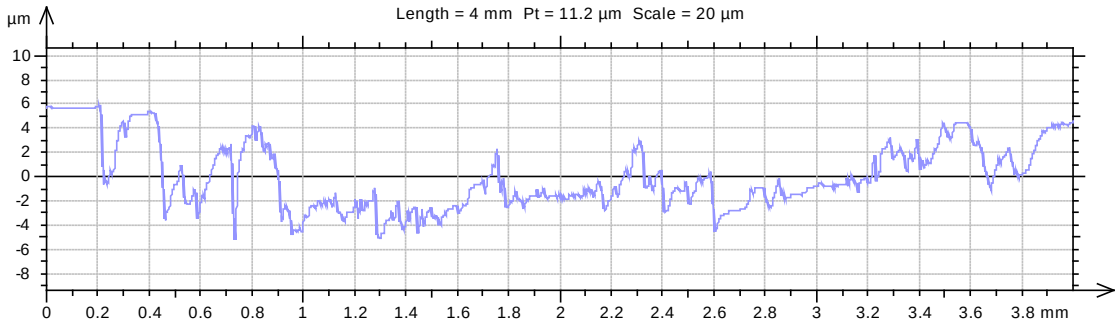

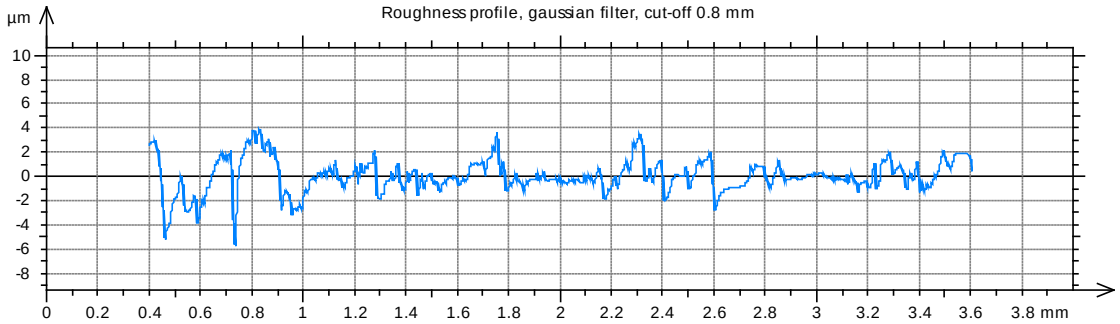

Parameters calculated on the profile mvk1

```
* Parameters calculated by mean of all the
sampling lengthes.
* A microroughness filtering is used, with a
ratio of 2.5 µm.

Roughness Parameters, Gaussian filter, 0.8 mm

   Ra    = 1.1 µm
   Rq    = 1.39 µm
   Rz    = 7.14 µm
   Rt    = 9.64 µm
```

2. Test No. 2

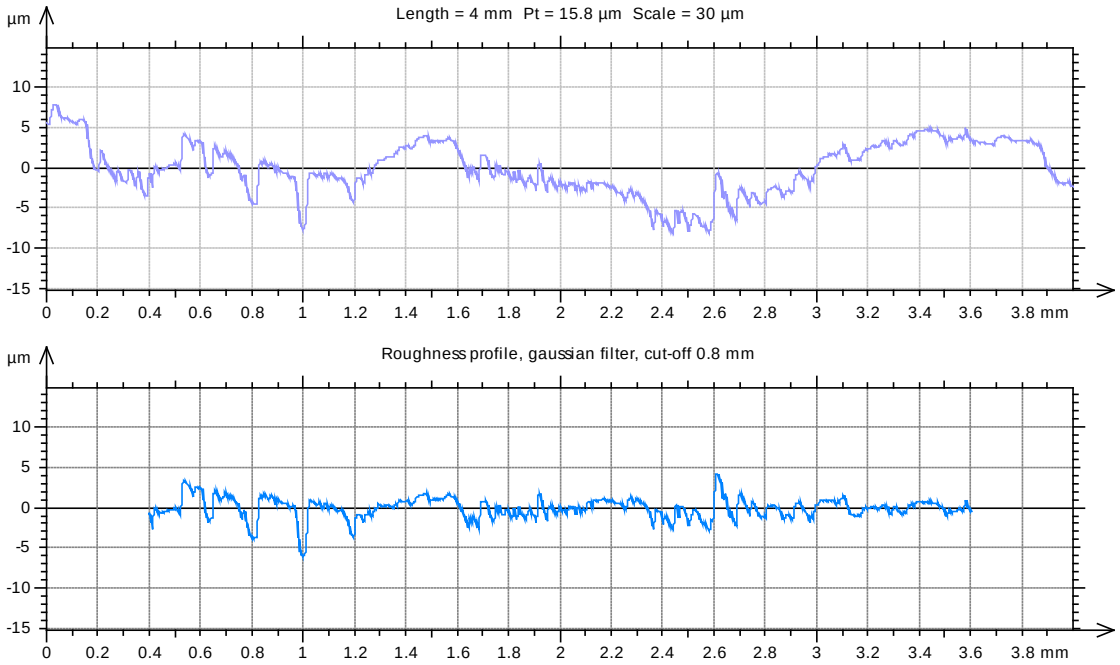

Parameters calculated on the profile mvk1

```
* Parameters calculated by mean of all the
sampling lengthes.
* A microroughness filtering is used, with a
ratio of 2.5 µm.

Roughness Parameters, Gaussian filter, 0.8 mm

   Ra    = 1.07 µm
   Rq    = 1.38 µm
   Rz    = 6.94 µm
   Rt    = 10.2 µm
```

3. Test No 19

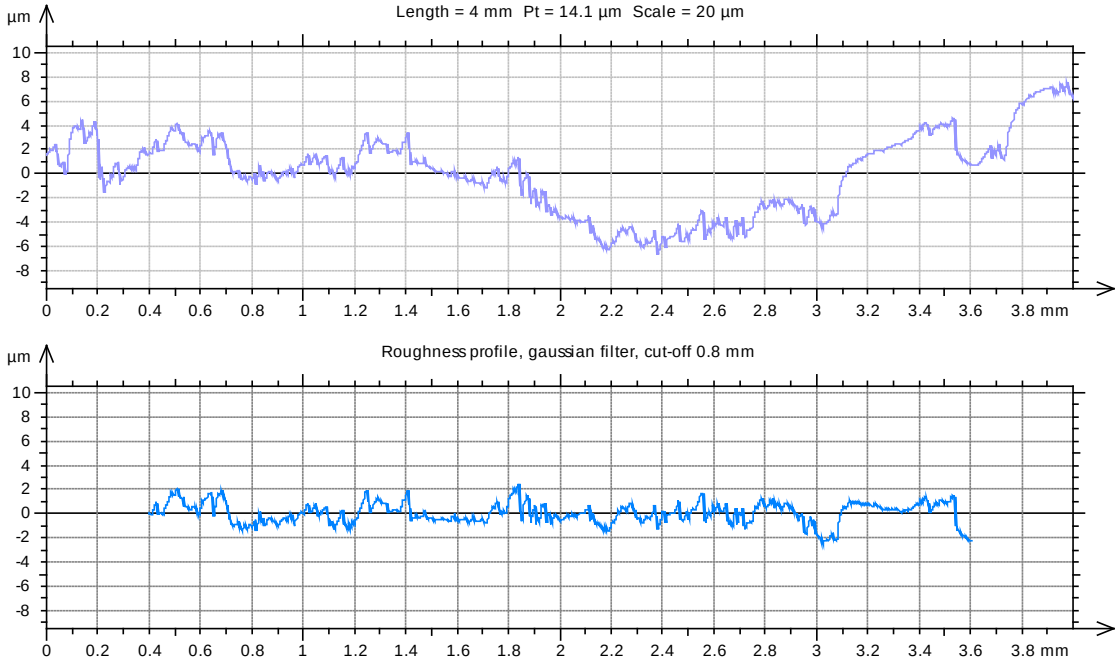

Parameters calculated on the profile mvk1

```
* Parameters calculated by mean of all the
sampling lengthes.
* A microroughness filtering is used, with a
ratio of 2.5 µm.

Roughness Parameters, Gaussian filter, 0.8 mm

   Ra    = 0.624 µm
   Rq    = 0.768 µm
   Rz    = 3.27 µm
   Rt    = 4.93 µm
```

4. Test No. 21

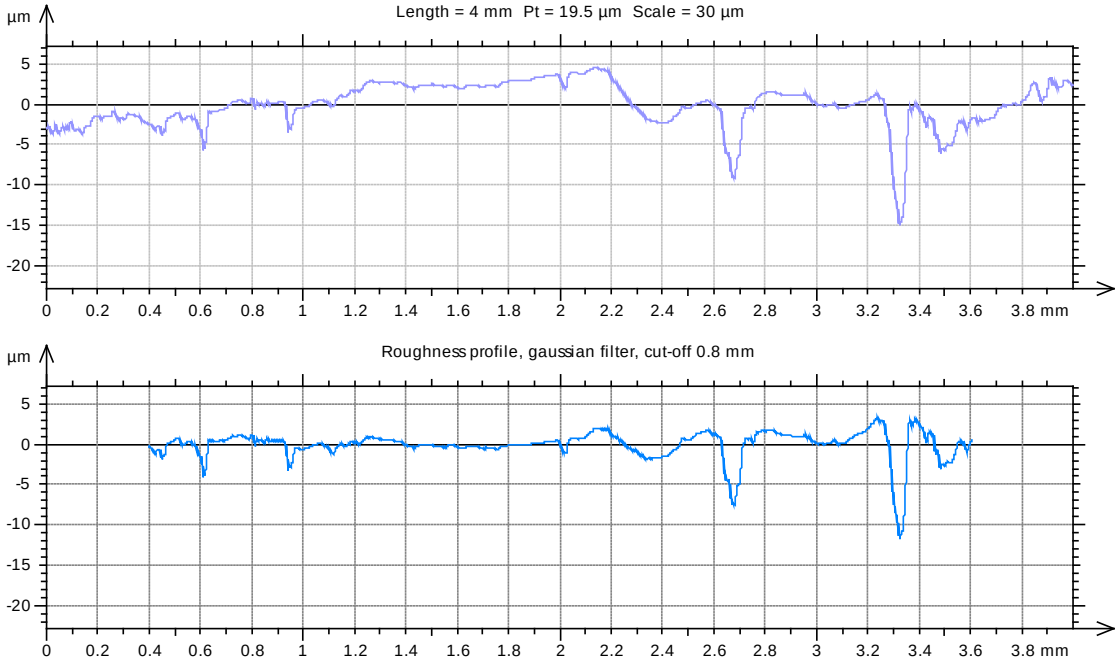

Parameters calculated on the profile mvk1

```
* Parameters calculated by mean of all the
sampling lengthes.
* A microroughness filtering is used, with a
ratio of 2.5 µm.

Roughness Parameters, Gaussian filter, 0.8 mm

   Ra    = 0.804 µm
   Rq    = 1.09 µm
   Rz    = 5.44 µm
   Rt    = 14.8 µm
```

5. Test No 8

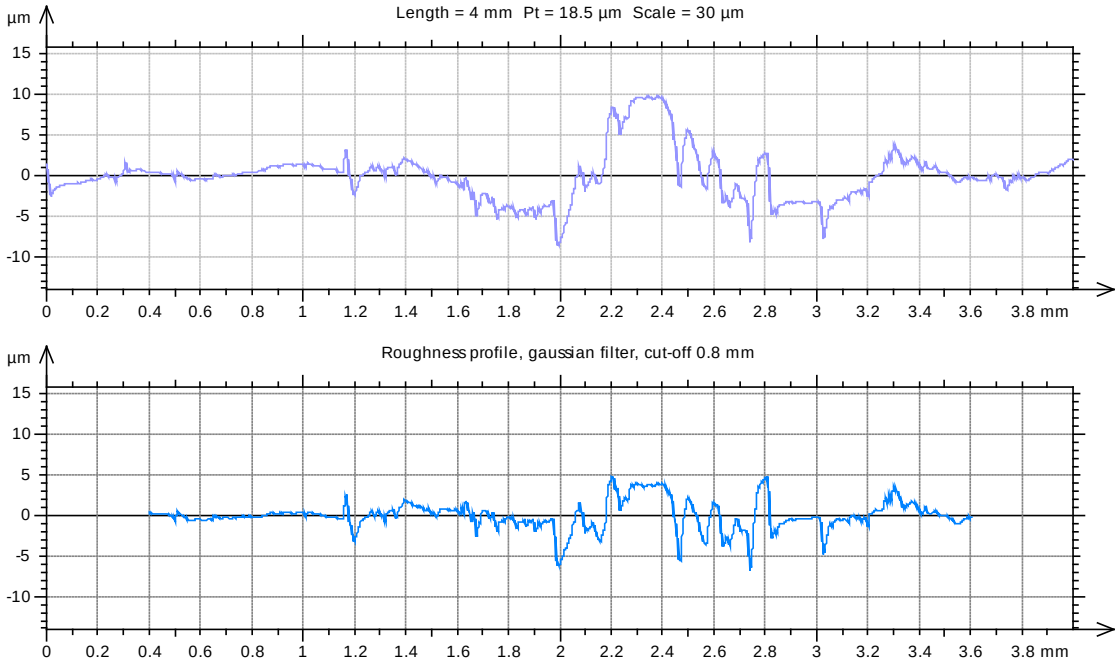

Parameters calculated on the profile mvk1

```
* Parameters calculated by mean of all the
sampling lengthes.
* A microroughness filtering is used, with a
ratio of 2.5 µm.

Roughness Parameters, Gaussian filter, 0.8 mm

   Ra    = 1.25 µm
   Rq    = 1.59 µm
   Rz    = 8.45 µm
   Rt    = 11.6 µm
```

6. Test No 12

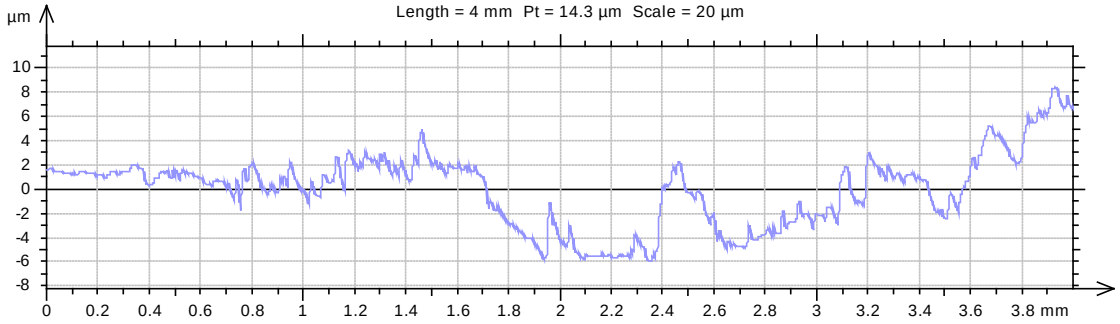

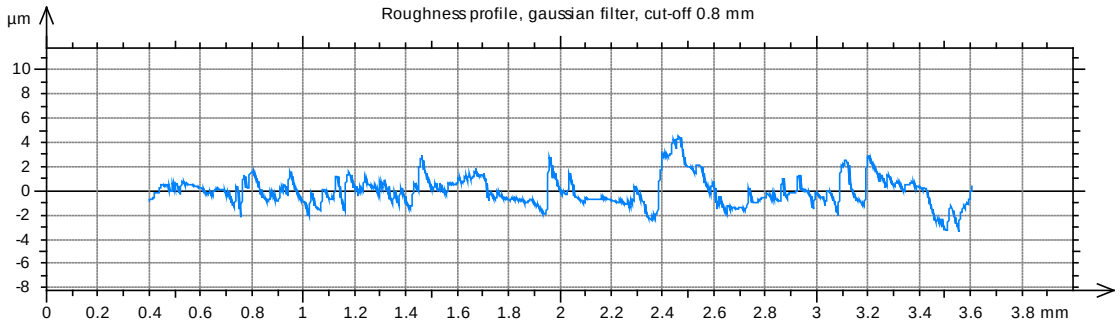

Parameters calculated on the profile mvk1

```
* Parameters calculated by mean of all the
sampling lengthes.
* A microroughness filtering is used, with a
ratio of 2.5 µm.

Roughness Parameters, Gaussian filter, 0.8 mm

   Ra    = 0.884 µm
   Rq    = 1.11 µm
   Rz    = 5.14 µm
   Rt    = 7.74 µm
```

APPENDIX-III

Experimental Results

Sr. No	Coded Values			Actual values			Mass of workpiece (grams)		Mass of workpiece Material removed (grams)	Volume of material removed (mm^3)	Grinding time (s)	Specific Tangential grinding force (N/mm)	Response		
	X_1	X_2	X_3	SiC Vol %	Feed (mm/s)	Depth of grind (*a*, μm)	Before grinding	After grinding					y_1 (*u*, J/mm^3)	y_2 ($Q_w^{'}$ mm^3/ mm.s)	y_3 (R_a, μm)
1	-1	-1	-1	8	60	8	37.098	36.941	0.157	57.634	9.52	2.71	148.772	0.477	1.05
							36.906	36.747	0.159	58.231	9.52	2.64	142.398	0.482	1.1
							36.327	36.151	0.176	64.636	9.52			0.535	1.08
2	-1	-1	0	8	60	12	37.006	36.809	0.197	72.362	9.52	2.98	129.642	0.599	1.07
							36.634	36.455	0.179	65.849	9.52	2.82	122.461	0.598	1.12
							36.89	36.693	0.197	72.359	9.52			0.545	1.09
3	-1	-1	1	8	60	16	36.863	36.630	0.232	85.318	9.52	3.63	134.849	0.706	1.13
							36.708	36.485	0.223	81.822	9.52	3.55	136.432	0.677	1.18
							36.135	35.924	0.211	77.640	9.52			0.642	1.14
4	-1	0	-1	8	70	8	32.595	32.455	0.141	51.658	9.60	1.84	113.064	0.424	1.1
							32.175	32.024	0.152	55.711	9.60	1.83	115.376	0.412	1.22
							32.439	32.302	0.137	50.190	9.60			0.457	1.18
5	-1	0	0	8	70	12	33.753	33.547	0.206	75.782	9.60	2.17	90.908	0.622	1.13
							33.633	33.424	0.209	76.607	9.60	2.09	86.342	0.628	1.22
							33.324	33.137	0.188	68.962	9.60			0.566	1.16
6	-1	0	1	8	70	16	32.508	32.257	0.251	92.179	9.60	2.46	84.603	0.756	1.19
							31.910	31.682	0.228	83.883	9.60	2.56	83.923	0.793	1.26
							32.362	32.099	0.263	96.660	9.60			0.688	1.22

Sr. No	Coded Values			Actual values			Mass of workpiece (grams)		Mass of workpiece Material removed (grams)	Volume of material removed (mm^3)	Grinding time (s)	Specific Tangential grinding force (N/mm)	Response		
	X_1	X_2	X_3	SiC Vol %	Feed (mm/s)	Depth of grind (*a*, μm)	Before grinding	After grinding					y_1 (*u*, J/mm^3)	y_2 ($Q_w^{'}$ mm^3/ mm.s)	y_3 (R_a, μm)
7	-1	1	-1	8	80	8	32.834	32.649	0.184	67.674	9.24	2.20	99.044	0.577	1.15
							32.727	32.562	0.165	60.631	9.24	1.84	92.719	0.517	1.22
							32.562	32.379	0.183	67.300	9.24			0.574	1.17
8	-1	1	0	8	80	12	32.788	32.537	0.251	92.021	9.24	2.33	77.173	0.784	1.24
							32.407	32.179	0.228	83.739	9.24	2.17	75.548	0.745	1.29
							32.645	32.407	0.238	87.449	9.24			0.714	1.25
9	-1	1	1	8	80	16	36.785	36.485	0.300	110.095	9.24	2.54	70.485	0.938	1.29
							36.602	36.341	0.261	95.998	9.24	2.28	72.574	0.818	1.3
							36.341	36.068	0.273	100.186	9.24			0.854	1.3
10	0	-1	-1	10	60	8	35.573	35.405	0.168	61.585	9.52	2.56	128.909	0.509	0.81
							35.303	35.150	0.153	56.042	9.52	2.64	131.623	0.521	0.88
							35.475	35.303	0.172	62.998	9.52			0.464	0.86
11	0	-1	0	10	60	12	35.801	35.595	0.206	75.465	9.52	2.79	116.272	0.624	0.85
							35.68	35.471	0.209	76.334	9.52	3.00	123.542	0.631	0.92
							35.328	35.141	0.188	68.673	9.52			0.568	0.86
12	0	-1	1	10	60	16	36.024	35.777	0.247	90.488	9.52	3.41	115.960	0.733	0.89
							35.523	35.303	0.220	80.611	9.52	3.45	114.582	0.783	0.90
							35.88	35.621	0.259	94.617	9.52			0.667	0.91
13	0	0	-1	10	70	8	37.514	37.336	0.178	65.270	9.60	2.34	113.850	0.535	0.86
							37.41	37.232	0.178	65.254	9.60	2.46	119.342	0.535	0.95
							37.232	37.034	0.198	72.432	9.60			0.594	0.87
14	0	0	0	10	70	12	36.551	36.331	0.220	80.438	9.60	2.33	91.937	0.660	0.91
							35.769	35.569	0.200	73.199	9.60	2.58	95.097	0.706	0.99
							36.187	35.952	0.235	86.090	9.60			0.600	0.93

Sr. No	Coded Values			Actual values			Mass of workpiece (grams)		Mass of workpiece Material removed (grams)	Volume of material removed (mm^3)	Grinding time (s)	Specific Tangential grinding force (N/mm)	Response		
	X_1	X_2	X_3	SiC Vol %	Feed (mm/s)	Depth of grind (*a*, μm)	Before grinding	After grinding					y_1 (*u*, J/mm^3)	y_2 ($Q_w^{'}$ mm^3/ mm.s)	y_3 (R_a, μm)
15	0	0	1	10	70	16	37.444	37.185	0.259	94.819	9.60	2.56	85.551	0.778	0.95
							37.186	36.913	0.273	99.723	9.60	2.63	83.598	0.818	1.0
							36.564	36.267	0.297	108.698	9.60			0.892	0.95
16	0	1	-1	10	80	8	35.525	35.276	0.249	91.079	9.24	2.56	85.726	0.776	0.92
							35.147	34.885	0.262	95.712	9.24	2.51	87.276	0.748	0.98
							35.387	35.147	0.240	87.809	9.24			0.816	0.95
17	0	1	0	10	80	12	37.692	37.381	0.311	113.744	9.24	2.63	70.565	0.969	0.97
							37.503	37.206	0.297	108.819	9.24	2.57	72.192	0.927	1.01
							37.206	36.923	0.283	103.507	9.24			0.882	0.98
18	0	1	1	10	80	16	37.810	37.440	0.370	135.403	9.24	3.04	68.605	1.154	1.04
							36.648	36.276	0.373	136.352	9.24	3.13	72.746	1.117	1.09
							37.342	36.984	0.358	131.107	9.24			1.162	1.04
19	1	-1	-1	12	60	8	37.428	37.254	0.174	63.251	9.52	2.57	127.501	0.523	0.62
							37.084	36.920	0.164	59.944	9.52	2.31	121.398	0.496	0.67
							36.346	36.168	0.178	64.740	9.52			0.535	0.66
20	1	-1	0	12	60	12	37.558	37.344	0.214	78.074	9.52	2.96	116.802	0.646	0.73
							37.102	36.901	0.201	73.389	9.52	3.08	122.334	0.654	0.83
							37.433	37.216	0.217	79.112	9.52			0.607	0.76
21	1	-1	1	12	60	16	37.322	37.072	0.250	90.945	9.52	3.52	121.956	0.752	0.8
							37.177	36.942	0.235	85.542	9.52	3.33	122.397	0.708	0.85
							36.734	36.450	0.284	103.506	9.52			0.856	0.81
22	1	0	-1	12	70	8	37.361	37.181	0.180	65.750	9.60	1.76	84.657	0.539	0.65
							36.909	36.726	0.183	66.743	9.60	1.54	79.895	0.502	0.71
							37.257	37.089	0.168	61.232	9.60			0.547	0.69

Sr. No	Coded Values			Actual values			Mass of workpiece (grams)		Mass of workpiece Material removed (grams)	Volume of material removed (mm^3)	Grinding time (s)	Specific Tangential grinding force (N/mm)	Response		
	X_1	X_2	X_3	SiC Vol %	Feed (mm/s)	Depth of grind (*a*, μm)	Before grinding	After grinding					y_1 (*u*, J/mm^3)	y_2 ($Q_w^{'}$ mm^3/ mm.s)	y_3 (R_a, μm)
23	1	0	0	12	70	12	39.239	39.013	0.225	82.157	9.60	1.98	76.603	0.674	0.75
							39.109	38.899	0.210	76.659	9.60	1.87	77.492	0.629	0.86
							38.539	38.305	0.233	85.092	9.60			0.698	0.79
24	1	0	1	12	70	16	37.536	37.269	0.267	97.190	9.60	2.14	69.877	0.797	0.82
							37.126	36.841	0.285	103.698	9.60	1.98	67.328	0.766	0.89
							37.382	37.126	0.256	93.422	9.60			0.851	0.84
25	1	1	-1	12	80	8	37.750	37.514	0.236	85.867	9.24	2.15	76.436	0.732	0.69
							37.619	37.380	0.239	87.252	9.24	2.28	79.573	0.744	0.76
							37.315	37.100	0.214	78.139	9.24			0.666	0.72
26	1	1	0	12	80	12	37.698	37.368	0.330	120.148	9.24	2.54	64.305	1.024	0.76
							37.201	36.875	0.326	118.905	9.24	2.32	61.391	0.984	0.85
							37.518	37.201	0.317	115.442	9.24			1.013	0.78
27	1	1	1	12	80	16	37.251	36.894	0.357	130.302	9.24	2.81	66.105	1.103	0.85
							36.053	35.720	0.333	121.367	9.24	2.58	64.926	1.034	0.96
							37.518	37.201	0.317	115.442	9.24			1.065	0.87

APPENDIX-IV

NSGA-II CODES FOR MULTI OBJECTIVE OPTIMISATION

```
/*********  **********************   ******************
                        Multiobjective Genetic Algorithm: Modified Dec 2011
                *********  **********************   ******************/
import java.io.*;

class Individual              //class for each individual
{
private int Chrom1[], Chrom2[], Chrom3[];
private double Rank;
private int maxBits1, maxBits2, maxBits3, maxRange1, maxRange2, maxRange3;
private double MRR, SE, RA;       // CF
private int SIC, F, DOC;

Individual()
          {
          maxBits1 = 4;
          maxBits2 = 7;
          maxBits3 = 4;
```

```
        maxRange1 = 4;
        maxRange2 = 20;
        maxRange3 = 8;
        Chrom1 = new int[maxBits1];
        Chrom2 = new int[maxBits2];
        Chrom3 = new int[maxBits3];
        SIC = (int) (maxRange1 * Math.random() + 8.0);
        F = (int) (maxRange2 * Math.random() + 60.0);
        DOC = (int) (maxRange3 * Math.random() + 8.0);

        Chrom1 = DecToBin(SIC, maxBits1);
        Chrom2 = DecToBin(F, maxBits2);
        Chrom3 = DecToBin(DOC, maxBits3);

        ComputeObjectives();
        }
void ComputeObjectives()
        {
        SIC = BinToDec(Chrom1, maxBits1);
        F = BinToDec(Chrom2, maxBits2);
        DOC = BinToDec(Chrom3, maxBits3);

        MRR=-15.0+3.555+0.1727*SIC-0.1205*F-0.0380*DOC-0.0136*SIC*SIC+0.0008*F*F+0.0001
*DOC*DOC+0.0015*SIC*F+0.0018*SIC*DOC+0.0007*F*DOC;
```

```
        //              CF=-25.159+0.756574*SIC+1.11635*F+2.35111*DOC-0.0959259*SIC*SIC-0.00749259*F*F-
0.0174537*DOC*DOC+0.00897222*SIC*F-0.01875*SIC*DOC-0.00247222*F*DOC;

                SE=841.217+13.045*SIC-16.5058*F-19.0852*DOC-
1.29902*SIC*SIC+0.100311*F*F+0.707089*DOC*DOC+0.050053*SIC*F+0.428645*SIC*DOC-0.0581*F*DOC;

                RA=1.94077-0.23832*SIC+0.012329*F-0.00403*DOC+0.008739*SIC*SIC+0.000000455*F*F-0.000315*DOC*DOC-
0.000881*SIC*F+0.001891*SIC*DOC+0.000128*F*DOC;
                }
        static int[] DecToBin(int DeciVal, int maxB)
                {
                int j, chr[] = new int[maxB];
                int Decimal = DeciVal;

                for(j=0; j<maxB; j++)
                        chr[j] = 0;
                j = maxB-1;

                while(Decimal>0)
                        {
                        chr[j] = Decimal%2;
                        Decimal = Decimal/2;
                        j--;
```

```
                }
        return chr;
        }
static int BinToDec(int chr[], int maxB)
        {
        int j=0, Sum;
        Sum = chr[j];

        for(j=1; j<maxB; j++)
                Sum = Sum*2 + chr[j];

        return Sum;
        }
double getFitness()
        {
        return Rank;
        }
void setFitness(double r)
        {
        Rank = r;
        }
int[] getChromosome1()
        {
        int newChrom1[] = new int[maxBits1];
```

```
		for(int i=0; i<maxBits1; i++)
			newChrom1[i] = Chrom1[i];
		return newChrom1;
		}
int[] getChromosome2()
		{
		int newChrom2[] = new int[maxBits2];
		for(int i=0; i<maxBits2; i++)
			newChrom2[i] = Chrom2[i];
		return newChrom2;
		}
int[] getChromosome3()
		{
		int newChrom3[] = new int[maxBits3];
		for(int i=0; i<maxBits3; i++)
			newChrom3[i] = Chrom3[i];
		return newChrom3;
		}
double getObj1()
		{
		return MRR;
		}

/*		double getObj2()
```

```
        {
        return CF;
        }
*/

double getObj3()
        {
        return SE;
        }

double getObj4()
        {
        return RA;
        }
String displayParameters()
        {
        String param = " SIC: " + Integer.toString(SIC) + "\tF: " + Integer.toString(F) + "\tDOC: " + Integer.toString(DOC);
        return param;
        }

void putChromosome(int chr[], int which)
        {
        if(which == 1)
                Chrom1 = chr;
```

```
        if(which == 2)
                Chrom2 = chr;
        if(which == 3)
                Chrom3 = chr;
        ComputeObjectives();
        }

Individual makeCopy()
        {
        Individual offsp = new Individual();

        for(int i=0; i<maxBits1; i++)
                {
                offsp.Chrom1[i] = Chrom1[i];
                }

        for(int i=0; i<maxBits2; i++)
                {
                offsp.Chrom2[i] = Chrom2[i];
                }
        for(int i=0; i<maxBits3; i++)
                {
                offsp.Chrom3[i] = Chrom3[i];
                }
```

```
            offsp.Rank = Rank;
            offsp.MRR = MRR;
//                  offsp.CF = CF;
            offsp.SE = SE;
            offsp.RA = RA;
            offsp.SIC = SIC;
            offsp.F = F;
            offsp.DOC = DOC;

            return offsp;
            }
}                   //end of Individual class

class MultiObjGA          // class for Multiobjective Genetic Algorithm using Non-dominated Sorting of solutions
{
private Individual Pop[];
private Individual NextPop[];
private int N, ROUL;
private int n1, n2, n3, gencount, maxGen;
private int min1 = 8, min2 = 60, min3 = 8;
private int max1 = 12, max2 = 80, max3 = 16;
private double Pc;
private double Pm;
int RoulWheel[];
```

```
int noOfSol;
Individual nonDomSol[];
WriteResults writer;

MultiObjGA(String commandLine, String resultsFilename, int popsize, int maxgen, double Pcross, double Pmute)
        {
        N = popsize;
        n1 = 4;
        n2 = 7;
        n3 = 4;
        gencount = 0;
        maxGen = maxgen;
        Pc = Pcross;
        Pm = Pmute;
        ROUL = 1080;
        RoulWheel = new int[ROUL];
        noOfSol = 0;
        nonDomSol = new Individual[2*N];
        Pop = new Individual[N];
        NextPop = new Individual[N];
        for(int i=0; i<N; i++)
                Pop[i] = new Individual();
        writer = new WriteResults(resultsFilename);
        writer.writeToFile("RSMOptimaztion Program\n");
```

```
                writer.writeToFile("Parameters passed: Results Filename, Population Size, Limit for Generations, Crossover Prob, Mutation Prob\n\n");
                writer.writeToFile(commandLine);
                }

        public void PerformEvolution()
                {
                int result;
                double avMRR, avSE, avRA;       //avCF
                System.out.println("Processing started....");
                System.out.println("Average values of Objectives:");
                writer.writeToFile("Results of program run with above parameters: \n\n");
                ComputeFitness();
                result = EvalGen();
                gencount++;
                while(gencount < maxGen && result < 0.8*N)
                        {
                        NewGen();
                        ComputeFitness();
                        result = EvalGen();
                        gencount++;
                        if(gencount%100 == 0)
                                {
```

```
                writer.writeToFile("The NonDominating Solutions at Generation " + gencount + " (Parameters followed by Objectives):\n");
                avMRR = 0;
        //              avCF = 0;
                avSE = 0;
                avRA = 0;
                for(int k=0; k<noOfSol; k++)
                        {
                        nonDomSol[k].ComputeObjectives();
                        if((k+1) < 10)
                                writer.writeToFile("Sol "+(k+1)+"\t\t>>");
                        else
                                writer.writeToFile("Sol "+(k+1)+"\t>>");
                        writer.writeToFile(nonDomSol[k].displayParameters());
                        writer.writeToFile("\t>> MRR: "+round2((15+nonDomSol[k].getObj1()))+
        "\tSE: "+round2(nonDomSol[k].getObj3())+"\tRA: "+round2(nonDomSol[k].getObj4())+"\n");  //  "\tCF: "+round2(nonDomSol[k].getObj2())+
                        avMRR += (15 + nonDomSol[k].getObj1());
        //              avCF += nonDomSol[k].getObj2();
                        avSE += nonDomSol[k].getObj3();
                        avRA += nonDomSol[k].getObj4();
                        }
                System.out.println("At Gen "+gencount+" --> AvMRR: "+round2(avMRR/noOfSol)+"\tAvSE: "+round2(avSE/noOfSol)+"\tAvRA: "+round2(avRA/noOfSol));  // "\tAvCF: "+round2(avCF/noOfSol)+
```

```
                    writer.writeToFile("At Gen "+gencount+" --> AvMRR: "+round2(avMRR/noOfSol)+"\tAvSE:
"+round2(avSE/noOfSol)+"\tAvRA: "+round2(avRA/noOfSol)+"\n");          // "\tAvCF: "+round2(avCF/noOfSol)+
                    writer.writeToFile("\n");
                    }
                }
            System.out.println();
            writer.closeFile();
            }

    public int EvalGen()                                                // to evaluate the population at specific generation
            {
            double temp;
            int ind, Maxcount=0, Currcount=1;
            double fitPop[] = new double[N];

            for(int i=0; i<N; i++)
                fitPop[i] = Pop[i].getFitness();

            for(int i=0; i<N; i++)
                {
                for(int j=1; j<(N-i); j++)
                    {
                    if(fitPop[j] > fitPop[j-1])
                        {
```

```
                    temp = fitPop[j];
                    fitPop[j] = fitPop[j-1];
                    fitPop[j-1] = temp;
                    }
                }
        }

// find the largest number of similar values
for(ind=1; ind<N; ind++)
        {
if(fitPop[ind] == fitPop[ind-1])
                Currcount++;
        else
                {
        if(Currcount > Maxcount)
                    Maxcount = Currcount;
                Currcount = 0;
                }
        }
if(ind == N)
        {
        if(Currcount > Maxcount)
                Maxcount = Currcount;
        }
```

```
        return Maxcount;
        }
public void ComputeFitness()                                    // to compute fitness of an individual
        {
        double fit;
        double[][] First, Second, Third, Fourth;

        First = new double[N][2];
//              Second = new double[N][2];
        Third = new double[N][2];
        Fourth = new double[N][2];
        for(int i=0; i<N; i++)
                {
                First[i][0] = i;
                First[i][1] = Pop[i].getObj1();
//                      Second[i][0] = i;
//                      Second[i][1] = Pop[i].getObj2();
                Third[i][0] = i;
                Third[i][1] = Pop[i].getObj3();
                Fourth[i][0] = i;
                Fourth[i][1] = Pop[i].getObj4();
                }

        int k=0;
```

```
        while(k<N)
                {
                fit = (double) dominateCount(k, First, Third, Fourth);      //Second
                Pop[k].setFitness(fit);
                k++;
                }
        }
public void NewGen()      //Creating the next generation
        {
        int newSize=0;
        Individual MatePool[];
        Individual NewPop[] = new Individual[N];

        SetRoulette();

        while(newSize < N)
                {
                MatePool = Selection();
                MatePool = CrossOver(MatePool);
                MatePool = Mutation(MatePool);
                NewPop[newSize] = MatePool[0].makeCopy();
                newSize++;
                NewPop[newSize] = MatePool[1].makeCopy();
                newSize++;
```

```
                }
        nonDominatedSort(NewPop);
        for(int i=0; i<N; i++)
                Pop[i] = NewPop[i].makeCopy();
        }  //end of  function NewGen
void SetRoulette()    //Setup Roulette wheel
        {
        int val, index=0;
        double sum=0.0;
        double temp[] = new double[2];
        double Fit[][] = new double[N][2];

        for(int i=0; i<ROUL; i++)
                        RoulWheel[i] = 0;

        for(int i=0; i<N; i++)
                {
                Fit[i][0] = i;
                Fit[i][1]= Pop[i].getFitness();
                sum = sum + Fit[i][1];
                }
        if(sum == 0.0)
                sum = 1.0;
```

```
for(int i=0; i<N; i++)
        {
        for(int j=1; j<(N-i); j++)
                {
                if(Fit[j][1] > Fit[j-1][1])
                        {
                        temp = Fit[j];
                        Fit[j] = Fit[j-1];
                        Fit[j-1] = temp;
                        }
                }
        }

for(int i=0; i<N; i++)
        {
        val = (int) ((Fit[i][1]/sum)*ROUL);
        for(int j=0; j<val; j++)
                {
                if((index+j) < ROUL)
                        RoulWheel[index+j] = (int) Fit[i][0];
                else
                        break;
                }
        index = index + val;
```

```
                }
        }

Individual[]  Selection()    //Selection operator for reproduction
        {
        Individual MatePool[] = new Individual[2];

        for(int i=0; i<2; i++)
                {
                int randNo = (int) (ROUL*Math.random());
                int chr = RoulWheel[randNo];
                MatePool[i] = Pop[chr].makeCopy();
                }

        return MatePool;
        }  // end of func selection

Individual[]  CrossOver(Individual MatePool[])    //to implement crossover operator
        {
        int Dec1, Dec2, r, count, temp;

                if (Math.random() < Pc)
                {
                int Chrom11[];
```

```
int Chrom12[];
count = 0;
do      {
        Chrom11 = MatePool[0].getChromosome1();
        Chrom12 = MatePool[1].getChromosome1();
        r=(int)((n1-1)*Math.random());

        for(int k=r; k<n1; k++)
                {
                temp = Chrom11[k];
                Chrom11[k] = Chrom12[k];
                Chrom12[k] = temp;
                }
        Dec1 = Individual.BinToDec(Chrom11, n1);
        Dec2 = Individual.BinToDec(Chrom12, n1);
        count++;
        } while(((Dec1 < min1) || (Dec1 > max1) || (Dec2 < min1) || (Dec2 > max1)) && (count < 5));

if(count < 5)
        {
        MatePool[0].putChromosome(Chrom11, 1);
        MatePool[1].putChromosome(Chrom12, 1);
        }
```

```
int Chrom21[];
int Chrom22[];
count = 0;
do      {
        Chrom21 = MatePool[0].getChromosome2();
        Chrom22 = MatePool[1].getChromosome2();
        r=(int)((n2-1)*Math.random());

        for(int k=r; k<n2; k++)
                {
                temp = Chrom21[k];
                Chrom21[k] = Chrom22[k];
                Chrom22[k] = temp;
                }
        Dec1 = Individual.BinToDec(Chrom21, n2);
        Dec2 = Individual.BinToDec(Chrom22, n2);
        count++;
        } while(((Dec1 < min2) || (Dec1 > max2) || (Dec2 < min2) || (Dec2 > max2)) && (count < 5));

if(count < 5)
        {
        MatePool[0].putChromosome(Chrom21, 2);
        MatePool[1].putChromosome(Chrom22, 2);
        }
```

```
int Chrom31[];
int Chrom32[];
count = 0;
do      {
        Chrom31 = MatePool[0].getChromosome3();
        Chrom32 = MatePool[1].getChromosome3();
        r=(int)((n3-1)*Math.random());

        for(int k=r; k<n3; k++)
                {
                temp = Chrom31[k];
                Chrom31[k] = Chrom32[k];
                Chrom32[k] = temp;
                }
        Dec1 = Individual.BinToDec(Chrom31, n3);
        Dec2 = Individual.BinToDec(Chrom32, n3);
        count++;
        } while(((Dec1 < min3) || (Dec1 > max3) || (Dec2 < min3) || (Dec2 > max3)) && (count < 5));

if(count < 5)
        {
        MatePool[0].putChromosome(Chrom31, 3);
        MatePool[1].putChromosome(Chrom32, 3);
```

```
                    }
                }

        return MatePool;
        }                                                   //end of function CrossOver

Individual[] Mutation(Individual MatePool[])   //Function to perform mutation
        {
        int r, Dec, count;

        for(int i=0; i<2;  i++)
                {
                if (Math.random() < Pm)
                        {
                        int Chrom1[];
                        count = 0;
                        do      {
                                Chrom1 = MatePool[i].getChromosome1();
                                r = (int)(n1*Math.random());
                                if(Chrom1[r] == 0)
                                        Chrom1[r] = 1;
                                else
                                        Chrom1[r] = 0;
                                Dec = Individual.BinToDec(Chrom1, n1);
```

```
        count++;
        } while(((Dec < min1) || (Dec > max1)) && (count < 5));

if(count < 5)
        MatePool[i].putChromosome(Chrom1, 1);

int Chrom2[];
count = 0;
do      {
        Chrom2 = MatePool[i].getChromosome2();
        r = (int)(n2*Math.random());
        if(Chrom2[r] == 0)
                Chrom2[r] = 1;
        else
                Chrom2[r] = 0;
        Dec = Individual.BinToDec(Chrom2, n2);
        count++;
        } while(((Dec < min2) || (Dec > max2)) && (count < 5));

if(count < 5)
        MatePool[i].putChromosome(Chrom2, 2);

int Chrom3[];
count = 0;
```

```
                    do      {
                            Chrom3 = MatePool[i].getChromosome3();
                            r = (int)(n3*Math.random());
                            if(Chrom3[r] == 0)
                                    Chrom3[r] = 1;
                            else
                                    Chrom3[r] = 0;
                            Dec = Individual.BinToDec(Chrom3, n3);
                            count++;
                            } while(((Dec < min3) || (Dec > max3)) && (count < 5));

                    if(count < 5)
                            MatePool[i].putChromosome(Chrom3, 3);
                    }
            }

    return MatePool;
    } //end of func mutation

void nonDominatedSort(Individual[] newPop)          // Non dominated sorting of combined population
    {
    int i=0, j, index=0;

    noOfSol = 0;
```

```
while(i < N)
        {
        j = 0;
        while(j < N)
                {
                if(i != j)
                        {
                        if(isNonDominated(Pop[i], Pop[j]))
                                {
                                if(!Contains(nonDomSol, noOfSol, Pop[i]))
                                        nonDomSol[noOfSol++] = Pop[i].makeCopy();
                                if(!Contains(nonDomSol, noOfSol, Pop[j]))
                                        nonDomSol[noOfSol++] = Pop[j].makeCopy();

                                if(index < N)
                                        NextPop[index++] = Pop[i].makeCopy();
                                if(index < N)
                                        NextPop[index++] = Pop[j].makeCopy();
                                }
                        }
                j++;
                }
        j = 0;
        while(j < N)
```

```
                {
                if(isNonDominated(Pop[i], newPop[j]))
                        {
                        if(!Contains(nonDomSol, noOfSol, Pop[i]))
                                nonDomSol[noOfSol++] = Pop[i].makeCopy();
                        if(!Contains(nonDomSol, noOfSol, newPop[j]))
                                nonDomSol[noOfSol++] = newPop[j].makeCopy();

                        if(index < N)
                                NextPop[index++] = Pop[i].makeCopy();
                        if(index < N)
                                NextPop[index++] = newPop[j].makeCopy();
                        }
                j++;
                }
        i++;
        }

i=0;
while(i < N)
        {
        j = 0;
        while(j < N)
                {
```

```
                    if(i != j)
                        {
                        if(isNonDominated(newPop[i], newPop[j]))
                            {
                            if(!Contains(nonDomSol, noOfSol, newPop[i]))
                                nonDomSol[noOfSol++] = newPop[i].makeCopy();
                            if(!Contains(nonDomSol, noOfSol, newPop[j]))
                                nonDomSol[noOfSol++] = newPop[j].makeCopy();

                            if(index < N)
                                NextPop[index++] = newPop[i].makeCopy();
                            if(index < N)
                                NextPop[index++] = newPop[j].makeCopy();
                            }
                        }
                    j++;
                    }
                i++;
                }
        }

boolean isNonDominated(Individual first, Individual second)
        {
        boolean flag=false;
```

```
        if((first.getObj1() >= second.getObj1()) && (first.getObj3() < second.getObj3()) && (first.getObj4() < second.getObj4()))
// (first.getObj2() < second.getObj2()) &&
                flag = true;
        if((first.getObj1() < second.getObj1()) &&  (first.getObj3() < second.getObj3()) && (first.getObj4() < second.getObj4()))
// (first.getObj2() >= second.getObj2()) &&
                flag = true;
        if((first.getObj1() < second.getObj1()) && (first.getObj3() >= second.getObj3()) && (first.getObj4() < second.getObj4()))
// (first.getObj2() < second.getObj2()) &&
                flag = true;
        if((first.getObj1() < second.getObj1()) &&  (first.getObj3() < second.getObj3()) && (first.getObj4() >= second.getObj4()))
// (first.getObj2() < second.getObj2()) &&
                flag = true;

        return flag;
        }

boolean Contains(Individual[] array, int size, Individual ind)
        {
        boolean flag=false;

        for(int i=0; i<size; i++)
                {
```

```
                    if(isIdentical(array[i].getChromosome1(), ind.getChromosome1()) && isIdentical(array[i].getChromosome2(),
ind.getChromosome2()) && isIdentical(array[i].getChromosome3(), ind.getChromosome3()))
                        flag = true;
                    }

            return flag;
            }

        boolean isIdentical(int[] chro1, int[] chro2)
            {
            boolean flag=true;

            for(int i=0; i<chro1.length; i++)
                {
                if(chro1[i] != chro2[i])
                    flag = false;
                }

            return flag;
            }

        int dominateCount(int k, double[][] First,  double[][] Third, double[][] Fourth)      // double[][] Second,
            {
            int dcount=0;
```

```
        int j=0;
        while(j < N)
                {
                if((First[k][1] < First[j][1]) ||  (Third[k][1] < Third[j][1]) || (Fourth[k][1] < Fourth[j][1]))
                        dcount++;                                       // (Second[k][1] < Second[j][1]) ||
                j++;
                }

        return dcount;
        }
double round2(double num)
        {
        double numfloor;
        double numround;

        numfloor = Math.floor(100*num);
        numround = numfloor/100;

        return numround;
        }
} //end of MGA class
```

REFERENCES

Abdullah, A., Pak, A., Farahi, M., Mohsen and Barzegari, M. (2007). "Profile wear of resin-bonded nickel-coated diamond wheel and roughness in creep-feed grinding of cemented tungsten carbide." *Journal of Materials Processing Technology,* 183(2-3), 165–168.

Agarwal, B.D. and Broutman, L.J. (1980). "*Analysis and performance of fiber composites*." John Wiley & Sons, New York, 3-12.

Agarwal, S. and Rao, P.V. (2005). "A probabilistic approach to predict surface roughness in ceramic grinding."*International Journal of Machine Tools & Manufacture,* 45(6), 609–616.

Agarwal, S. and Rao, P.V. (2008). "Experimental investigation of surface/subsurface damage formation and material removal mechanisms in SiC grinding."*International Journal of Machine Tools & Manufacture,* 48(6), 698–710.

Allison, J.E. and Cole, G.S. (1993). "Metal matrix composite in the automotive industry: opportunities and challenges." *Journal of Minerals & Materials Characterization & Engineering, 45,* 19–24.

Ames, W. and Alpas, A.T. (1995). "Wear mechanisms in hybrid composites of graphite-20% SiC in A356 aluminium alloy (Al-7% Si-0.3% Mg)." *Metallurgical and Materials Transactions A*, 26(1), 85-98.

Aniban, N., Pillai, R.M. and Pai, B.C. (2002). "An analysis of impeller parameters for aluminium metal matrix composites synthesis." *Materials and Design,* 23(6), 553-556.

Anjum, M.F., Tasadduq, I. and Al-Sultan K. (1997). "Response surface methodology: A neural network approach."*European Journal of Operational Research*, 101(1), 65-73.

Arsenault, R. J., Wang, L. and Feng, C.R. (1991). "Strengthening of composites due to micro-structural changes in the matrix." *Acta metallica and Material Science,* 39(1), 47-57.

ASM Hand book (1989) Machining, *ASM International* 783-802

ASM Hand book (2001) Composites, Miracle, D.B. and Donaldson, S.L (Volume Chair). *ASM International* 130-138

Asokan, P, Bhaskar, N., Babu, K., Prabhaharan, G. and Saravanan, R. (2005). "Optimization of surface grinding operations using particle swarm optimization technique." *Journal of Manufacturing Science and Engineering*, 127(4), 885-892.

Bas, C., Arslan, G., Zehra, F. and Muluk. (2010). "On multiple response optimization: desirability functions and artificial neural networks." *Proc., 24th Mini EURO Conference on Continuous Optimization and Information-Based Technologies in the Financial Sector (MEC EurOPT 2010)*, June 23–26, 2010, Izmir, TURKEY.

Bhaskar, V., Gupta, S.K. and Ray, A.K. (2001). "Multiobjective optimization of an industrial wiped film reactor: some further insights." *Computers & Chemical Engineering*, 25(1-3), 391–407.

Bianchi, E.C., Silva, E.J., Varga,s V.L., Magagnin, T.C., Monici, R.D., Filho, O.V. and Aguiar, P.R(2002). "The grinding wheel performance in the transverse cylindrical grinding of an eutetic alloy." *Materials Research*. 5(4), 433-438.

Bifano, T. G. and Fawcett, S. C. (1991). "Specific grinding energy as an in-process control variable for ductile-regime grinding." *Journal of Precision Engineering*, 113(2), 256-262.

Bowman, R.R, Misra, A.K. and Arnold, S.M. (1995). "Processing and mechanical properties of Al_2O_3 fiber-reinforced NiAl composites." *Metallurgical and Materials Transactions*. 26 A 615- 628.

Brinksmeier, E., Aurich, J.C., Govekar. E., Heinzel, C., Hoffmeister, H.W., Klocke, F., Peters, J., Rentsch, R., Stephenson, D. J., Uhlmann, E., Weinert, K. and Wittmann, M. (2006). "Advances in modeling and simulation of grinding processes." *Annals of the CIRP*. 55(2), 667–696.

Brinksmeier, E. and Giwerzew, A. (2003). "Characterization of the size effect and its influence on the workpiece residual stresses in grinding." *1st Colloquium Processscaling*, October 28-29, 2003, Bremen, Germany.

Brinksmeier, E., Tönshoff, H.K., Czenkusch, C. and Heinzel, C. (1998). "Modelling and optimisation of grinding processes." *Journal of Intelligent Manufacturing*, 9(4), 303-314.

Brockenbrough, J. R., Suresh, S. and Wienecke, H. A., (1991). "Deformation of metal-matrix composites with continuous fibers: geometrical effects of fiber distribution and shape." *Metallurgical and Materials Transactions* A. 39(5), 735-742.

Carlos, A.C., Veldhuizen, D.A. and Lamont, G.B.(2002). "*Evolutionary algorithms for solving multi-objective problems*." First edition, Kluwer Academic New York.

Castillo, D. E., Montgomery, D.C. and D.R. McCarville, D.R.(1996). "Modified desirability functions for multiple response optimization." *Journal of Quality Technology,* 28(3), 337-345.

Chen, X., Rowe, W.B., Mills, B. and Allanson, D.R (1996). "Analysis and simulation of the grinding process Part III: comparison with experiment." *International journal of machine tools and Manufacture,* 36(8), 897-906.

Chiu, N. and Malkin, S. (1993). "Computer simulation for cylindrical plunge grinding." *Annals of the CIRP*. 42(1), 383-387.

Ch'ng C.K., Quah S. and Low H.C. (2008). "A new approach for multiple response optimization." *Quality Engineering,* 17(4), 621-626.

Choudhury, I.A. and El-Baradieb, M.A. (1999). "Machinability assessment of inconel 718 by factorial design of experiment coupled with response surface methodology." *Journal of Materials Processing Technology,* 95(1-3), 30-39.

Christman, T., Needleman, A., Nutt, S. and Suresh, S. (1989). "On micro-structural evolution and mechanical modeling of deformation of a whisker-reinforced metal-matrix composite." *Materials Science Engineering,* 107 A, .49-61.

Christodoulou, L., Parrish, P. A. and Crowe, C. R. (1988). "XD titanium aluminide composites." *Proc., Int. Symp. on High Temperature/High Performance Composites:, April 5-7, 1988. Reno, Nevada,* 29-34.

Clyne, T. W. and Whithers, P. J. (1993). "*An introduction to metal matrix composites*." First edition, Cambridge University *Press*, London, 12-24.

Comley, P, Walton, I., Jin, T. and Stephenson, D.J. (2006). "A high material removal rate grinding process for the production of automotive crankshafts." *Annals of the CIRP*. 55(1), 347-350.

Corbin, S.F. and Wilkinson, D.S. (1994). “Influence of matrix strength and damage accumulation on the mechanical response of a particulate metal matrix composite.” *Acta metallica and material Science,* 42(4), 1319–1328.

Correia, D.S., Gonçalves, C.V, da Cunha, S.S. Jr. and Ferraresi, V.A. (2005). “Comparison between genetic algorithms and response surface methodology in GMAW welding optimization.” *Journal of Materials Processing Technology,* 160(1), 70–76.

Cronjager L. and Meister D. (1992), “Machining of fibre and particle-reinforced aluminium”, *Annals of CIRP* 41 (1), pp. 63–66

D’Souza, R.G.L., Chandrasekaran, K. and Kandasamy, A. (2010). “Improved NSGA-II based on a novel ranking scheme.”*Journal of Computing,* 2(2), 91-95.

Das, S, Prasad V, Ramachandran, T.R. (1989). “Microstructure and wear of cast (Al-Si alloy)-graphite composites”. Wear, 133 pp. 173-187.

Davidson, M.J., Balasubramanian, K. and Tagore, G.R.N.(2008). “Surface roughness prediction of flow-formed AA6061 alloy by design of experiments.”*Journal of Materials Processing Technology,* 202(1-3), 41–46.

Davim, J.P. (2003). “Study of drilling metal–matrix composites based on the Taguchi techniques.” *Journal of Materials Processing Technology,* Vol.132(1-3), 250-254.

Dean, A.M. and Voss, D. (1999). “*Design and Analysis of Experiments*” Springer USA.

Deb K.(2008). “*Multiobjective Optimization using evolutionary algorithms*.” Wiley Interscience Series in Systems and Optimization, John Wiley & Sons, 245-253.

Deb, K., Pratap, A., Agarwal, S. and Meyarivan, T. (2002).”A fast and elitist multiobjective genetic algorithm: NSGA-II.” *IEEE Transactions Evolutionary Computation.* 6(2), 182–197.

Deming, S.N. (1991). “Multiple-criteria optimisatiuon.” *Journal of Chromotography* A, 550, 15-25.

Derringer, G. and Suich R. (1980). “Simultaneous optimization of several response variables.” *Journal of Quality Technology,* 12(4), 214-219.

Di Ilio, A. and Paoletti, A. (2000). "A comparison between conventional abrasives and superabrasives in grinding of SiC-aluminium composites."*International Journal of Machine Tools & Manufacture,* 40(2), 173–184

Di Ilio, A., Paoletti, A. and D'Addona, D (2009). "Characterization and modelling of the grinding process of metal matrix Composites."*CIRP Annals - Manufacturing Technology*, 58(1), 291–294.

Di Ilio, A., Paoletti, A., Tagliaferri, V. and Venialiii F. (1996). "Experimental study on grinding of silicon carbide reinforced aluminium alloys." *International Journal of Machine Tools & Manufacture*, 36(6673-685).

Dragone, T. L. and Nix, W. D., (1990). "Geometric factors affecting the internal stress distribution and high temperature creep rate of discontinuous fiber reinforced metals." *Acta metallica and material Science*, 38(10), 1941–1953.

El-Gallab, M. and Sklad, M. (1998). "Machining of Al/SiC particulate metal matrix composites Part II: Workpiece surface integrity." *Journal of Materials Processing Technology, International Journal of Advanced Manufacturing Technology,* 83(1-3), 277–285.

Eshelby, J. D. (1957). "The determination of the elastic field of an ellipsoidal inclusion, and related problems." *Procedings of the Royal Society .of London series A, on Mathematical and physical sciences*, 241(1226), 376-396.

Fisher, J. R. and Gurland, J. (1981). "Void nucleation in spheroidized carbon steels. part 1: experimental." *Metal Science,* 15(5), 185-192.

Fonseca, C.M. and Fleming, P.J. (1993). "Genetic algorithms for multiobjective optimization: Formulation, discussion and generalization." *Proc., 5th Int. Conf. on Genetic Algorithms, San Mateo.* 416-423.

Ghani, J.A., Choudhury, I.A. and Hassan, H.H. (2004). "Application of Taguchi method in the optimization of end milling operations." Journal of Material Processing Technology, 145(1), 84–92.

Ginta, T.L., Amin, A.K.M., Radzi, H.C.D. and Lajis M.A. (2009). "Tool life prediction by response surface methodology in end milling titanium alloy Ti-6Al-4V using uncoated WC-Co inserts." *European Journal of Scientific Research*, 28(4), 533-541.

Goldberg, D.E. (1989). "*Genetic algorithm in search optimization and machine learning*."First edition, Addison-Wesley Longman, Inc.

Gopala Krishna, A. and Rao, M.K (2006). "Multi-objective optimisation of surface grinding operations using scatter search approach." *International Journal of Advanced Manufacturing Technology*, 31(3-4), 475–480.

Gopala Krishna, A. (2007). "Optimization of surface grinding operations using a differential evolution approach."*Journal of Materials Processing Technology*, 183(2-3), 202-209.

Halpin, J. C. and Tsai, S.W. (1967). "Environmental factors in composite design," Air Force Materials Laboratory, AFML-TR-67-423.

Hecker R L, Liang S Y. (2003). "Predictive modeling of surface roughness in grinding", *International Journal of Machine Tools & Manufacture* 43(8), 755-761.

Harrington, E.C. (1965). "The desirability function." *Industrial Quality Control*, 21, 494-498.

Holland, J.H. (1975). "Adaptation in natural and artificial systems." *Ann Arbor, MI:* University of Michigan Press.

Hood, R., Lechner, F., Aspinwall, D.K. and Voice, W.(2007). "Creep feed grinding of gamma titanium aluminide and burn resistant titanium alloys using SiC abrasive." *International Journal of Machine Tools & Manufacture*, 47(9), 1486–1492.

Hooke, R. and Jeeves, T.A. (1960). "Direct search solution of numerical and statistical problems."*Journal of Association for Computing Machinery*, 8 212-229.

Hsu, C.M. (2004). "An integrated approach to enhance the optical performance of couplers based on neural networks, desirability functions and tabu search." *International Journal of Production Economics*. 92(3), 241-254.

Huda, D., El-Baradie, M.A. and Hashmi, M.S.J. (1996). "Analytical study for the stress analysis of metal matrix composites." *Journal of Materials Processing Technology*, 56(1-4), 429–434.

Humphreys, F. J. (1998). "Deformation and annealing mechanisms in discontinuously reinforced metal matrix composites." in *9th* Rise *Int. Symp. On Metallurgy and Materials*

Science, Rise National Laboratory Roskilde, Denmark 51-74.

Hung, N.P., Zhong, Z.W. and Zhong, C.H. (1997). "Grinding of metal matrix composites reinforced with silicon-carbide particles." *Journal of Materials and Manufacturing Processes* 12(6), 1075 – 1091.

Hwang, T.W. and Malkin. S. (1999). "Upper bound analysis for specific energy in grinding of ceramics." *International Journal of Wear*. 231(2), 161–171.

Hwang, T.W., Evans, C.J. and Malkin, S. (1999). "Size effect for specific energy in grinding of silicon nitride." *International Journal of Wear (part-2) (225–229), 862–867.*

Hwang, C.L., Paidy, S.R., Yoon, K. and Masud, A.S.M. (1980). "Mathematical programming with multiple objectives: a tutorial." *Computational Operation Research,* 7(1-2), 5-31.
Inasaki, I. (1988). "Speed Stroke Grinding of Advanced Ceramics." *Annals of the CIRP*. Vol. 37(1), 299 – 302.

Ishibuchi, H. and Murata T. (1996). "Multi-objective genetic local search algorithm." in *Proc. of IEEE Int. Conf. on Evolutionary Computation (ICEC'96),* Nagoya, Japan, 119–124.

Islam, A., Nikoloutsou, Z., Sakkas, V., Papatheodorou, M. and Albanisa, T. (2010). "Statistical optimisation by combination of response surface methodology and desirability function for removal of azo dye from aqueous solution." *International Journal of Environmental Analytical Chemistry*, 90(3–6), 497–509.

Jeong, I.J. and Kim, K.J. (2008). "An interactive desirability function method to multiresponse optimization." *European Journal of Operational Research*, 2008, 195(2), 412-426.

Jeyapaul, R., Shahabudeen, P. and Krishnaiah, K. (2006). "Simultaneous optimization of multi-response problems in the Taguchi method using genetic algorithm."*International Journal of Advanced Manufacturing Technology*, 30(9-10), 870–878.

Jing, W, HE-Zhen, OH Jin-ho, and PARK Sung-hyun, (2008). "Multi-response robust optimization using desirability function." *IEEE symp. on Advanced Management of information for globalized Enterprises* 28-29 Sept. 2008, Tianjin, china, 1-3.

Johnson, E.C., Li, R., Shih, A.J. and Hanna, H. (2008). "Design of experiments based force modeling of the face grinding process."*Transactions of NAMRI/SME* 36, 241-248.

Jones, D.G., Mirrazavi, S.K. and Tamiz, M. (2002). “Multiobjective meta-heuristics: An overview of current state-of-the-art.” *European Journal of Operational Research*, 137(1), 1-9.

Jones, P.M, Tiwari, A., Roy, R. and Corbett, J. (2004). “Optimisation of the high efficiency deep grinding process with fuzzy fitness function and constraints.”*Congress on evolutionary computations* 19-23 June 2004, 1 574-581.

Jones, R. M., (1992). *Mechanics of composites materials*. McGraw Hill Publication, Tokyo.

Kaczmar, J.W. (1989). “Effect of production engineering parameters on structure and properties of Cu-W composite powders.” *Powder Metallurgy*, 32(3), 171-175.

Kainer, K.U. (2006). *Metal matrix composites. custom-made materials for automotive and aerospace engineering*, WILEY-VCH Verlag GmbH & Co. Weinheim, Germany. 12-25.

Kannan, S. and Kishawy, H.A. (2006). “Surface characteristics of machined aluminium metal matrix composites.” *International Journal of Machine Tools & Manufacture*, 46(15), 2017–2025.

Kaw, A.K. (1997). *Mechanics of composites materials*. *CRC press*, New York, 31-43.

Khuri, A .I. and Conlon, M. (1980). “Simultaneous optimization of multi responses represented by polynomial regression functions.” *Technometrics*, 23(4), 363-375.

Kilickap, E., Huseyinoglu, M. and Yardimeden, A. (2010). “Optimization of drilling parameters on surface roughness in drilling of AISI 1045 using response surface methodology and genetic algorithm.” *International Journal of Advanced Manufacturing Technology*, 52(1-4), 79-82.

Kim, K.J. and Lin, D.K.J. (2000). “Simultaneous optimization of mechanical properties of steel by maximizing exponential desirability functions.” *Applied Statistics*, 49(3), 311-326.

Knowles, J.D. and Corne, D.W. (2000). “Approximating the non-dominated front using the Pareto archived evolution strategy.” *Evolutionary Computing*, 8 142-172.

Kodali, S.P., Kudikala, R. and Deb, K. (2008). “Multi-objective optimization of surface grinding process using NSGA II.” *First Int. Conf. on Emerging Trends in Engineering and Technology, IEEE computer society*, Nagpur India. 16-18 July 2008.

Konak, A., Coit, D.W., Smith, A.E., (2006). “Multi-objective optimisation using genetic

algorithms: A Tutorial". *Reliability Engineering and System Safety*, 91 992-1007

Krajnik, P., Sluga, A. and Kopac, J. (2005). "Design of grinding factors based on response surface methodology." *Journal of Materials Processing Technology*, 162–163 629–636.

Krajnik, P., Sluga, A. and Kopac J. (2006). "Radial basis function simulation and metamodelling of surface roughness in centreless grinding." *Journal of Achievements in Materials and Manufacturing Engineering*, 14(1-2), 104-110.

Kutz, M. (2008). Mechanical Engineering Hand Book -Materials and Mechanical Design, John-Wiley and Sons New York. 383-403.

Kwak, J.S. (2005). "Application of Taguchi and response surface methodologies for geometric error in surface grinding process." *International Journal of Machine Tools & Manufacture*, 45(3), 327–334.

Kwak, J.S. and Kim, Y.S.(2008). "Mechanical properties and grinding performance on aluminum-based metal matrix composites." *Journal of materials processing Technology*, 201 (1-3), 596-600.

Kwak, J.S. and Song, J.B. (2001). "Trouble diagnosis of the grinding process by using acoustic emission signals." Int. *Journal of machine tools and Manufacture*, 41(6), 899-913.

Kwak, J.S., Sim, S.B. and Jeong, Y.(2006). "An analysis of grinding power and surface roughness in external cylindrical grinding of hardened SCM440 steel using the response surface method." *International Journal of Machine Tools & Manufacture*, 46(3-4), 304–312.

Lee, T.S., Ting, T.O. , Lin, Y.J. and Htay, T. (2007). "A particle swarm approach for grinding process optimization analysis."*International Journal of Advanced Manufacturing Technology*, 33(11-12), 1128–1135.

Levy, A. and Papazian, J.M. (1991). "Elastoplastic finite element analysis of short fibre reinforced SiC/Al composites: Effects of thermal treatment." *Acta metallica and material science* 39(10), 2255-2266.

Lewandowski, J. J., Liu, C., and Hunt, W. H. Jr. (1988). "Processing and properties for powder metallurgy composites." (P. Kumar, A. Ritter, and K. Vedula, eds.), *The Metallurgical Society*, Warrendale, Pennsylvania. 117- 138.

Li, X., Zhao, G., Guan, Y. and Ma, M. (2009). “Optimal design of heating channels for rapid heating cycle injection mold based on response surface and genetic algorithm.”*Materials and Design*. 30(10), 4317–4323.

Li, Y., Rowe, W.B. and Mills, B. (1999). “Study and selection of grinding conditions part 1”. *Proc. Institution of Mech. Engrs*. 213(2), 119-129.

Lin, J.T., Bhattacharya, D. and Lane C. (1995). “Machinability of silicon carbide reinforced Metal Matrix Composites.” *Wear Part-2*, 181-183, 883-888.

Lin, T.R. (2002). “Experimental design and performance analysis of TiN coated carbide tool in face milling stainless steel.” *Journal of Material Processing Technology*, 127(1), 1–7.

Ling Yin, L., Huang, H., Ramesh, K. and Huang T. (2005). “High speed versus conventional grinding in high removal rate machining of alumina and alumina–titania.” *International Journal of Machine Tools & Manufacture*, 45(7-8), pp. 897–907.

Llorca, J., Needleman, A. and Suresh, S. (1991). “An analysis of the effects of matrix voids growth on deformation and ductility in metal-ceramic composites”. *Acta metallica and material Science*, 39(10), 2317-2335.

Lloyd, D. J. (1989). “The solidification microstructures of particulate reinforced Al/SiC composites.” *Comp. Sci. & Tech.*, 35(2), 159-180

Lloyd, D. J. (1994). Particle reinforced aluminium and magnesium matrix composites, *Inter. Mater. Reviews*, 39(1), 1-23.

Malkin, S. and Guo, C., (2008). Grinding technology: *Theory and applications of machining with abrasives* second edition Industrial Press Inc. New York 120-128.

Malkin, S. and Ritter, J.E. (1989). “Grinding mechanisms and strength degradation for ceramics.” *Journal of Engineering for Industry*, 111- 167.

Manna, A. and Bhattacharayya, B. (2003). A study on machinability of Al/SiC-MMC, *Journal of Materials Processing Technology*, 140,(1-3), 711-716.

Manoharan, M. and Lewandowski, J.J. (1990). Fracture initiation and growth toughness of an aluminium metal matrix composites, *Acta metallica and material Science*, 38, 489-496.

Marinescu, I. D., Hitchiner, M., Uhlmann, E. and Rowe, W. B. (2007). *Handbook of Machining with grinding wheels* CRC Press 82-84.

McDanels, D. L., (1985). "Analysis of stress-strain, fracture, and ductility of aluminum matrix composites containing discontinuous silicon carbide reinforcement." *Metall. Trans. A*, 16 1105-1115.

Monici R.D., Bianchi, E.C., Catai, R.E. and Aguiar, P.R.(2006). "Analysis of the different forms of application and types of cutting fluid used in plunge cylindrical grinding using conventional and superabrasive CBN grinding wheels." *International Journal of Machine tools and Manufacture*, 46(2), 122-131.

Montgomery, D.C. (2005). *Design and analysis of experiments*, John Wiley and Sons, New York.

Motorcu, A.R. (2010). "The optimization of machining parameters using the taguchi method for surface roughness of AISI 8660 hardened alloy steel." *Journal of Mechanical Engineering*, 56(6), 391-401.

Mukherjee, I. and Ray, P.K. (2008). "Optimal process design of two-stage multiple responses grinding processes using desirability functions and metaheuristic technique." *Applied Soft Computing*, 8(1), 402–421.

Nardone, V. C. and Prewo, K. M., (1986). "On the strength of discontinuous silicon carbide-reinforced aluminium composites." *Scripta Metallurgica*, 20(1), 43-48.

Nguyen, H., Jang, N., and Choi, S.H. (2009). "Multiresponse optimization based on the desirability function for a pervaporation process for producing anhydrous ethanol." *Korean J. Chem. Eng*., 26(1), 1-6.

Osyczka, A. and Kundu, S. A. (1995). "A new method to solve generalized multicriteria optimization problems using the simple genetic algorithm." *Structural Optimization*.10 (2), 94-99.

Padkin, A.J., Boreton, M. F. and Plumbridge, W. J. (1987). "Fatigue crack growth in two-phase alloys." *Mater. Sci. Tech*, 3(3), 217-223.

Palanikumar, K. (2008). “Application of Taguchi and response surface methodologies for surface roughness in machining glass fiber reinforced plastics by PCD tooling.” *International Journal of Advanced Manufacturing Technology*, 36(1-2), 19–27.

Phadke, M.S. (1989). *Quality engineering using robust Design*, Englewood Cliffs, NJ: Prentice-Hall.

Piggott, M. R. (1980). *Load bearing fiber composites*, Oxford, Pergamon Press.

Puri, A.B. and Bhattacharyya, B. (2005). “Modeling and analysis of white layer depth in a wire-cut EDM process through response surface methodology.” *International Journal of Advanced Manufacturing Technology*, 25(3-4), 301–307.

Raissi, S, Farsani, R. (2009). “Statistical process optimization through multi-response surface methodology.” *world Academy of Science, Engineering and Technology*, 51, 267-271.

Ramesh, K., Yeo, S.H., Gowri, S. and Zhou, L.(2001). “Experimental evaluation of super high-speed grinding of advanced ceramics.” *International Journal of Advanced Manufacturing Technology*, 17(2), 87–92.

Reddy, S.K. and Rao, P.V. (2006). “Experimental investigation to study the effect of solid lubricants on cutting forces and surface quality in end milling.”*International Journal of Machine Tools & Manufacture*, 46(2), 189–198.

Ren, Y.H. Zhang, B. and Zhou, Z.X. (2009). “Specific energy in grinding of tungsten carbides of various grain sizes.” *CIRP Annals - Manufacturing Technology*, 58(1), 299–302

Rohatgi, P.K. (1993). “Metal matrix composites”. *Defence Science Journal*, 43(4), 323-349.

Ronald, A.B. Vijayaraghavan, L. and Krishnamurthy, R. (2009). “Studies on the influence of grinding wheel bond material on the grindability metal matrix composites.”*Materials and Design* 30(3), 679-686.

Ross, S.M. (2004). *Introduction to probability and statistics for engineers and scientists*. Academic Press 291-296.

Rowe, W.B. (2009). *Principles of Modern grinding Technology*, William Andrew Publications

Saravanan, R. and Sachithanandam M. (2001). “Genetic algorithm for multivariable surface grinding process optimisation using a multi-objective function model.”*International Journal of Advanced Manufacturing Technology*, 17(5), 330–33.

Saravanan, R., Asokan, P. and Sachidanandam, M.(2002). “A multi-objective genetic algorithm approach for optimization of surface grinding operations.” *International Journal of Machine Tools & Manufacture*, 42(12), 1327–1334.

Schaffer, J. D. (1985). “Multiple objective optimisation with vector evaluated genetic algorithms, Genetic Algorithms and their Applications.” *Proc. of 1st International Conference on Genetic Algorithms*, Lawrence Erlbaum, Hillsdale, USA. 93–100.

Seeman, M., Ganesan, G., Karthikeyan, R. and Velayudham, R. (2010). “Study on tool wear and surface roughness in machining of particulate aluminum metal matrix composite-response surface methodology approach.” *International Journal of Advanced Manufacturing Technology*, 48(5-8), 613–624.

Shaw, M.C. (1996). Principle of Abrasive Processing, *Springer* 314-345

Shen, J.Y., Luo, C.B., Zeng, W.M., Xu, X.P. and Gao, Y.S. (2002). “ceramics grinding under the condition of constant pressure.” *Journal of Materials Processing Technology*, 129(1-3), 176-181.

Shetty, R., Pai, B.R., Rao, S.S. and Nayak, R (2009). “Taguchi’s technique in machining of metal matrix composites.” *Journal of the Brazilian Society of Mechanical Sciences and Engineering*, 31(1), 12-20.

Shetty, R., Pai, B.R., Rao, S.S. and Kamath, V. (2008). ”Machinability study on discontinuously reinforced aluminium composites (DRACs), using response surface methodology and Taguchi’s design of experiments under dry cutting condition.”*Maejo International Journal of Science and Technology*, 2(1), 227-239.

Shi, N. and Arsenault, R. J. (1994).”Plastic flow in SiC/Al composites – strengthening and ductility.” *Ann. Rev. Mater. Sci*., 24, .321-357.

Shih, A.J., Scattergood, R.O. and Curry, A.C. (2003). “Cost-effective grinding of zirconia using the dense vitreous bond silicon carbide wheel.” *Journal of Manufacturing Science and*

Engineering, 125(2), 297-303.

Sidda Reddy, B., Suresh Kumar, J., and Reddy, V. K. (2009). "Prediction of surface roughness in turning using adaptive neuro-fuzzy inference system." *Jordan Journal of Mechanical and Industrial Engineering,* 3(4), 252-259.

Sivasakthivel, P.S., Velmurugan, V. and Sudhakaran, R. (2010). "Prediction of tool wear from machining parameters by response surface methodology in end milling." *International Journal of Engineering Science and Technology,* 2(6), 1780-1789.

Slowik, A. and Slowik, J. (2008). "Multi-objective optimization of surface grinding process with the use of evolutionary algorithm with remembered Pareto set." *International Journal of Advanced Manufacturing Technology*, 37(7-8), 657–669.

Sodhi, M.S. and Tiliouin, K. (1996). "Surface roughness monitoring using computer vision." *Int. J. Mach. Tools Manufact*. 36(7), 817-828.

Song, S. G., Shi, N., Gray G. T. III and Roberts, J. A. (1996). "Reinforcement shape effects on the fracture behavior and ductility of particulate-reinforced 6061-Al matrix composites." *Metall. and Mater. Trans*. 27A, 3739-3746.

Srinivas, N. and Deb, K. (1993). "Multiobjective optimization using nondominated sorting in genetic algorithms." *Evolutionary Computation* 2(3), 221-248.

Surappa, M.K. (2003). "Aluminium matrix composites: Challenges and opportunities." *Sadhana* .28, Parts 1 & 2, 319–334.

Suresh, P.V.S., Rao, P.V. and Deshmukh, S.G. (2002). "A genetic algorithmic approach for optimization of surface roughness prediction model." *International Journal of Machine Tools & Manufacture,* 42(6), 675–680.

Swamy A. R. K., Ramesha A., Veeresh Kumar G.B. and Prakash J.N. (2011). "Effect of Particulate Reinforcements on the Mechanical Properties of Al6061-WC and Al6061-Gr MMCs" *Journal of Minerals & Materials Characterization & Engineering.* 10(12), 1141-1152

Tawakoli, T., Westkaemper, E. and Rabiey, M. (2007). "Dry grinding by special conditioning." *International Journal of Advanced Manufacturing Technology,* 33(3-4), 419–424.

Ting, T.O., Lee, T.S. and HTay, T. (2005). "Performance analysis of grinding process via particle swarm optimization."*Proc. of the 6th Int. Conf. on Computational Intelligence and Multimedia Applications (ICCIMA'05).* Las Vegas USA.

Tonshoff. H.K., Peters, J., Inasaki, I. and Paul, T. (1992). "Modelling and simulation of grinding processes." Annals of the CIRP. 41(2), 677–688.

Tvergaard, V. (1990). "Analysis of Tensile Properties for a Whisker-reinforced metal matrix composite." *Acta metallica and material Science,* 38(2), 185- 194.

Veeresh Kumar, G.B., Rao, C.S.P., Selvaraj, N., and Bhagyashekar, M.S. (2010). "Studies on Al6061-SiC and Al7075-Al2O3 metal matrix composites." *Journal of Minerals & Materials Characterization & Engineering,* 9(1), 43-55.

Venu Gopal, A. and Rao, P.V. (2003). "Selection of optimum conditions for maximum material removal rate with surface finish and damage as constraints in SiC grinding."*International Journal of Advanced Manufacturing Technology*, 43(13), 1327-1336.

Venu Gopal, A. and Rao, P.V. (2003). The optimisation of the grinding of silicon carbide with diamond wheels using genetic algorithms." *International Journal of Advanced Manufacturing Technology*, 22(7-8), 475–480.

Watt, D. F., Xu, X. Q. and Lloyd, D. J. (1996). "Effects of particle morphology and spacing on the strain fields in a plastically deforming matrix." *Acta metallica and material Science,* 44(2), 789-799.

Wattanutchariya, W. and Pintasee, B. (2006). "Optimization of metallic milling parameters for surface finishing." *Proc., of 7th Asia Pacific on Industrial Engineering and Management Systems Conference. 17-20 December 2006,* Bangkok, Thailand.

Wen, X.M, Tay, A.A.O. and Nee, A.Y.C. (1992). "Micro-computer based optimization of the surface grinding process."*Journal of Materials Processing Technology*, 29(1-3), 75–90.

Whitehouse, A.F. and Clyne, T. W. (1993). "Effects of reinforcement content and shape on cavitation and failure in metal matrix composites." *composites*, 24(3), 256-261.

Wilk, W. and Barbara, S.B. (2008). “Abrasive machining of metal matrix composites.” 8th International *Conference on Advanced Manufacturing operations* 2008 Bulgaria.

Xi-Ping Li, Guo-Qun Zhao, Yan-Jin Guan and Ming-Xing Ma. (2009). “Optimal design of heating channels for rapid heating cycle injection mold based on response surface and genetic algorithm.”*Materials and Design* 30(10), .4317–4323.

Xu, C. and Shin, Y.C. (2007). “Control of cutting force for creep-feed grinding processes using a multi-level fuzzy controller.” *ASME Transactions: Journal of Dynamic Systems measurement and control*. 129(3), 539-550.

Xue, L., Naghdy, F. and Cook, C. (2002). “Monitoring of wheel dressing operations for precision grinding.”*IEEE International conference on Industrial Technology, December* 2002. Bankok Thailand.

Zhang, L., Subbarayan, G., Hunter, B.C. and Rose, D. (2005). “Response surface models for efficient, modular estimation of solder joint reliability in area array packages.”*Microelectronics Reliability*. 45(2), 623–635.

Zhong, Z.W. (2003). “Grinding of aluminium-based metal matrix composites reinforced with Al_2O_3 or SiC particles.”*International Journal of Advanced Manufacturing Technology*, 21(2), 79–83.

Zhong, Z. W. and Hung, N.P. (2002). “Grinding of alumina/aluminium composites.” *Journal of Materials Processing Technology*, 123(1), 13–19.

Zhou, X. and Xi, F. (2002). “Modeling and predicting surface roughness of the grinding process.” *International Journal of Machine Tools & Manufacture*, 42(8), 969–977.

Zitzler, E., Deb, K. and Thiele, L. (2000). “Comparison of multi objective evolutionary algorithms: Empirical results.” *Evolutionary Computation.* 8(2), 173-195.